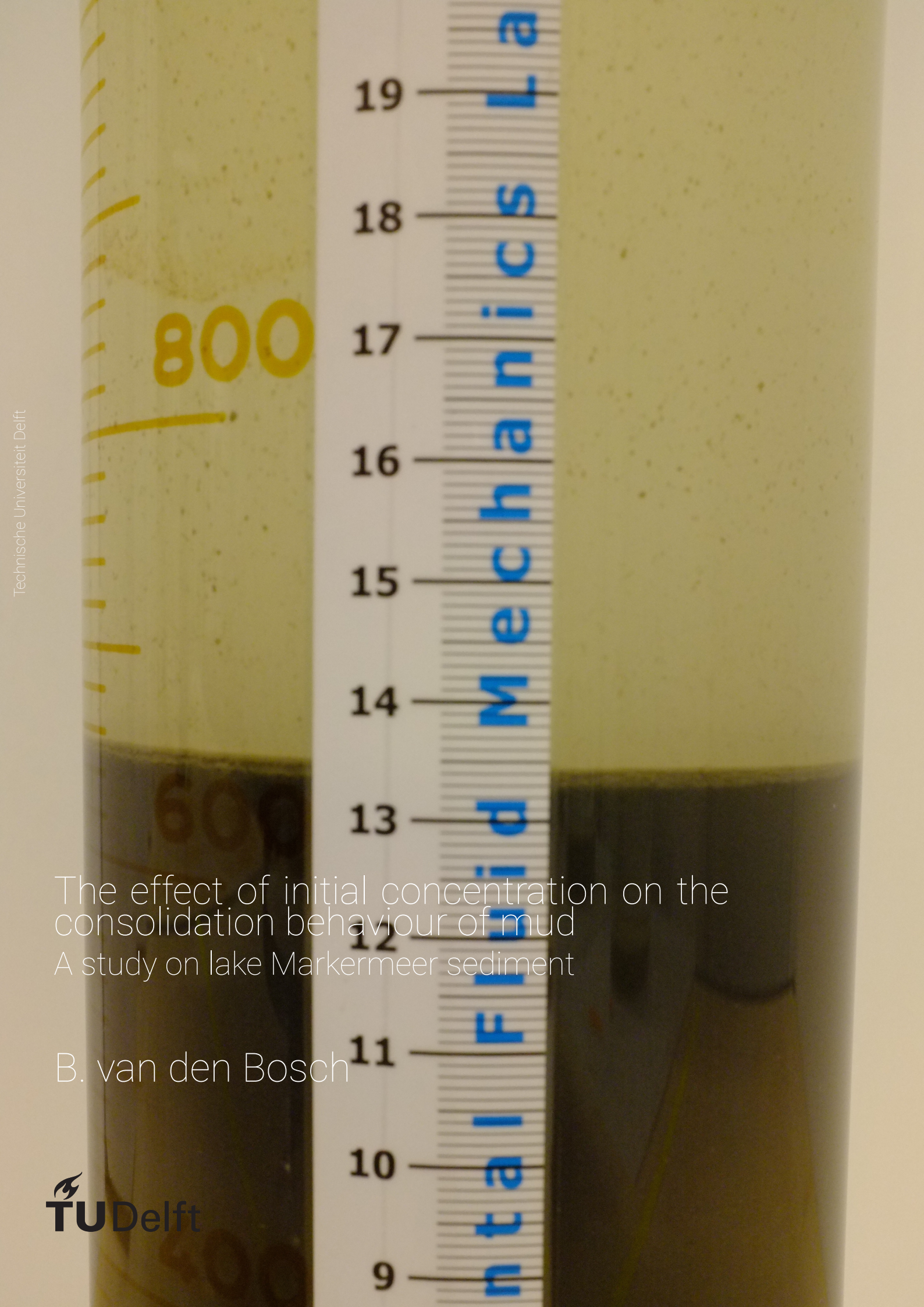

The effect of initial concentration on the consolidation behaviour of mud

A study on lake Markermeer sediment

B. van den Bosch

TU Delft

The effect of initial concentration on the consolidation behaviour of mud

A study on lake Markermeer sediment

by

Barend A. P. van den Bosch

to obtain the degree of Master of Science
at the Delft University of Technology,
to be defended publicly on Thursday December 1, 2016 at 15:00.

Student number:	1539108	
Project duration:	February 1, 2016 – December 1, 2016	
Thesis committee:	Prof. dr. ir. J.C. Winterwerp,	Delft University of Technology, chair
	Ir. M. Barciela Rial,	Delft University of Technology, supervisor
	Ir. H. J. Luger,	Deltares
	Dr. ir. L. A. van Paassen,	Delft University of Technology
	Ir. T Vijverberg,	Royal Boskalis Westminster N.V.

An electronic version of this thesis is available at `http://repository.tudelft.nl/`.

TU Delft Deltares

Preface

This research marks the completion of my Master of Science degree at Delft University of Technology. This work will contribute to a better understanding of the consolidation of mud and the Building With Nature project the Marker Wadden. Utilising the forces of nature to contribute to a safe and better environment attracted my attention towards this project. Throughout the course of my studies I worked on several Building With Nature projects and I hope to continue doing so in the future.

This research was carried out at the Deltares FCL laboratory, where there is a lot of expertise on experimental work with fine cohesive sediments. During this research I was given the opportunity to learn and work in a professional environment. This experience was part of the preparation to start my life as an engineer.

The realisation of this thesis was made possible by a great number of people and I wish to express my gratitude. First of all, I would like to thank Deltares for allowing me to work in the laboratory to conduct my experiments. I would like to thank my colleges Miguel, Maria, Luca, Bernadette and especially Saskia who helped me a lot with the experiments and work in the laboratory. During this research I was guided by my graduation committee. I am very grateful to the chair of my committee Han Winterwerp for his expertise and to Maria Barciela Rial for the support and encouragement during my research. Dirk Luger, Leon van Paassen and Thomas Vijverberg thank you for being part of my graduation committee, support and finding the time to help me graduate. Finally, I would like to thank my parents who are the greatest motivators and who helped me to reach this goal. Thank you for enabling me to get an education, which is the greatest investment a person can do.

Barend van den Bosch
Delft, December 2016

Summary

Land reclamations in deltaric areas provide space to meet the demand for a safe place to live and work. In coastal zones granular sediments, a traditional filling material for land reclamations, is becoming more scarce. An alternative filling material is mud. A land reclamation starts with pumping a high density mud slurry in an enclosed area where the solids will settle and form a bed. If this process is repeated a bed will rise above the water level. Such a land reclamation project is being constructed in lake Markermeer, the Netherlands. An islands archipelago is being constructed with mud from the bottom of the lake itself to serve as a habitat for flora and fauna.

Mud as a filling material poses some challenges. Mud consists of clay, silt, sand, organic material, water and gas [Winterwerp and Van Kesteren, 2004]. The versatility of the material makes it difficult to predict its consolidation behaviour. A clay particle has a high specific surface area and an electrical charge distribution. This gives mud cohesive properties and the ability to form flocs. Flocs are aggregated mud particles with a very high water content that forms an open clay-water matrix that traps other particles in it.

The objective of this research is to determine if the consolidation behaviour is a function of the initial conditions. To assess the effect of the initial concentration of mud on the bed formation settling column experiments were performed. These experiments were divided in two cases; case 1 has an initial concentration below the gelling point and case 2 has an initial concentration that exceeds the gelling point. The gelling point marks the concentration of the sediment-water mixture where the settling phase ends and self-weight consolidation phase begins. A settling curve is derived from monitoring the mud-water interface. From the settling curve material parameters can be derived, but only when the two phases, settling and self-weight consolidation, are present in the settling curve. The implication of this is that for the second case of the settling column experiment the material parameters cannot be determined from the settling curve. To determine material parameters for the high initial concentration case, a second set experiments needs to be performed. When the equilibrium bed height is reached the density profile and strength of the bed was measured to determine final conditions of the bed. The second set of experiments, a seepage induced consolidation (SIC) test, is a measuring device that performs direct measurements on a mud sample. The SIC tests were performed on mud samples that originated from the high initial concentration settling column experiments. A SIC test consolidates a sample by applying a load. During load steps the permeability is measured.

From these two experimental methods two sets of material parameters are obtained. The material parameters obtained from the two methods were of a different order of magnitude. Therefore, the material parameters are dependent on the initial concentration. With a 1-DV model it is possible to model the density profile at different stages of the consolidation process. The two sets of material parameters are used to model the density profile and are compared to the measured density profile. The material parameters obtained from the SIC test provide better results, in terms of predicting the final bed height and the shape of the density profile. This profile fits better to the measurement. Then the material parameters of the columns were interchanged and the density profiles were modelled again. The results show that when material parameters were interchanged the profile did not fit as good as the previous modelled density profile. Therefore, it can be concluded that there is an effect of initial concentration on the final conditions. The 1-DV model simulates swelling in high concentrated mud. The modelled density profiles are consistent with the measured density profiles. In the low concentration density profiles the swelling does not occur. Hence, the initial concentration has an effect of the consolidation behaviour.

The outcome of this research is relevant for land reclamations with mud as a filling material. The objective of this research is to gain a better understanding of the consolidation behaviour of high concentration mud slurry. Knowing that the consolidation behaviour, material parameters and final conditions are dependent of the initial concentration makes building with mud a possible solution for land reclamations.

Contents

List of symbols

A_p	DELCON parameter for effective stress	[Pa]
A_k	DELCON parameter for permeability	[Pa]
A	Shear strength fractal dimension parameter	[Pa]
B_p	DELCON parameter for effective stress	[Pa]
B_k	DELCON parameter for permeability	[Pa]
c_0	Initial concentration	$[g/l]$
c_{gel}	Gelling concentration	$[g/l]$
c_u	Undrained shear strength	$[g/l]$
c_v	Consolidation coefficient	$[m^2/s]$
c_s	Swelling coefficient	$[m^2/s]$
d	Particle diameter	$[m]$
D_p	Primary particle diameter	$[\mu m]$
D_f	Floc diameter	$[\mu m]$
e	Void ratio	[-]
g	Gravitational acceleration	$[m^2/s]$
h	Bed height	$[m]$
h_∞	Final bed height	$[m]$
k	Permeability	$[m/s]$
K_k	Permeability coefficient	$[m/s]$
K_p	Effective stress coefficient	[Pa]
$K_{p,0}$	Coefficient accounting for creep	[Pa]
m	Factor accounting for non-linear effects	[-]
n_f	Fractal dimension	[-]
n	$n = 2/(3 - n_f)$	[-]
t	Time	$[s]$
u	Pore water pressure	[Pa]
w_s	Effective settling velocity	$[m/s]$
$w_{s,r}$	Settling velocity for non-spherical particles	$[m/s]$
$w_{s,0}$	Settling velocity individual mud floc	$[m/s]$
Γ_c	Consolidation coefficient	$[m^2/s]$
ρ_s	Particle density	$[kg/m^3]$
ρ_b	Bulk density	$[kg/m^3]$
ρ_w	Density of water	$[kg/m^3]$
σ	Total stress	[Pa]
σ'	Effective stress	[Pa]
τ	Peak stress	[Pa]
ϕ	Volumetric concentration	[-]
$\bar{\phi}$	Average volumetric concentration	[-]
ϕ_p	Volumetric concentration of primary particle	[-]
ϕ_s^{sa}	Volumetric concentration solids sand fraction	[-]
ϕ_s^m	Volumetric concentration solids mud fraction	[-]
ζ_s	Gibson height account for sand	$[m]$
ζ_m	Gibson height account for mud	$[m]$

1 Introduction

1.1. Background information

Coastlines are the transition between water and land. The coastal zone inhabits a large part of the earths population. A variety of reasons makes it very attractive to live in a coastal area and the demand for space is increasing. Land reclamation and nourishments are a solution to cope with this demand for new space to live and work. The availability of a fill material is usually an issue. This is mainly the case in land reclamation projects in Asia, where sand, the most common hydraulic fill material, is less available. Usually there is an abundance of mud present. Which can be used as an alternative filling material for land reclamations. In the past there have been reclamations done with mud as a fill material. Dredged mud from maintenance dredging in ports etc. is reused as a filler material instead of being discarded into open water which could have a negative impact on the environment [van 't Hoff and Nooy van der Kolff, 2012].

In the Netherlands a land reclemation project is being constructed in 2016 where dredged mud is being used as a hydraulic fill material to create wetlands. This is a showcase project in which the possibilities of building with mud are shown. The mud is dredged with the purpose to be used as a building material and not as a result of maintenance dredging. The land reclamation project is called the Marker Wadden, situated in lake Markermeer and exists of several small islands that will be suitable as a living environment for flora and fauna. The construction of the islands is explained in figure 1.1.

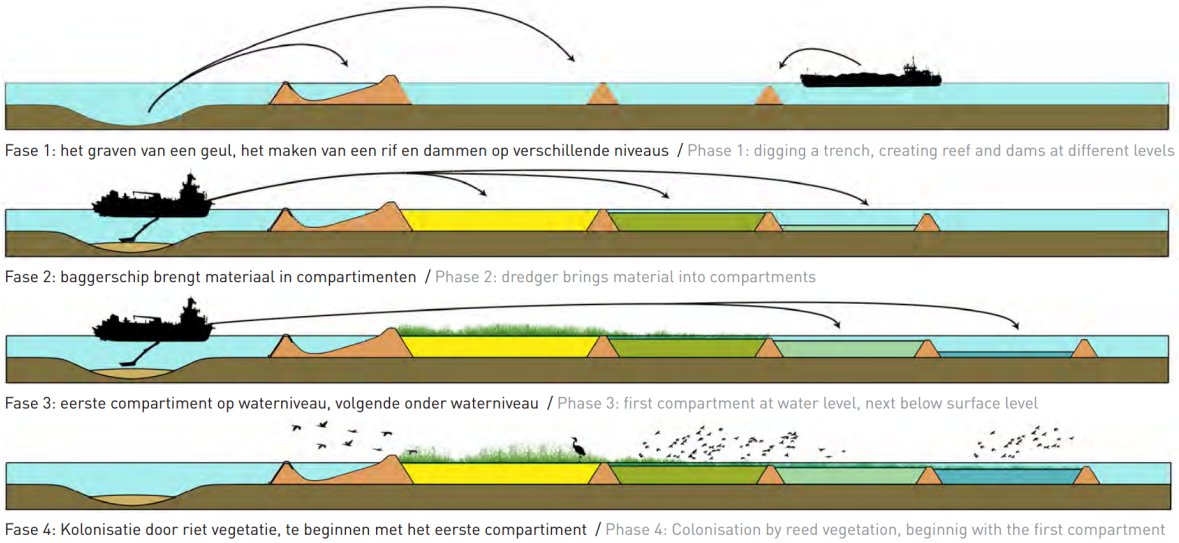

Figure 1.1: Method to build the artificial islands of the Marker Wadden [Geretsen, 2014]. Sand dams enclose several areas, at different heights, where mud is contained to form a habitat for flora and founa.

To reclaim land with dredged mud it is essential to trap it in an enclosed area. The dredged mud forms a slurry and should be contained in an area where the fluid mud can settle, explained in figure 1.2. The

solid and water particles rearrange in the water column and eventually the mud has all settled on the bed of the lake. This process can be described in two phases. The first phase consists of particles falling trough the water column until they reach the bottom and start to build a structure skeleton by making contact with other particles, this is called the settling phase. In the second phase, the particles have formed a structure skeleton, the weight of the layer itself drives water out of the material. This is called self-weight consolidation. After some time the self-weight consolidation reaches an equilibrium and a bed of mud is formed. These phases can be monitored by an interface of clear water and mud that is moving down in the vertical direction.

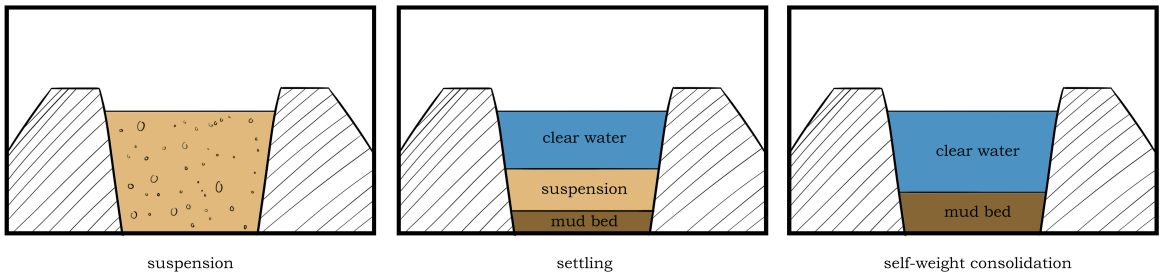

Figure 1.2: Schematised process of creating wetland in three phases. Phase 0; small dikes enclose an area in which fluid mud is deposited. Phase 1; particles settle in the suspension to the bottom and form a bed, a layered water column is observed. Phase 2; a mud bed has formed, all particles have settled, which consolidates under its own weight.

Reclamation of land with mud is a technique that has been used before, but introduces some challenges. The challenges are to predict the consolidation height and density profile over time. To design and construct a land reclamation the material properties of mud should be known. The material properties of mud depend on a variety of factors, such as salinity, agitation, concentration, composition etc. Opposed to sand, which is a predictable and a well studied building material, the properties of mud from an engineering perspective have a wide variability, which makes it difficult to predict its behaviour. Also chemical conditions influence the electrostatic interaction between clay particles. It is difficult to understand the factors that influence the behaviour of mud and this is what engineers and researchers are still struggling with today. The heterogeneity of the material makes it difficult to predict the consolidation behaviour. The uncertainties in predicting consolidation behaviour induce risks. In a land reclamation project risks are preferably avoided. This research contributes to the understanding and prediction of the consolidation behaviour, so that risks can be reduced. Reducing risks makes building with mud a more appealing solution for land reclamations.

During this research two fields of expertise, fluid mechanics and soil mechanics meet. Fluid mechanics focuses mainly on the flow of water around particles during settling, whereas soil mechanics focuses on consolidated particles that have formed a stiff soil. This research studies the consolidation behaviour of mud and is located at the interface between fluid and soil mechanics. From a fluid mechanics point of view the researches goes down into the vertical direction from water to a more dense slurry. A soil mechanics point of view goes in the upward direction, from very stiff soil to a fluid mud layer.

1.1.1. Case Marker Wadden

Lake Markermeer was created for safety reasons in 1967 by finishing the Houtribdijk that separates lake Markermeer from lake IJselmeer. Before in 1932, the first closure had been constructed to close the Zuiderzee, an inlet of the North sea, to create lake IJselmeer. Figure 1.3 shows the historical situation were de Zuiderzee is a tidal inlet. These closures have created two fresh water lakes. The original plan was to create a polder, the Markerwaard. Due to political discussions the polder was actually never created and the lake remains as created in 1967. Figure 1.4 shows the present day situation of the fresh water lakes in the Netherlands.

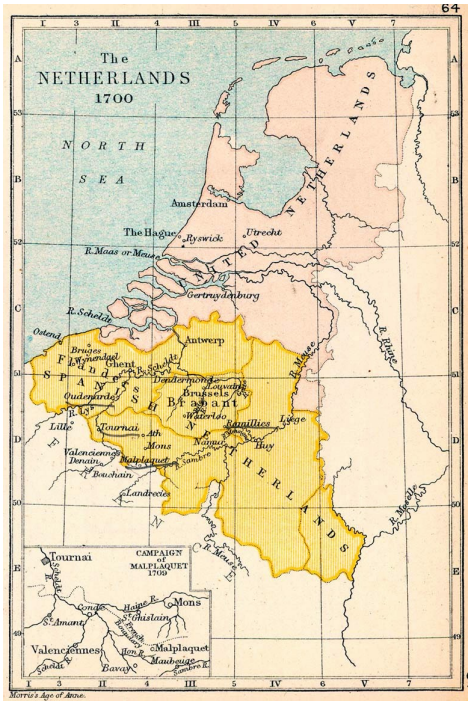

Figure 1.3: Map of the Netherlands in 1700 with the Zuiderzee still present at that time (www.wikipedia.org).

Figure 1.4: Map of the Zuiderzee works were lake IJselmeer and lake Markermeer are created (www.wikipedia.org).

Lake Markermeer serves as an important fresh water basin which is a resource for drinking water and a buffer in case of heavy precipitation or as a resource during drought. The lake Markermeer spans an area of almost 700 km^2 and is a large natural reserve in the Netherlands and protected by Natura 2000 legislations due to its ecological value [Evans, 2012].

However, the lake is presently in a state were the ecological value is low [Noordhuis et al., 2015]. Around the lake dikes were constructed cutting of the flushing mechanism of the lake and removing the soft transitions from water to land. This has lead to an accumulation of fine sediments in the lake and a soft silt layer that has deposited on the bottom of the lake. Wind driven waves can stir up the fine sediment and influence the water quality negatively by increasing the turbidity. Raised turbidity levels decrease the light penetration trough the water, which reduces the quality of life for flora and fauna. Not only the turbidity levels affect the water quality, but also nutrients in the water.

This issue has lead to the ideology of the Marker Wadden. In which 'Wadden' refers to the barrier islands in the Wadden Sea in front of the northern part of the Dutch coastline. The concept of this project is to create wetland by reclamation of small islands to form a archipelago that consists of shallow areas, soft banks and smooth transitions between water and land. This will mainly provide a habitat for flora and fauna and additionally improve the water quality locally.

The Islands will be constructed with resources that are locally available. The initial idea was to remove the top fluffy silt layer from the bottom of the lake to reduce turbidity and use that as a filling material. This has proven to be an unrealistic solution, because of the vast amount of area that has to be dredged to collect enough filling material. The practical solution is to create a silt trap, by dredging a trench of several meters deep and use the dredged Holocene clay from the deeper bottom layer as a filling material. The fluffy silt material that will accumulate over time in the silt trap might have a constructional use in later time.

The final design is presented in figure 1.5. Sand dams provide protection against waves from the governing wind direction and enclose sections were mud can settle and consolidate. Behind the sand dams a marsh-pond habitat is created that is attractive for birds.

Figure 1.5: Design of the Marker Wadden project with a borrow pit in the north and silt trap in the east[Geretsen, 2014]. Sand dams provide protection against wave attack and enclose areas to trap deposited mud. Behind the sand dams a marsh-pond habitat is created that is attractive for birds.

1.2. Problem description

Building the Marker Wadden with soft cohesive sediment poses some challenges. Building with mud is less studied as opposed to building with sand. This traditional filling material is investigated extensively, whereas the properties of soft cohesive sediment or mud as a building material are relatively unknown. The challenge lies in the versatility of the material. Winterwerp and Van Kesteren [2004] stated: 'Mud is a mixture of clay, silt, sand, organic material, water and sometimes gas'. The versatility makes it difficult to predict the behaviour and define material properties.

The consolidation behaviour can be described with material parameters and bed properties. Other researchers, such as Been and Sills [1981] Merckelbach [1999] Berlamont et al. [1993] have investigated specific samples from sights in marine and freshwater environment. But there is not yet an established empirical data base with information about mud, such as the Atterberg limits in soil mechanics for stiffer clays.

A physical understanding of the consolidation behaviour is necessary to build with mud. This understanding is an ongoing process. Two experimental methods are being practiced, first a classic settling experiment, second a more advanced experimental method called a Seepage Induced Consolidation (SIC) test, but there is not yet a clear relation found between these two. Commonly consolidation experiments take much time, because consolidation is a slow process.

The majority of the research was done on low concentration mud suspensions and that has provided useful relations and formulations, although they are mainly empirically derived. In practice low concentration suspension are not handled during land reclamations. A dredging vessel transports a high density mixture of mud and water that is called a slurry. The density of the slurry is beyond a point such that the particles do not settle anymore, this is called the gelling point. The particles form a structure skeleton and the slurry will consolidate after being deposited, without first the settling phase, indicated by phase 1 in figure 1.2. This case in which the initial concentration c_0 of the mud is beyond the gelling concentration c_{gel} will be the main point of interest during this research. Mainly because this is the case in which in practice the slurry will be deposited.

1.3. Research objective

The objective of this research is within the context as sketched in the previous sections. This research investigates the effect of initial concentration on the behaviour of mud. Soft cohesive sediments are dredged and used as building material. To successfully build with mud the final conditions and behaviour should be predicted. The behaviour of mud depends on many initial conditions, such as composition, dynamics when depositing and chemical structure. In this research the focus is on sediment from lake Markermeer and the concentration in which sediment will be deposited. The high initial concentration of deposited sediment will be investigated during this research. These conditions can be modelled physically so that the consolidation behaviour can be studied. The results determine, whether the material parameters, final conditions and consolidation behaviour of the soft mud in lake Markermeer are affected by the initial concentration. The main objective follows:

Determine if the consolidation behaviour is a function of the initial conditions.

1.3.1. Research questions

Research questions are used as a tool to reach the objective of this research. These questions will be answered during the course of this research. The research questions are stated as main questions and sub questions. The main research question follows:

- *Is the consolidation behaviour a function of the initial concentration?*
- *Are the material parameters a function of the initial concentration?*
- *Are the final conditions a function of the initial concentration?*

The main research questions are followed by a set of sub-research questions. These sub-research questions relate more to the practical side of this research and will serve as a guideline to answer the main research questions.

- *Which material parameters are relevant in the consolidation process?*
- *Is there a relation between a classic settling experiment and a Seepage Induced Consolidation test?*

1.4. Research approach

1.4.1. Methodology

This research was started with a literature survey and how this research can provide additional knowledge to the existing research. Secondly, two experimental methods were performed. For the experiments a mud sample is used that was dredged from a borrow pit for the Marker Wadden close to Lelystad. The mud that was collected is a representative sample for this research.

The first experimental method was a series of settling column experiments. The settling column experiments were divided in two cases. The first case is a classic settling column experiment with the initial concentration below the gelling concentration, case $c_0 < c_{gel}$. With the settling curve from these series of experiments and equations described by fractal theory the material parameters can be determined by following the method of Merckelbach and Kranenburg [2004a]. The second case involves high concentration slurries, in which the initial concentration exceeds the gelling concentration $c_0 > c_{gel}$.

The second experimental method is a Seepage Induced Consolidation (SIC) test. This is a state of the art laboratory test that makes it possible to deduce the material parameters for the higher initial concentration mud. The sample is consolidated by applying a load and by inducing seepage on the sample. Material parameters can be determined from this test.

The material parameters obtained from these two methods were later used in a 1-DV model [Winterwerp, 1999]. The 1-DV model produces a density profile, which is an important measure to compare the two experimental methods. Several measurements were performed on the bed from the settling column experiments. The density and the strength of the bed was measured. The density profile derived from the density measurement was compared with the model simulations. How well a simulated profile compares to the measurement is based on the final bed height and the density profile.

The results from these experiments and measurements allow to draw conclusions. These conclusion will answer the research questions. When the research questions are answered the objective of this research is met. The final part of this research includes recommendations for further research and the industry that is active in the field of dredging and land reclamations of mud.

1.4.2. Report outline

The content of this thesis is summarised in this section. In chapter 2 a literature survey is conducted to place this research in perspective. This research follows the fractal theory and this is explained into detail to properly follow the steps in this research. Besides this the, nature of cohesive sediment is explained to understand why this research lies in a different field than the use of sand as a building material for land reclamations.

Chapter 3 describes consist of the methods that apply and the materials that were used. The measuring procedures are explained and how the measuring devices are set-up. In chapter 4 the results are presented, subsequently in chapter 5 the results are discussed. The final chapter consists of the conclusions and recommendations. In this final chapter the research questions are answered and recommendations for future research are stated.

2

Literature survey

In this chapter the existing and relevant knowledge is explored. The composition of cohesive sediment and the nature of the cohesive behaviour is explained first. Secondly is explained how mud behaves as an individual particle and as an aggregated floc. For this self-similarity is assumed, which is described by fractal theory. This research is based on this very influential assumption. Based on this theory the three phases of the settling curve are explained. Next two experimental methods are discussed. The two methods are explained into detail and their limitations are discussed. Finally a discussion on the literature survey is held. This section discusses how this research will add to the existing knowledge.

2.1. Cohesive sediment description

Sediment is a naturally occurring material that is broken down by processes of weathering and erosion [Monroe and Wicander, 2011]. It can be transported by wind, ice, water and the gravitational force acting on the particle. Cohesive sediment is often referred to as mud and consists of a mixture of clay, silt, sand, organic material, water and possible gas. The amount in which these components occur, with chemical, historical and biological factors determine cohesive behaviour of mud. Cohesive behaviour relates to ductile behaviour when the sediment is remoulded [Winterwerp and Van Kesteren, 2004]. Cohesive sediment consists of granular, mineral and organic solids. These three categories will be discussed in the next three sections.

2.1.1. Granular composition

Sediment consists of granular material that settles in water by gravity. The granular size distribution and composition are of great influence on the mechanical behaviour. Clay particles and organic content characterise the liquid phase and determine the cohesive behaviour. The solid phase is characterised by the particle size distribution. Classifications are standardised, such as the Dutch NEN 5104 standard see fig 2.2. The classification is based on the particle diameter and does not tell the difference in composition, it only refers to size. This means that a size fraction can contain organic and mineral material.

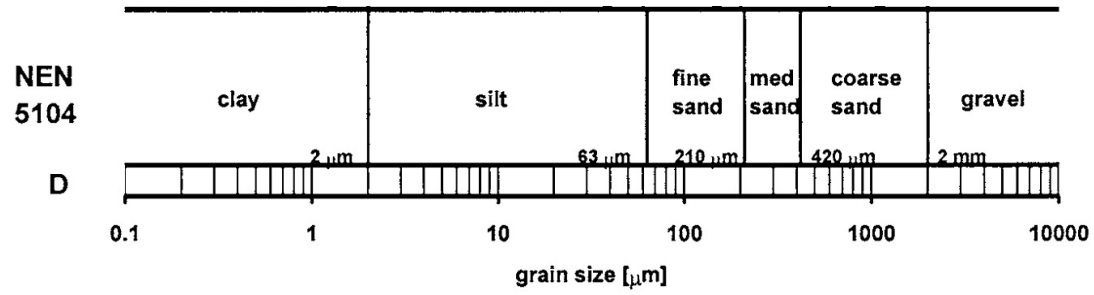

Figure 2.1: NEN 5104 standard adapted from Winterwerp and Van Kesteren [2004]. This standard only refers to particle size, not to composition.

The size classification consists of clay, silt, sand and a gravel fraction. In practice the gravel fraction is assumed to be absent in mud. A common statement is that particles smaller than $63\mu m$ is called the mud

fraction. So mud consists according tho the NEN standard of clay and silt. In the clay fraction there is a sub fraction that is not displayed in figure 2.2, this is the colloidal fraction. Brownian motion, random motion of particles suspended in fluid, causes this fraction to not settle in the water column. The size of these particles are 0.1 μm or less. This fraction is mainly of influence for the behaviour of clay particles while in suspension in the water column.

2.1.2. Mineral composition

A major component in the mineral solids fraction are silicates. Silicates are minerals that vary in composition and structure. Most common silicates in the silt fraction ($2\mu m < d < 63\mu m$) are quartz and feldspar. The clay fraction ($d < 2\mu m$) mainly consists of clay minerals, such as kaolinite, illite, smecite and chlorite. These clay minerals are usually found in a marine environment. No clay minerals are present in the sand fraction ($d > 63\mu m$). Clay minerals are responsible for the cohesive behaviour of mud. This is partially attributed to the size and the plate like shape of a particle. Due to this shape particles have a very high specific surface area and an electrical charge distribution. Depending on the type of silica, they can build up and form a certain layer structure of a clay mineral. Several types of structures exist and have their own properties.

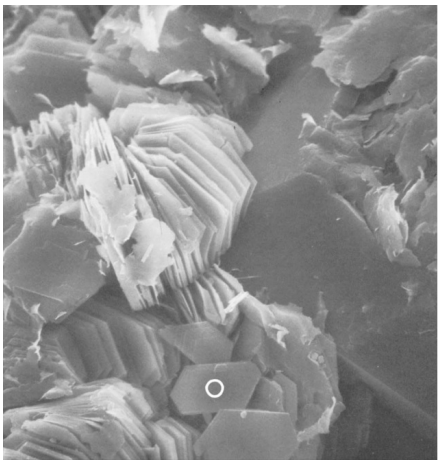

Figure 2.2: Kaolonite mineral structure [Welton, 1984]. Particles have a plate like shape with a high specific surface area and an electrical charge distribution.

2.1.3. Organic composition

Organic matter mainly consist of organic polymers. In mud organic matters exists of particulate organic matter and dissolved organic matter. Organic matter can be produced within the sediment by biological processes, or has an origin from outside of the sediment. When organic matter is deposited from the water column fermentation processes can occur, producing methane and carbon dioxide. As a result gas is trapped in the bed. In this research the main focus is not on organic matter, but the influence of organic matter is of great impact on the behaviour of mud, mainly on flocculation in the water column, which will be explained later. Thus, the influence of organic matter will be taken into account.

2.1.4. Cohesive behaviour of sediment

Clay particles have the peculiar property to form flocs. In a suspension of mud the clay particles form a very open structure with a high water content, called a floc. Flocs are characterised by a very high water content 80-98% by volume [Winterwerp and Van Kesteren, 2004]. These open structures form a clay-water matrix that traps other particles in it, such as silt and possible sand. In marine environment almost all cohesive sediment is flocculated. This phenomenon is the main difference between sand and mud. Therefore, the behaviour of mud varies very much from that of sand.

The cohesive behaviour of sediment can be attributed to the clay particles present. Only 5-10% of clay is needed for the sediment to start showing cohesive behaviour. Besides the clay particles mineralogy, chemical properties and organic matter play an important role in the cohesive behaviour of mud.

2.2. Flocculation

Mehta [2014] defines a floc as: an agglomeration of a large number of primary clay mineral particles cohering by attractive electrochemical forces, biochemical bonding or binding. This process, agglomeration of primary particles, is called flocculation. The following section will elaborate on mud flocs and how they are formed.

2.2.1. Fractal structure of flocs

Self-similarity is a conceptual model that describes the hierarchal structure of flocs. Krone [1986] was one of the first to investigate the mud flocs as a function of their structure. He stated the hierarchal structure from clay particle to flocculi, which become full flocs due to their cohesive nature. The aggregated flocs form larger aggregates and so on [Kranenburg, 1994]. Treating mud flocs as self-similar fractal structures at a hierarchy of scales is a well accepted assumption and from now on referred to as fractal theory. Figure 2.3 describes the conceptual model of the fractal structure of a mud floc.

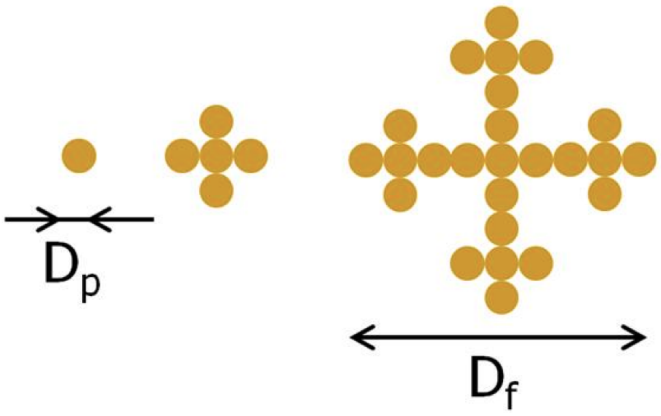

Figure 2.3: Conceptual description of the fractal theory, where D_p= primary particle diameter and D_f= floc diameter [Winterwerp and Van Kesteren, 2004].

Fractal theory implies that various physical processes follow power-law behaviour. Properties of cohesive sediment follow this behaviour, such as permeability and effective stress. As an approximation mud flocs are treated as self-similar fractals. However, Kranenburg [1994] suggested to treat mud in the bed also as these self similar structures, but it is not realistic to assume that they would form exact self-similar aggregates.

The fractal dimension n_f describes the self-similar fractal as a growing object. Here formally defined as [Kranenburg, 1994]:

$$n_f = \frac{number\ of\ primary\ particles}{linear\ length\ of\ aggregate} \tag{2.1}$$

The range of the fractal dimension is $1 \leq n_f \leq 3$. Measurements of the fractal dimension of flocs in the water column give values between $n_f = 1.4-2.2$ [Winterwerp and Van Kesteren, 2004]. This represents fragile flocs to strong flocs. Within the bed the fractal dimension is much higher, $2.6 < n_f < 2.8$ [Kranenburg, 1994]. When a bed is completely consolidated the fractal dimension approaches 3.0. The range of these values show that when the fractal dimension increases the size of a floc decreases. Later the fractal dimension will prove to be a very important parameter, as it highly influences the behaviour of mud.

2.2.2. Aggregation and break-up processes

Flocculation is a process of aggregation and break-up. Aggregation is the result of coherence of particles after collisions. Aggregation and break-up is caused by shear stress and collisions. Flocculations is governed by three main processes [Winterwerp and Van Kesteren, 2004]:

- Brownian motions
- Differential settling velocities
- Shear stress

When there is a balance between aggregation and break-up an equilibrium is reached, this is called flocculation time. In general it is accepted that in coastal environments the first two processes are negligible and the governing process for flocculation is shear stress caused by turbulence. In figure 2.4 the relation between floc size, shear rate and suspended sediment concentration is shown. Shear rate is a surrogate of shear stress. What can be seen is that floc size increases with shear rate, until it reaches a maximum, then floc size decreases with increasing shear rate as flocs break-up more than there is aggregation of flocs.

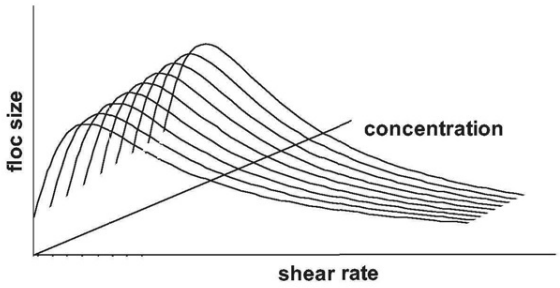

Figure 2.4: Three-dimensional relationship between floc diameter, suspended sediment concentration and shear stress [Winterwerp and Van Kesteren, 2004]

2.3. Settling and consolidation

In a controlled environment, such as a laboratory, where sediment settles only sedimentation takes place. In nature sedimentation and erosion occurs. For this research erosion is of less interest, because the experiments will be performed in a closed column. When a slurry is deposited in an enclosed area to create wetland erosion also does not play a roll. The main focus of this research is on the settling and consolidation of cohesive sediment. In this section the settling and consolidation of mud is explained. Figure 2.5 shows a schematic overview of a settling curve. The figure indicates three phases. In the following sections these phases will be explained. First the settling of a single floc is explained, this is to later understand how a group of flocs settle during the hindered settling phase. In consolidation phase I all particles have settled and the mud bed that is formed is consolidating under its own weight. In consolidation phase II the deformation in the mud bed is small until it reaches an equilibrium height.

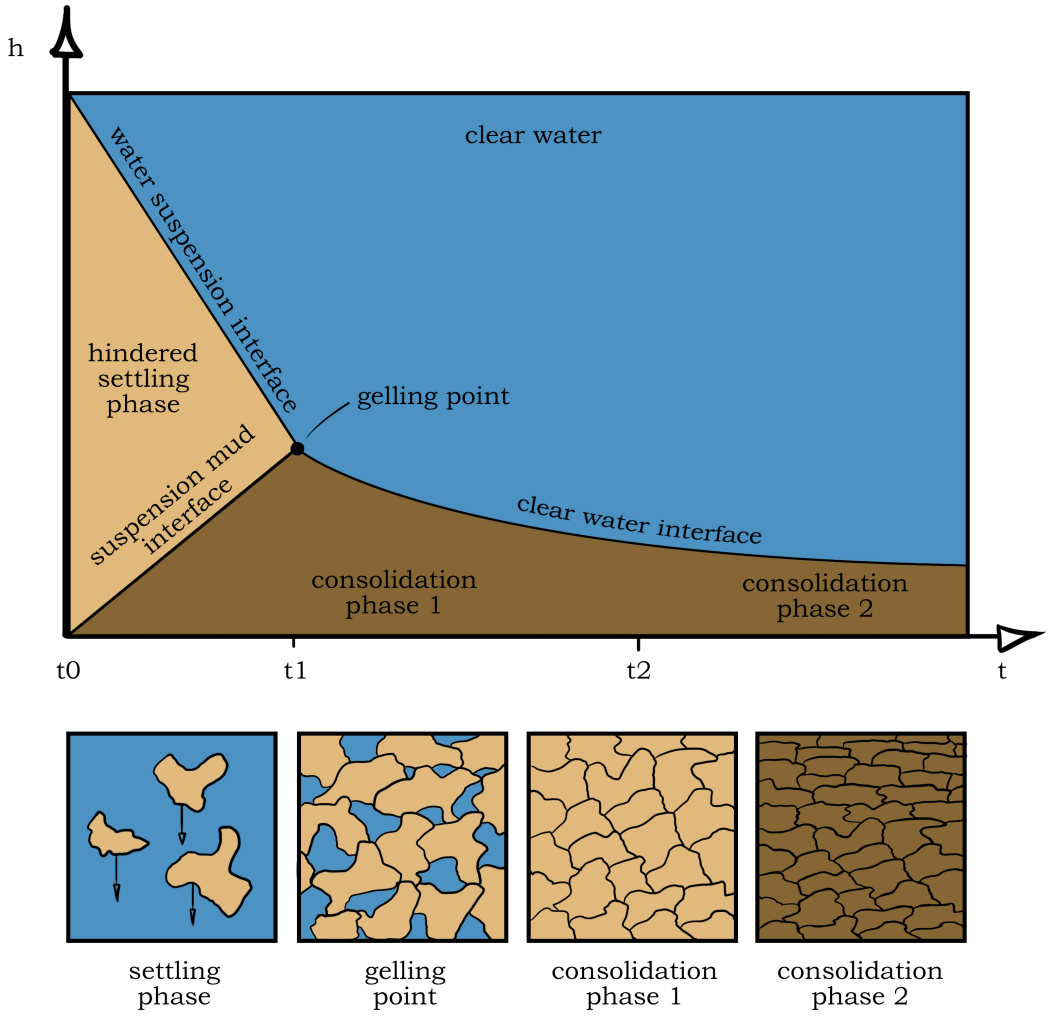

Figure 2.5: Schematised settling curve with three indicated phases and the indicated interfaces. The lower boxes illustrate schematically how the mud flocs are behaving in the water column or as a bed.

2.3.1. Single floc settling in still water

To derive the settling function for a floc it is inevitable to first look at the settling of a single spherical particle. Stokes wrote a formulation where a Euclidian particle settles in a viscous fluid. Which follows:

$$w_s = \frac{(\rho_s - \rho_w) g D^2}{18\mu} \tag{2.2}$$

Stokes derived this classic formulation by assuming that the drag force is in equilibrium with the gravity force, given that they work in opposite direction. This formulation applies for large particles. However, settling of mud flocs cannot be described with the stokes law. To account for the size, shape and density of the floc a different formulation applies [Winterwerp, 2002].

$$w_{s,r} = \frac{\alpha(\rho_s - \rho_w)g}{18\beta\mu} D_p^{3-n_f} \frac{D^{n_f-1}}{1+0.15Re_p^{0.687}} \tag{2.3}$$

In this formulation α and β are shape parameters, D_p is the diameter of the primary particle and Re_p is the particle Reynolds number. When a particle is massive and spherical ($\alpha = \beta = 1, n_f = 3$) equation 2.3 approaches equation 2.2, Stokes' law.

2.3.2. Hindered settling

When a mud suspension is settling individual flocs will start to hinder each other along the way down. When the concentration is high enough a traffic jam of mud flocs occurs. The effective settling velocity is influenced by the presence of the particles hindering each other. This is called hindered settling. This is expressed in the following function [Dankers and Winterwerp, 2007]:

$$w_s = w_{s,0} \frac{(1-\phi)^m(1-\phi_p)}{1+2.5\phi} \tag{2.4}$$

With:
w_s = effective settling velocity [m/s]
$w_{s,0}$ = settling velocity individual mud floc [m/s]
ϕ =volumetric concentration [-]
ϕ_p= volumetric concentration of primary particles [-]
The exponent m accounts for possible non-linear behaviour of the return flow behind the particle. With this factor it is possible to account for hydrodynamic effects. In practice m is chosen at 2.

2.3.3. Gelling concentration

When a single floc in a fluid settles it follows the adapted stokes law equation 2.3. When the concentration of particles becomes higher particles start hindering each other during settling. When the concentration increases further particles tend to become in contact with each other and build up a framework of particles. At this point the framework starts to build up some strength. This is the transition point from a water supporting system to a sediment supporting system. This transition point is called the gelling point[Dankers and Winterwerp, 2007]. The gelling concentration is the concentration of the suspension at that transition point. The gelling point marks the transition between settling and consolidation.

The gelling concentration (c_{gel}) can be determined by three methods. The first method is to measure the concentration of the settled bed with a conductivity probe as done by Dankers [2006]. A second method is to determine the gelling concentration based on the mass balance of the settling profile and from average concentrations above and below the lower interface. This method gives an approximation of the gelling concentration when there is no consolidation. The third method is by setting up two settling column experiments with different initial concentrations. By measuring the velocity of the lowering interface $w_{s,0}$ and using equation 2.4, this gives two equations and two unknowns w_s and c_{gel}. So this system of equations can be solved. The first two methods are not very practical. The third method is commonly used and applied during this research.

2.3.4. Self-weight consolidation

After sedimentation, when flocs have settled and they form a framework of particles, the flocs that arrived first are squashed by the ones on top. When mud flocs settle they form a skeleton that is highly compressible [Been and Sills, 1981]. Pore water is redistributed out of the space between the flocs. This rearranging of particles and fluid is called self-weight consolidation, because this process is driven by the weight of the flocs itself. Self-weight consolidation is characterised by vertical deformations of the bed.

Self-weight consolidation is commonly expressed by the Gibson equation [Gibson et al., 1967]. To get a better understanding of self-weight consolidation it is useful to examine the equation. It follows:

$$\frac{\partial\phi}{\partial t} + \left(\frac{\rho_s - \rho_w}{\rho_w}\right)\frac{\partial k\phi^2}{\partial z} + \frac{\partial}{\partial z}\left(\frac{k\phi}{g\rho_w}\frac{\partial\sigma'}{\partial z}\right) = 0 \tag{2.5}$$

With:
t = time [s]
ϕ = volumetric concentration [-]
ρ_s = density of solids [kg/m^3]
ρ_w = density of water [kg/m^3]
k = permeability [m/s]
σ' = effective stress in vertical direction [Pa]

To solve this equation expressions for permeability and effective stress are needed. Just as the Gibson equation permeability and effective stress are a function of the void ratio e or can be expressed as a function of ϕ. The third term of the Gibson equation represents the consolidation coefficient c_v. During this research large strains are common. When strains are small the consolidation equation reduces to the classic Terzaghi principle [Winterwerp and Van Kesteren, 2004]. The Terzaghi principle follows:

$$\sigma = \sigma' - u \tag{2.6}$$

In which u is the pore water pressure and σ is the total vertical stress.

2.3.5. Material functions from fractal theory

The formation of a bed from a mud suspension can be expressed in three phases. These three distinguished phases are shown in figure 2.5. These phases are: hindered settling phase, consolidation phase I and consolidation phase II. When a suspension of mud is set to rest over time these phases can be observed. Merckelbach and Kranenburg [2004a] proposed a method to determine material parameters by monitoring the mud-water interface during these three phases over time. Figure 2.5 shows a schematic settling curve in which the hindered settling phase ends at the gelling point and the consolidation phases starts. These phases will be elaborated separately in the following sections. Here the link between settling, gelling concentration and self-weight consolidation is explained.

Hindered settling phase

Hindered settling is explained in section 2.3.2. During this phase a mud-water interface is observed moving down in vertical direction following a linear trend, unless segregation of particles occur. When the flocs form a framework of particles there is no more settling and the gelling concentration is reached. This is indicated by the gelling point in figure 2.5. If segregation of particles occurs the linear trend ends in a smooth curve. This is due to the different settling velocities of the particles with different sizes that induce the segregation.

Consolidation phase I

During the first consolidation phase a network structure of flocs builds up. Here the mud builds up strength even though it is very small, assumed to be negligible. This phase is characterised by permeability. The Gibson equation then reduces to this:

$$\frac{\partial \phi}{\partial t} + \left(\frac{\rho_s - \rho_w}{\rho_w} \right) \frac{\partial k \phi^2}{\partial z} = 0 \tag{2.7}$$

This simplification can be made assuming that the small stresses that are building up are balanced by water flowing out of the bed. Evaluating this equation the change of volumetric concentration over time is determined by the permeability of the bed. To solve the simplified Gibson equation the material function or constitutive relation for permeability should be known. Merckelbach and Kranenburg [2004b] parameterised permeability as follows:

$$k = K_k \left(\frac{\phi_p^m}{1 - \phi_s^{sa}} \right)^{-\frac{2}{3-n_f}} \tag{2.8}$$

Where ϕ_s^{sa} is the volume concentration of solids in the sand fraction, ϕ_p^m the volumetric concentration of solids in the mud fraction and K_k is the permeability coefficient. It is difficult to measure the permeability directly, but Merckelbach and Kranenburg [2004b] proposed a method to derive the permeability. They propose a method where the K_k can be derived by measuring the moving mud-water interface over time. The procedure is to plot the height of the mud-water interface against time and fit the function 2.9 to obtain n_f and K_k.

$$h(t) - \zeta_s = \left(\frac{2-n}{1-n}\right)^{\frac{1-n}{2-n}} (n-2) K_k \left(\frac{\rho_s - \rho_w}{\rho_w}\right)^{\frac{1}{2-n}} t^{\frac{1}{2-n}} \tag{2.9}$$

Here ζ_s is the Gibson height accounting for sand, ζ_m is the Gibson height accounting for mud, h is the height of the mud-water interface and $n = 2/(3-n_f)$. Equation 2.9 is a power law function and plotted on double logarithmic paper it will appear as a straight line.

Consolidation phase II

During the second phase the deformations in the bed are small. This phase is characterised by the effective stress that develops in the consolidating bed. After some time the final consolidation height is reached and the bed has reached its equilibrium state. In this phase the full Gibson equation 2.5 will be solved. Just as in consolidation phase I to solve the full Gibson equation the permeability and effective stress relations, material functions, should be known. The material function for effective stress in vertical direction follows:

$$\sigma' = K_p \left(\frac{\phi_p^m}{1-\phi_s^{sa}}\right)^{\frac{2}{3-n_f}} - K_{p,0} \tag{2.10}$$

Here $K_{p,0}$ account for creep effects and K_p is the coefficient for effective stress. In the following derivations the effect of creep is neglected. The final bed height is used in equation 2.11 to obtain K_p from the following function[Merckelbach and Kranenburg, 2004b]:

$$h_\infty = \zeta_s + \left(\frac{n}{n-1}\right) \frac{K_p}{g(\rho_s - \rho_w)} \left(\frac{g(\rho_s - \rho_w)}{K_p} \zeta_m\right)^{\frac{n-1}{n}} \tag{2.11}$$

When consolidation has reached equilibrium and parameters n_f, K_k and K_p are derived the consolidation parameter can be determined. This consolidation coefficient is denoted with c_v in soil mechanics, but in this research also as Γ_c. The formulations follows:

$$\Gamma_c = c_v = \frac{2}{3-n_f} \frac{K_k K_p}{g\rho_w} \tag{2.12}$$

If the fractal descriptions for permeability, effective stress and the consolidation coefficient are substituted into the Gibson equation, an advection-diffusion equation can be derived. Rewriting the Gibson equation into an advection-diffusion equation makes it easy to solve. The advection-diffusion equation that is simplified for sediment without sand is derived by substituting equation 2.12 into equation 2.5 and it follows:

$$\frac{\partial \phi}{\partial t} + \left(\frac{\rho_s - \rho_w}{\rho_w}\right) \frac{\partial k\phi^2}{\partial z} + \Gamma_c \frac{\partial^2 \phi}{\partial z^2} = 0 \tag{2.13}$$

2.4. Cohesive sediment experiments

To model consolidation of cohesive sediment a classic approach is to use a simple settling column. This is done by many researchers in the past, such as Been and Sills [1981], De Lucas Pardo [2014], Merckelbach [2000], Townsend and McVay [1990] . These columns are easy to set up and conditions can be controlled precisely in a laboratory environment. Settling column experiments can give a good understanding of the consolidation behaviour of mud, while they also have their limitations. In this section the settling column experiments are described. Also common measurement techniques and alternative methods will be discussed.

2.4.1. Considerations of a settling column experiment

A settling experiment models the sedimentation of cohesive sediment for a harbour, estuary or a land reclamation. Usually sediment and water from a particular site is chosen for the experiment. A predetermined concentration of sediment in water is put into the column. The suspension is gently mixed, then the experiment starts. While monitoring the moving mud-water interface in the column settling and consolidation behaviour is observed. With the methods from Dankers [2006] and Merckelbach and Kranenburg [2004b] material properties and parameters can be determined. They are derived from the lowering mud-water interface and power law curve fitting, as explained in section 2.3.

Settling column size

Settling columns vary in size mainly determined by the type of measurements that are needed. A glass or acrylic transparent column of 1L is sufficient [Hendriks, 2016]. Columns of a larger size allow for pore pressure measurements, drain pipe, Beeker sampling for density measurements [Meshkati Shahmirzadi et al., 2015] etc. During experiments in small settling columns wall effects start to play a role. A smaller diameter results in a slower consolidation rate. This is proven by Meshkati Shahmirzadi et al. [2015], during this research two column diameters 5.7 cm and 16 cm were compared. In literature columns with a diameter smaller than 10 cm are referred to as small by Johansen [1998], Lintern [2003] and Merckelbach [1998a]. Van Mieghem et al. [1997] recommends to use a column width of 10 cm for consolidation experiments, while Berlamont and Van Goethem [1984] had found no difference in the relative residual height in experiments done in columns of 10 cm and 100 cm. However, Michaels and Bolger [1962] showed a study in which flocculated kaolin suspensions was carried out in 4.8 cm diameter columns. From previous research it is noted that wall effect is something to take into account, but during this research due to practicality standard 2L columns are used with a diameter of approximately 8 cm.

The duration of consolidation is proportional to the height of the bed square ($t \propto h^2$). Migniot and Hamm [1990]showed that a higher initial deposit height does not significantly influence the density profile of the consolidated bed. Therefore, it is assumed that the column height of an experiment will not influence the results of a settling column experiment. For this research it is very convenient to use small columns as time is limited for this research. The consolidation time for sedimentation experiments in 2L columns can take from 3 weeks up to two months.

Initial concentration effect

By varying the initial concentration of the sediment mixture in the settling columns the influence in the behaviour of the mud can be observed. A concentration below the gelling point starts as a suspension and follows the settling curve from figure 2.5 from the beginning. The suspension settles, forms a bed, and then consolidates. For concentrations above the gelling point the starting point along the settling curve is different. Because the concentration is higher than the gelling concentration ($c_0 > c_{gel}$), the mixture is expected to directly start consolidating. The starting point lies somewhere beyond the gelling point or c_{gel} in figure 2.5. The consolidation behaviour of a a high concentration mixture is to a certain extent an unknown. This is one of the main topics in this research.

2.4.2. Seepage Induced Consolidation

Seepage induced consolidation test or SIC test is a state of the art measuring device that can perform more direct measurements on soft sediment samples. The test lets sediment consolidate by applying a load and permeability is measured at different stages by a pore water flow trough the sediment. This device is based on the method developed by Liu and Znidarčić [1991]. Permeability can be determined over a range of different void ratios with the constant flow rate and the law of Darcy. During the SIC test the flow rate through the sample are small, because the sample should not be disturbed to much. High, long and sudden flow rates trough the sample might induce a clogging filter. This highly influences the test results. A clogging filter is a common phenomenon in soil mechanical tests such as the oedometer test.

For deriving permeability and effective stress the data is fitted to power law functions. There are two sets of power law functions that are used. First method uses the material parameters from the fractal theory, in which ϕ is a function of σ' and k. In the second method σ' and k are a function of e. The material functions for the fractal theory are here repeated:

$$\sigma' = K_p \left(\phi_p^m\right)^n \tag{2.14}$$

$$k = K_k \left(\phi_p^m\right)^{-n} \tag{2.15}$$

The material functions for the second method follow:

$$\sigma' = \left(\frac{e}{A_p}\right)^{\frac{1}{-B_p}} - Z \tag{2.16}$$

$$k = A_k e^{B_k} \tag{2.17}$$

In which A and B are coefficients of the power law model and Z is coupled to the void ratio at zero effective stress. Typical values for the parameters are shown in table 2.1

Table 2.1: Typical values for parameters in the material functions 2.16 and 2.17.

A_p	B_p	Z	A_k	B_k
1-100	0.1-1	0-10^{-5}	10^{-8}-10^{-14}	1-10

The two methods use a different variables, volumetric concentration ϕ and void ratio e. Volumetric concentration ϕ is commonly used in fluid mechanics and void ratio e is used in soil mechanics. The volumetric concentration and void ratio are inversely related. When data is processed with these two methods what can be observed is that the angle of the fitted power law is influenced by choosing ϕ or e. This is because a dense packing of particles is expressed as a lower void ratio e and a high volumetric concentration ϕ. The choice of method, ϕ or e, influences the accuracy of the angle of the fitted equation. This is explained in figure 2.6. The accuracy of the angle of the fitted equation is affected, because higher values of the variable ϕ or e have a bigger influence on the angle of the fit than the lower values.

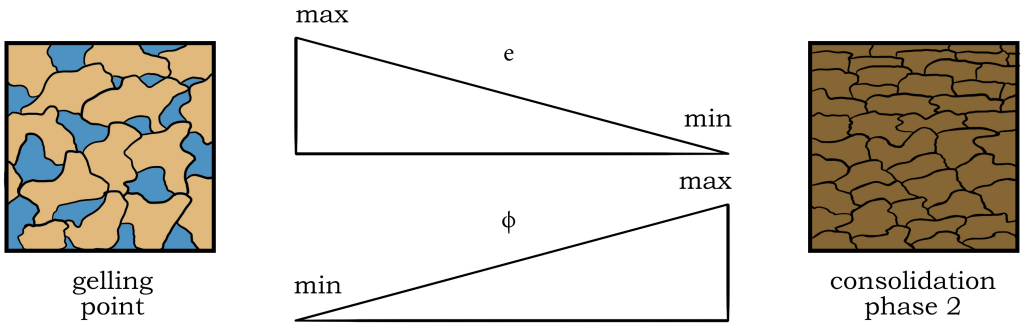

Figure 2.6: Schematised relation between volumetric concentration ϕ and void ratio e. A loose packing of mu at the gelling point has a high e and a low ϕ, a dense packing of mud during consolidation phase II has a high ϕ and a low e.

2.5. Discussion on literature survey

In the literature survey in the previous sections theory and research is described. The theory mainly describes the settling and consolidation of low concentration suspensions ($c_0 < c_{gel}$). In this research the objective is to determine if consolidation behaviour is a function of the initial conditions. The main focus will be on high concentration mud mixtures, so when the initial concentration is beyond the gelling concentration ($c_0 > c_{gel}$). This section will describe how this research will add to the existing knowledge. The assumptions made in the following section is based on the fractal theory (JC Winterwerp, personal communication, September 19, 2016).

2.5.1. Case low initial concentration

Many researchers, such as Dankers and Winterwerp [2007], De Lucas Pardo [2014], Merckelbach and Kranenburg [2004b] and many others were investigating the behaviour of a mud suspension below the gelling concentration, case $c_0 < c_{gel}$. The approach is to follow the settling curve trough each phase, i.e. hindered settling, consolidation phase I and consolidation phase II, as described in section 2.3. From the complete settling curve and the equations from section 2.3 the parameters: c_{gel}, n_f, K_k and K_p for the material can be determined. The most important material parameters are n_f, K_k and K_p from which the permeability and effective stress can be derived. Permeability and effective stress are the most influential factors on the settling and consolidation of mud.

When the material parameters for the bed are determined from a settling column experiment, when the case $c_0 < c_{gel}$ holds, they will always have the same order of magnitude. What this means is that the material parameters are independent of the initial concentration. It has already been proven that multiple settling column experiments with different initial concentrations will result in consolidated beds with material parameters in the same order of magnitude. In summary: the material parameters do not depend on the initial concentration for case $c_0 < c_{gel}$.

2.5.2. Case high initial concentration

When the initial concentration of a water-sediment mixture exceeds the gelling concentration, case $c_0 > c_{gel}$ the material parameters cannot be determined from the settling curve and by the equations 2.4, 2.9 and 2.11, if the Fractal approach is followed. When mud has a high initial concentration ($c_0 > c_{gel}$), it is assumed there is no hindered settling phase. The mud exceeds the gelling concentration. Therefore, it is assumed mud starts consolidating directly, because there is no complete settling curve, which follows the three phases: settling, consolidation phase C-I and consolidation phase C-II. Thus, the material parameters cannot be obtained from the settling curve and by using the equations described by the fractal approach.

When the fractal approach cannot be utilised to obtain the material parameters a different method is needed. For the case $c_0 > c_{gel}$ it is not yet proven if the material parameters are dependent or independent of the initial concentration and how the initial concentration influences the consolidation behaviour. This means that the statement from the previous section for this case ($c_0 > c_{gel}$) cannot be made, but leads to the question: are material parameters, consolidation behaviour and final conditions dependent on the initial concentration?

Answering this question is the objective of this research. It is possible to derive the material parameters from a SIC test. This makes it possible to compare material parameters from a settling column experiment and a SIC test and prove one of the statements above.

3

Methods

This chapter presents an overview of the performed experiments and work methods. The laboratory experiment are conducted at the Deltares FCL lab in Delft. Table 3.1 gives an overview of the experiments performed.

Table 3.1: Overview of experiments

Experiment	Output	Method
Settling column $c_0 < c_{gel}$	$w_s, c_{gel}, n_f, K_k, K_p$	[Dankers and Winterwerp, 2007] [Merckelbach and Kranenburg, 2004a]
Settling column $c_0 > c_{gel}$	settling curve	
Vane test	c_u, τ_p	[ASTM, 1989]
UHCM	density profile	[Berkhout, 1994]
SIC test	$\phi - k, \phi - \sigma'$	[Merckelbach and Kranenburg, 2004b]
SIC test	$k - e, e - \sigma'$	[Liu and Znidarčić, 1991]

The first set of experiments that will be discussed are the settling column experiments. The data can be evaluated with the provide method from Dankers and Winterwerp [2007] and Merckelbach and Kranenburg [2004a]. The results will give the material parameters of the consolidated bed. Further it is explained how the measurements were performed on the bed. In table 3.1 can be seen that the method from Dankers and Winterwerp [2007] and Merckelbach and Kranenburg [2004a] is not applicable for the case $c_0 > c_{gel}$, because the sediment does not follow the complete settling curve from settling to consolidation. The material parameters were determined by a different method. The sediment that is consolidated in settling column experiment was used for the SIC tests. From this test permeability and effective stress can be determined.

3.1. Materials

3.1.1. Markermeer clay

The sediment used in this experiment is from lake Markermeer taken from a borrow pit close to Lelystad. The sediment comes from the Holocene clay layer that lies meters below the bed of the lake. The sediment was taken during a field campaign prior to this research. For further reading about the properties of the sediment the reader is referred to [Barciela Rial, 2015]. The measured particle density for the sieved Markermeer sediment is $\rho_s = 2540$ kg/m^3.

For this experiment only the fraction smaller than 63 μm from the bulk sediment was used. The bulk sediment was sieved in three steps. Sieves with the mesh width of 1 mm, 0.5 mm and 63 μm were used. The sieving was done by diluting the sediment with water from lake Markermeer to let silt and clay particles pass through the sieve. The sieving process agitates the flocs in such a way that is is assumed that every floc is broken. After the sieving the sediment was rested for 9 days to let the particles aggregate into flocs again. After sieving the water content was derived to prepare high concentration mud in the columns. The sediment preparation had a duration of two weeks, in which the sediment spent time at room temperature (20-22 °C). The sediment for column c_0=400 g/l was treated differently: it was dried in an oven at 35 °C for 24

hours to reduce the water content. This was necessary because otherwise due to the water content the initial concentration of c_0=400 g/l could not have been prepared. Due to this extra pretreatment the experiment in this particular column started 1 day later.

3.1.2. Markermeer water

Water used to make the mud mixture in the columns and to dilute the sediment for sieving originates from lake Markermeer. It was taken from a field campaign prior to this research and stored in dark and cool storage room. Markermeer water is used to keep the same porewater chemistery as in natural environment. Measurements show that the water is almost pH neutral and has a low salinity level. Table 3.2 compares the Markermeer water with water taken from the sample in bulk and after sieving. The water taken from the sample shows a higher conductivity. This indicates the presence of salinity in the sediment from historic saline deposits in the Holocene clay layer.

Table 3.2: Measurements from water samples

Sample	Markermeer water	Water from bulk sample	Water from sieved sample
pH [-]	7.77	8.04	7.40
Measured at temp. [°C]	12.3	11.8	11.6
Conductivity [μS/cm]	923	1300	1302
Measured at temp. [°C]	9.0	8.1	7.6

3.2. Settling column experiments

The settling column experiments were performed in 2L columns. These columns were approximately 40 cm high and 8 cm inner diameter. Nine columns were set up with systematic varying initial concentration c_0. This experiment was divided in two cases. The first case is the low initial concentration experiment, case $c_0 < c_{gel}$. The second case is the high initial concentration experiment, case $c_0 > c_{gel}$. For case 2 $c_0 > c_{gel}$ two columns are duplicated to serve as control experiments. The initial concentrations for case $c_0 < c_{gel}$ are chosen in such a way that they were below the expected gelling concentration, but sufficiently high to clearly detect an interface. In Figure 3.1 the experimental set-up is shown with corresponding initial concentration. In the figure two separated cases and the duplicate experiments are shown. The columns were placed in a room with the lights switched on throughout the day and where the temperature ranges from 22 -24 °C.

The mud-water interface was monitored with a camera, Canon EOS70D. During the settling phase of the experiment a picture was taken every minute. During the consolidation phase the interval between pictures gradually decreased, varying from one per five minutes up to one per day. From this data settling curves were derived.

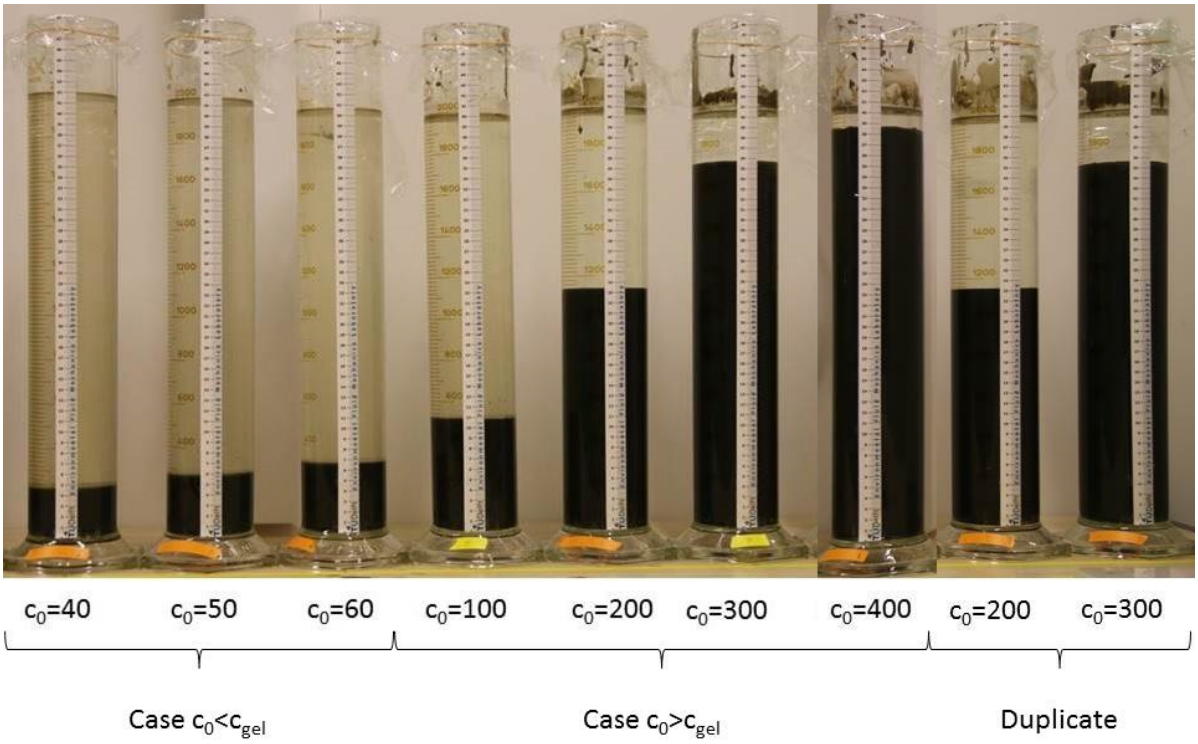

Figure 3.1: Settling column experiment set-up with indicated initial concentrations. Time of the experiment is t=8 days, except for column c_0 = 400 g/l t=7 days.

3.2.1. Sediment pretreatment

The prepared sediment had 9 days to rest after it was sieved prior to the start of the experiment. During this period supernatant water is extracted to reduce the water content and the sediment has the opportunity to flocculate. The water content was determined, by drying a subsample in an oven at 105°C to prepare the water-sediment mixture with a specific concentration per column. The sediment-water mixtures are rested in the columns for one more day to let it homogenise with respect to temperature and let flocs build up.

3.2.2. Experimental procedure

To start the experiment each column is gently mixed with a mixing rod in vertical direction. Each column is mixed with the same amount of strokes during the same amount of time following a protocol. This is done to make sure each column gets the same treatment for reliable and reproducible results.

At specific intervals a photo is taken from the columns. From these photos the mud-water interface is detected by a Fortran script. The Fortran script gives as output for each photo a pixel value per column. The pixel value is related to a reference in the picture. From this reference the height of the mud-water interface

can be derived by the measuring tape visible on the columns. To derive the height of the mud-water interface the amount of pixels per length is calibrated for each column individually. Individual calibration per column is needed due to varying distance from each column to the lens of the camera. During this experiment the camera moved a number of times. New calibration was needed for every time the camera moved to keep the results accurate.

After approximately 7 days the interface was determined by hand from the photos using Photoshop. These two methods of detecting the interface introduced two different errors. The first method detects the interface by a difference in brightness of the pixels. This is a systematic approach that has a small error which is related to the resolution of the picture. The pictures from the experiment have a resolution of 3888x2592. It is assumed this error is negligible. The second method detects the interface by eye while the picture is zoomed in at 600 %. But assuming the error is in the order of one or two pixels, this means that the error is less than a millimetre. This is a reasonable error to produce reliable results.

3.3. Vane test

The strength of the sediment was tested by measuring the undrained shear strength or remoulded strength with a rheometer. When a sample is tested, this is done in-situ, so that they are disturbed as little as possible.

3.3.1. Experimental set-up

The material that will be tested has a low strength. The measurements device is able to measure in Pascal, which are low values for measuring strength. In classic soil mechanics soil strength is expressed in kPa. The rheometer is equipped with a range of shear vanes for different soil strengths. Each soil has an expected range of strength and needs for testing the right vane. When the strength of soil is measured in-situ in a settling column an extension shaft is available to reach the soil.

The test method consists of inserting a vane in a undisturbed sample and rotating it at a constant rate to determine the torque required to cause a cylindrical surface that is sheared by the vane. The torque is converted to a shearing resistance of the cylindrical surface area. The torque is measured by torque transducer that is calibrated and attached to the vane. The set-up of this vane test is a rheometer Haake M1500 with an extension shaft, see figure 3.3.

3.3.2. Experimental procedure

Prior to inserting the vane in the settling column the water is removed by a peristaltic pump. A minimal amount of water remained on top of the bed. This could not be removed without disturbing the sample. In other cases when the sample is not in a settling column this is not necessary.

The vane is inserted into the bed until a given depth that is marked on the shaft of the vane. This gives the same depth at which each measurement is done. For columns with a bed height higher than a few centimetres multiple measurements are possible, by lowering the vane further. For a good measurement an undisturbed volume is needed. As a rule of thumb 5 cm should be between each measurement in the vertical direction and the diameter of the sample should be twice the diameter of the vane. When the test is started the vane rotates at a constant rate for 2 full rotations.

A vane test measures shear strength. This can be expressed as a peak strength τ_p and an undrained shear strength c_u. An example of a vane test measurement is shown in figure 3.2. Which clearly shows a peak and an average value between the first and the second rotation. The procedure is described in more detail in the ASTM [1989].

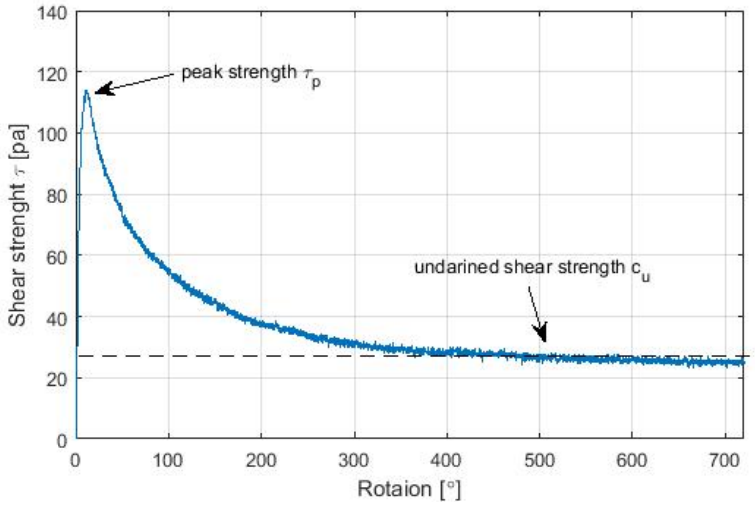

Figure 3.2: Strength measurement from a vane test in column $c_0 = 60 g/l$.

Figure 3.3: Vane test set-up rotovisco measuring system Haake M1500.

3.4. Density profile

The Density profile of a consolidated bed can be derived in two ways. First, by measurements with ultra-sonic sound that are taken from the consolidated bed from settling columns experiments. Second, by a 1-DV (one dimensional vertical) model [Winterwerp, 1999] that was further developed at Deltares, which solves the 1 dimensional vertical classic consolidation equation (the Gibson equation). Later these two methods can be compared. This section elaborates on how the experimental measurement is done.

3.4.1. Experimental set-up

The density measurements were done with an instrument developed by Deltares. This measuring device is called the Ultra-sonic High Concentration Meter (UHCM). The UHCM measures high concentrations of solid particles in liquids. Figure 3.4 shows the set-up of the UHCM measuring in the column. The measurement is based on the transmitting and receiving sound between two acoustic transducer. The acoustic principle is based on measuring the transmission of acoustic energy (ultra sound) through the measuring volume between the transmitter and the receiver probes [Berkhout, 1994].

3.4.2. Experimental procedure

Before starting the measurement the device is calibrated in a sediment-water mixture of which the density is known. It is important to use the same material, as particle size may influence the measurement. For the measurement the probes are lowered in the consolidated bed. A measurement was taken at a set interval over the vertical. This will give a density over height, a density profile. For a valid measurement the volume around the measurement volume should be sufficient. From experience and according to Van Kessel and Kranenburg [1996] measurements close to the bottom and near the surface give an unrealistic output. Also air or gas trapped inside the sediment will lead to an unrealistic output. An example of a typical density profile is shown in figure 3.5. A consolidated bed is expected to show a density profile with a convex shape. The density ranges typically between 1200 to 1400 kg/m^3 for a consolidated bed [Been and Sills, 1981]. In appendix C a more detailed description of the measurement procedure and data processing is given.

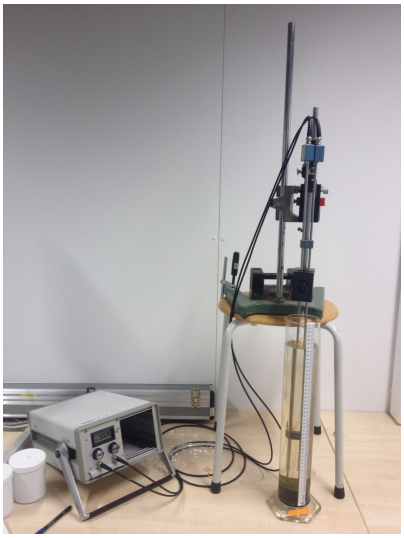

Figure 3.4: Density measurement set-up with UHCM.

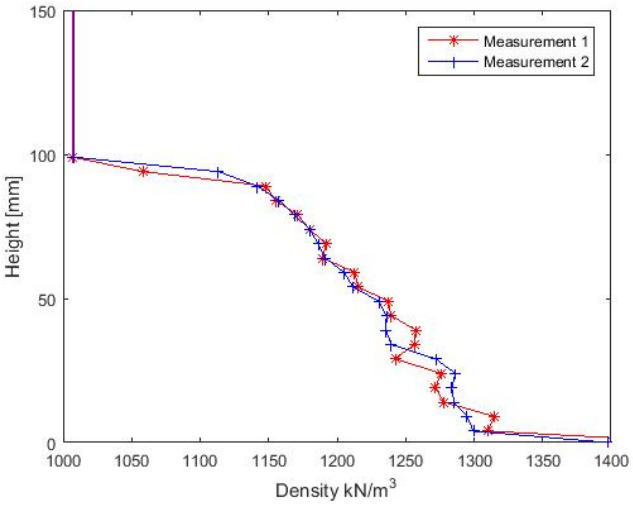

Figure 3.5: Density profile from column $c_0 = 100g/l$. Measurement 1 and 2 were done in the same column. The measurements show similar density profiles, which indicates the UHCM produces repeatable results assuming the sediment is homogeneously distributed in the horizontal plane.

3.5. Seepage Induced Consolidation (SIC)

The SIC test is an experimental method that is used to determine the consolidation characteristics of soft sediments like slurry. For these tests very soft and compressible materials are used with a low permeability. In this section the focus is on how the test was prepared and conducted, not on the physics.

3.5.1. Experimental set-up

A SIC test device is available at the Deltares FCL lab, see figure 3.6. It consist of a triaxial cell that holds the sample and a flow controlled piston pump. The triaxial cell is connected to a piston that can accurately apply a load and register the settlement of the sample. The piston pump generates an accurate controlled downward flow rate trough the sample, this causes a suction force. The pressure difference between the suction and the cell pressure is the differential pressure that is monitored during the test. When a load is applied the sample will consolidate by expelling pore water out trough the top of the sample. Reference is made to the publications of Liu and Znidarčić [1991] and Znidarčić et al. [2011] for a more detailed explanation.

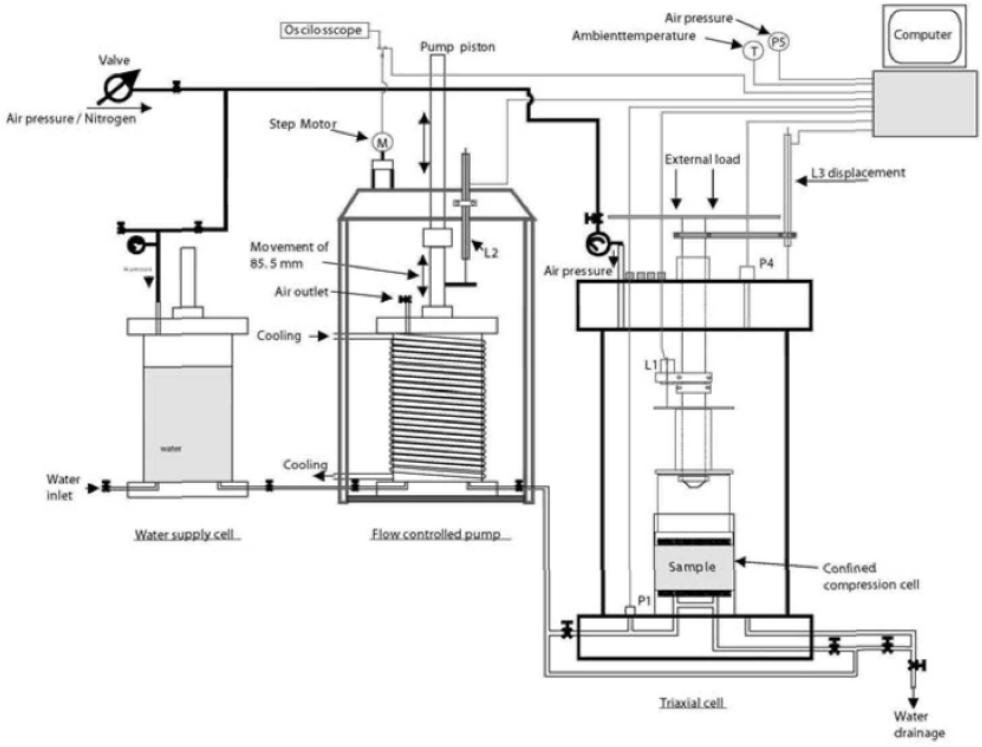

Figure 3.6: SIC test set-up at Deltares

3.5.2. Experimental procedure

A SIC test consists of inducing consolidation and permeability steps on a sample. The consolidation steps and permeability steps are listed in table 3.3. These settings for each step form a guide line for each test, but due to unforeseen circumstances such as, a jamming filter stone and high pressure drops, can be altered. The consolidation is undrained from the bottom, so that a pressure difference can be measured. The sample is submerged in water in the triaxial cell to extrude air during the permeability steps. Consolidation is induced by applying a load subsequently followed by a permeability step induced by a constant suction.

When the load is applied and the pressure is stabilised or after a set time period the sample has reached equilibrium settlement. Hereafter the permeability step is conducted by imposing a short suction, which induces a pressure increase, followed by a relaxation phase where the pressure reaches equilibrium again. During a permeability step the external load is maintained. When the pore water pressure reaches equilibrium a next permeability step can be carried out. This procedure is followed until the force limit is reached. For more accuracy in some steps multiple permeability steps were done. Figure 3.6 shows a schematised set-up of the SIC device. It shows the external load being applied and the suction imposed from bottom of the sample.

The sample that is used in the SIC tests has its origin from the settling column experiments. When the settling columns experiments are finished, the bed has reached equilibrium, the sediment from the bed is put into the SIC device. First, the water on top of the bed is removed from the columns as described in section 3.3. Then, the remaining sediment is transferred to a container in which it is mixed gently to homogeneous the sample. It is assumed that making the sample homogenise also removes gas trapped in the sediment. Then the sediment is put into the sample holder ring of the SIC device. After the sample is placed in the ring and left to rest for three days. Then the triaxial cell is closed and the measurement can start. From the remaining sediment in the container the water content is determined by drying a subsample in an oven at 105 °C to derive the void ratio.

After the SIC test the sample is taken out of the sample holder ring. The void ratio of the sample is determined by two methods. The first method involves the height of the sample that is derived from the settlement during the SIC test and the initial void ratio, which is known. From the initial void ratio and the final sample height the final void ratio can be determined. In the second method the void ratio is determined by drying a subsample in an oven at 105 °C. The difference between the outcome can be caused by the presence of gas in the sample, which was produced during the SIC test.

The height and weight is measured and the water content is determined. From these two measurements it is possible to determine if there was gas produced in the sample. When there is a difference in void ratio at the end of the SIC test determined by drying the sample in an oven at 105 °C and measuring the height of the sample, this would suggest there is gas in the remaining voids.

Multiple SIC tests were carried out. The sediment that goes into the sample ring is originating from the settling column experiment, with initial concentrations c_0 = 200 g/l, c_0 = 300 g/l and c_0 = 400 g/l. The SIC tests will be referred to as SIC200, SIC300 and SIC400, respectively. The number in this notation refers to the initial concentration of the settling column experiment. The sediment from settling column with $c_0 = 100 g/l$ was not suitable for a SIC test. Because there wasn't enough sediment to fill the sample holder ring.

Table 3.3: Load and permeability step settings for SIC tests

Phase	Load	Load	Discharge
	[N]	[Pa]	[mm^3/s]
Consolidation	2	112	
Permeability			0.5
Permeability			1
Consolidation	5	279	
Permeability			2
Permeability			1
Consolidation	10	558	
Permeability			1
Permeability			1.5
Consolidation	50	2809	
Permeability			1
Permeability			1.5
Consolidation	100	5584	
Permeabilty			1
Permeability			1.5
Consolidation	500	27920	
Permeability			1.5
Permeability			1
Permeability			0.2
Permeability			0.3
Consolidation	900	50257	
Permeability			0.3
Permeability			0.2
Permeability			0.15
Permeability			0.1

4

Results

The results of the settling column experiment, strength measurements, density measurements and SIC tests are presented and analysed in this chapter. The settling column experiments are divided in two cases. First, the classic case $c_0 < c_{gel}$, second the high initial concentration case $c_0 > c_{gel}$. The measurements in the bed by the vane test and the UHCM are displayed subsequently. The density measurement with the UHCM are compared with results from the 1-DV model. Followed by the results from the SIC test.

4.1. Settling column experiments for low initial concentration

Processed data from experiment $c_0 < c_{gel}$ generates settling curves figure 4.2. The first part of the curves present the hindered settling phase. The first part of the curve is characterised by the effective settling velocity w_s and the gelling concentration c_{gel}. Figure 4.1 gives an overview of the settling curve and the hindered settling phase. The hindered settling phase starts at $t = 0$ and ends $t = t_c$. At this moment the bed reaches the gelling concentration.

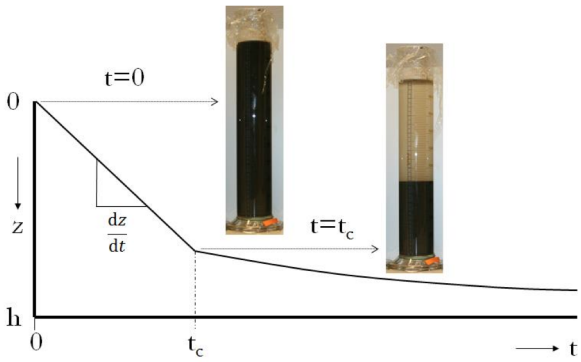

Figure 4.1: Schematised settling curve with indicated hindered settling phase with picture of a settling column that indicates the phase of the experiment from Winterwerp and Van Kesteren [2004] adapted by Hendriks [2016].

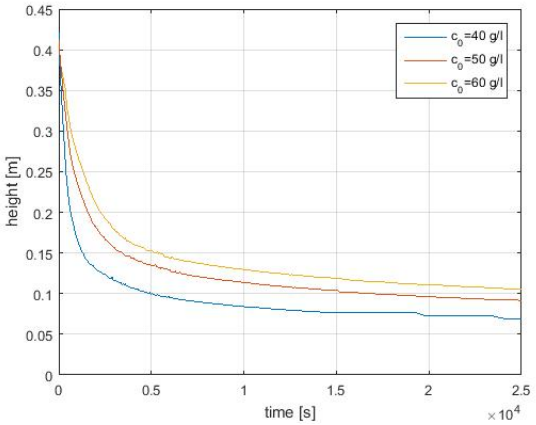

Figure 4.2: Settling curves from experiment case $c_0 < c_{gel}$.

The effective settling velocity is determined from the hindered settling phase by taking the derivative. Assuming this part of the curve is linear, this is indicated by the dz/dt term in figure 4.1.

4.1.1. Qualitative findings

The settling interface follows the same behaviour as a classic sedimentation consolidation experiment [Merckelbach and Kranenburg, 2004a]. An interface is seen moving downward, while the water above the interface is turbid. This low turbidity is present for approximately two days before a clear water interface develops. This

suggests that the sediment has a second interface that is lowering due to the presence of another sediment size fraction. This fraction has a smaller particle diameter and has a lower settling velocity. Many size fractions are present in the sediment. These fractions are responsible for the smooth transition from settling phase to consolidation phase that is observed in figure 4.3. In theory a clear transition should be noticed this is schematised in figure 2.5.

After three days the top layer of the bed develops a grey layer. This is an oxic layer developing on the anoxic settled bed [De Lucas Pardo, 2014]. After approximately two weeks a green layer started developing on top of the oxic layer. It is assumed that this is biofilm growing on top of the sediment. Also green material is suspended in the clear water and attached to the wall of the column. Around the fourth week of the experiment red colouring can be seen especially in the columns with $c_0 > c_{gel}$ columns. This oxidation of iron compounds present in the Markermeer sediments. This results in an interface that is not completely straight, but gives a wiggly interface. That may influence the accuracy of reading the interface measurements.

4.1.2. Effective settling velocity

The measured effective settling velocities range from 0.1 mm/s to 0.4 mm/s. The effective settling velocity decreases with increasing initial concentration. The hindering effect is clearly observed. For a higher concentration the effective settling velocity decreases considerably. See table 4.1 for effective settling velocities determined from figure 4.3.

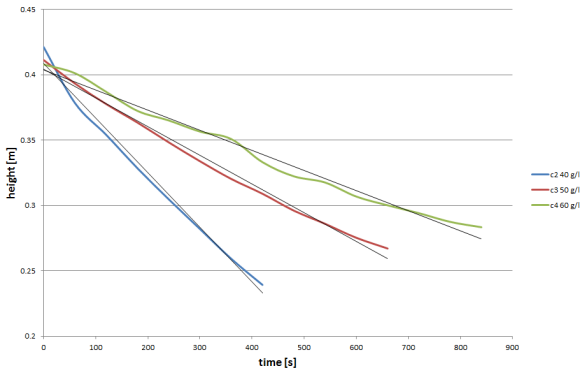

Figure 4.3: Effective settling velocity from mud-water interface measurements settling column experiments.

Table 4.1: Effective settling velocities for initial concentration from settling column experiments.

c_0 [g/l]	w_s [mm/s]
40	0.4
50	0.2
60	0.1

4.1.3. Gelling concentration

The gelling concentration can be determined with the effective settling velocity w_s and the equation 2.4 [Dankers and Winterwerp, 2007]. This is done by solving a system of three equations and two unknowns. This resolves in three values for the gelling concentration with accompanying settling velocity of a single floc in still water $w_{s,0}$. These values are presented in table 4.2 and compared with results from other research that used sediment from lake Markermeer. Comparing the values for c_{gel} with other research, the result seems plausible. For further calculations in this research a $c_{gel} = 80$ g/l is used.

Table 4.2: Gelling concentrations from settling column experiments and comparable research.

c_{gel} [g/l]	$w_{s,0}$ [mm/s]
79.8	3.76
80.2	3.63
81.0	3.55
82.0 [Barciela Rial, 2015]	-
70.0 [De Lucas Pardo, 2014]	0.6
85.0 [Hendriks, 2016]	-

4.1.4. Consolidation

After the settling phase the consolidation phases begin. The first consolidation phase C-I, governed by permeability and secondly the consolidation phase C-II, governed by effective stress. Applying fractal theory the

permeability coefficient K_k is characterised by phase C-I and the effective stress coefficient K_p by phase C-II. The fractal dimension n_f is characterised by both phases C-I and C-II. This is clarified in figure 4.4.

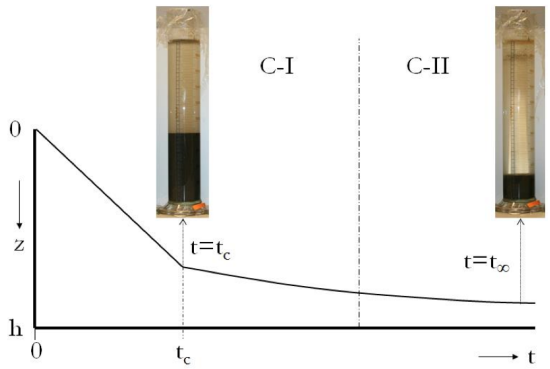

Figure 4.4: Schematised settling curve with indicated consolidation phase with picture of a settling column that indicates the phase of the experiment from Winterwerp and Van Kesteren [2004] adapted by Hendriks [2016]

Consolidation phase C-I

Parameters n_f and K_k are determined by curve fitting equation 2.9 to the mud-water interface measurements from phase C-I. The challenge is to find the start and end of this phase, as the transition is not so clear. To find the transitions the settling curve is plotted on double logarithmic scale (figure 4.6). A bend in the settling curve indicates the end of the settling phase. A power law relation appears as a straight line on double logarithmic scale. This describes phase phase C-I, see figure 4.5. When the interface measurements start to move away from the fitted straight line, this indicates the transition from phase C-I to phase C-II.

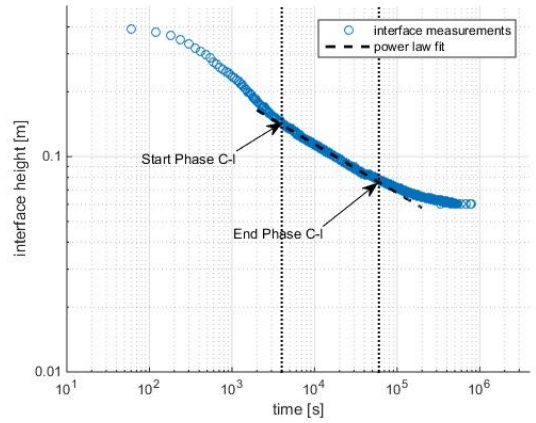

Figure 4.5: Curve fit equation 2.9 to interface measurements settling column experiment column $c_0 = 50$ g/l

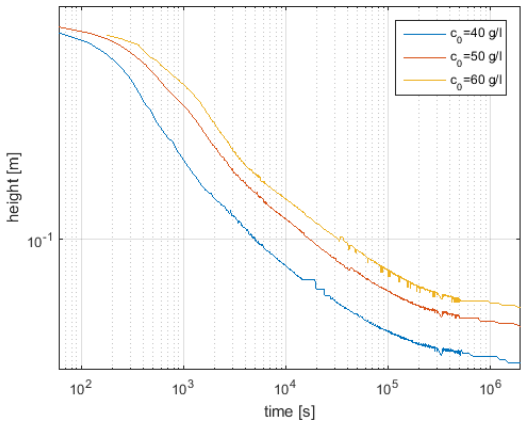

Figure 4.6: Settling curves for case $c_0 < c_{gel}$ plotted on logarithmic scale

Fitting the curve to the interface measurements of each settling column experiment ($c_0 < c_{gel}$) the following results are found, see table 4.3. The fractal dimension that is found correspond to the range $n_f = 2.6 - 2.8$ given by Winterwerp and Van Kesteren [2004]. The K_k parameters for varying c_0 are in the same order of magnitude. This indicates a valid result.

Table 4.3: Permeability coefficient and fractal dimension determined from phase C-I of the settling curve.

$c_0[g/l]$	$K_k[m/s]$	n [-]	$n_f[-]$
40	1.23E-13	6.6454	2.70
50	2.18E-13	6.4074	2.69
60	1.74E-13	6.6316	2.70

Consolidation phase C-II

The consolidation phase finishes with phase C-II. The bed shows only small deformations. This phase is characterised by the effective stress parameter K_p. This can be calculated with equation 2.11 [Merckelbach and Kranenburg, 2004a] when the bed has reached equilibrium. The final bed height was measured at t=67 days. This bed height is reached earlier, but the equilibrium bed height is assumed when the interface did not move for seven days. The measured final bed height and effective stress parameter are listed in table 4.4

Table 4.4: Effective stress coefficient determined from the final bed height of the settling column experiment.

c_0 [g/l]	h_∞ [m]	n_f [-]	K_p [Pa]
40	4.3	2.70	1.12E+07
50	5.3	2.69	8.10E+06
60	6.2	2.70	1.26E+07

Consolidation coefficient

The consolidation coefficient c_v or Γ_c is calculated with equation 2.12. The result is listed in the table 4.5

Table 4.5: Consolidation coefficient determined from settling column experiment.

c_0 [g/l]	h_∞ [cm]	n_f [-]	Γ_c [m^2/s]
40	4.3	2.70	0.93E-09
50	5.3	2.69	1.15E-09
60	6.2	2.70	1.51E-09

4.1.5. Summary of the low initial concentration settling experiment results

This section gives a summary of the results from the previous sections. The results are summarised in table 4.6.

Table 4.6: Results from settling column experiment case $c_0 < c_{gel}$ summarised.

c_0 [g/l]	w_s [mm/s]	$w_{s,0}[mm/s]$	K_k [m/s]	n_f [-]	h_∞ [mm]	K_p [Pa]	Γ_c [m^2/s]
40	0.4	3.76	1.23E-13	2.70	43	1.12E+07	0.93E-09
50	0.2	3.63	2.18E-13	2.69	53	0.81E+07	1.15E-09
60	0.1	3.55	1.74E-13	2.70	62	1.26E+07	1.51E-09

4.2. Settling column experiments with high initial concentration

The settling curves of the settling column experiment $c_0 > c_{gel}$ are shown in figure 4.7. The initial concentration is above the gelling concentration, so the fractal theory cannot be utilised. It is not possible to determine material parameters of the bed with the interface measurements as done for the settling columns with $c_0 < c_{gel}$.

Figure 4.7 shows the settling curves of five columns. The columns with the initial concentration c_0 = 200 g/l and c_0 = 300 g/l have a duplicate, to check if the experiments are repeatable. In figure 4.7 the settling curves of column c_0 = 200 g/l, c_0 = 300 g/l and the duplicates follow similar trends quite accuratly. Minor differences can be accounted for by different diameter of the columns and error in reading the interface. This shows that the experiment is repeatable and the protocol is followed correctly.

Peculiar behaviour can be seen in the first phase of this settling curve. A linear decrease of the settling curve is seen. This would suggest a hindered settling phase. However, in this case the hindered settling phase is skipped because the particles already form a supporting structure ($c_0 > c_{gel}$). Consolidation starts at the beginning of the experiment as the gelling concentration is already exceeded. This explained in figure 2.5. Consolidation behaviour follows an exponential decreasing trend which is expected here.

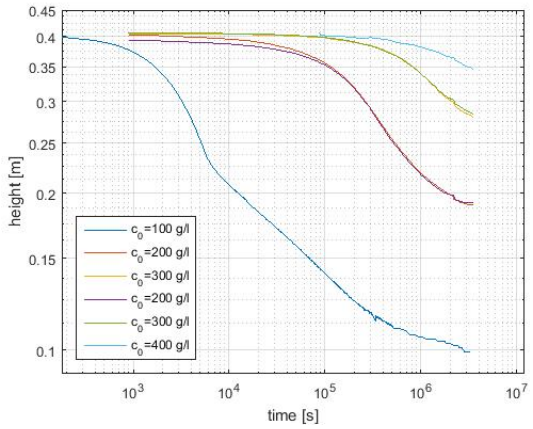

Figure 4.7: Settling curves for case $c_0 > c_{gel}$ plotted on double logarithmic scale.

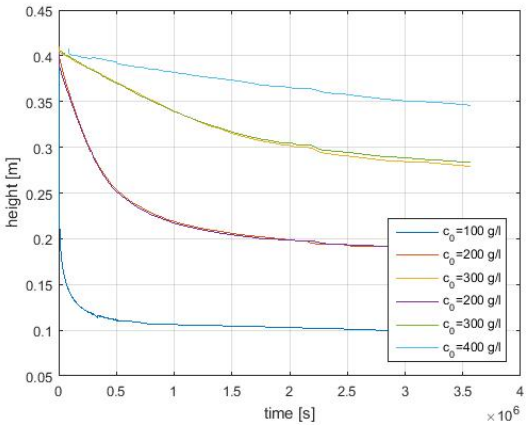

Figure 4.8: Settling curves for case $c_0 > c_{gel}$ plotted on linear scale.

4.3. Undrained shear strength

When consolidation was finished in the settling column experiment the undrained shear strength of the bed is determined. A shear vane was used to test the peak strength τ_p and the remoulded strength or undrained shear strength c_u of the bed. The vane is put directly into the settled bed in the column. Following the procedure as described in section 3.3. The settings for the used rheometer are in table 4.7.

Table 4.7: Settings vane test Haake M1500

Variable	Setting
Rate of rotation	0.5 rpm
Rotation	3
Duration	6 min
Vane	FL100
Vane diameter	16.5 mm
Vane height	22.1 mm
Vane depth	30.0 mm

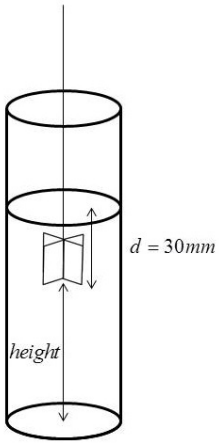

Figure 4.9: Schematised vane measurement in column. The depth of the van during the first measurement is 30mm. Further measurement are done at different heights indicated in table 4.9

4.3.1. Strength measurement

The obtained values from the vane test are presented in table 4.3.1 The measurements show similar results. The measurements are all taken at the same depth 30 mm below the surface (figure 4.9), hence the similar strength of the soil. It is expected that columns c_0 = 40 g/l, c_0 = 50 g/l and c_0 = 60 g/l have similar material properties, see figure 4.10, so the strength should be similar. For columns c_0 = 100 g/l, c_0 = 200 g/l, c_0 = 300 g/l and c_0 = 400 g/l it is the objective of this research to determine if the bed of the columns will have similar properties, regardless of the initial concentration. The results show that the strength is similar for the case $c_0 < c_{gel}$ and $c_0 > c_{gel}$ when column c_0 = 400 g/l is not taken into account. The results from case $c_0 > c_{gel}$ show similar undrained shear strength except for the column c_0 = 400 g/l. This value is rather high comparing to the other columns. The reason for this might be the case that the initial concentration of 400 g/l is a transition point of initial concentration in which this high concentration mud starts to build up considerable strength. The results from table 4.9 also show that the strength over height increases more than

other columns. Another explanation is that locally the bed was not homogeneously distributed. Locally the bed could have been stiff for an unknown reason and therefore the strength was considerably higher. The strength of the bed is twice as high in comparison with the other beds. However, the reason for this high strength is unknown. The measured strength from the column $c_{0,2}$ = 300 g/l also show a considerable lower value. Note that duplicate experiments are indicated with the number 2 in the subscript. This measurement was done at a different time than the other the measurements. The measurement in this column was done later, because the measuring device was not available. During this period the equipment was moved to another location. The equipment is rather old and sensitive, moving the equipment might have influenced the calibration of the torque transducer. What also was observed during measurements was that when an other electrical device was plugged into a socket in the same room this produced noise in the measurement. The sensitivity of the measuring device might be the explanation for the strength of $c_{0,2}$ = 300 g/l to deviate.

What should be kept in mind that the values are measured in Pa, which are rather low values. It is difficult to measure this accurately with the vane test. This is evident from the strength measured in column $c_{0,2}$ = 300 g/l and column c_0 = 400 g/l. So the accuracy of this test method in this range is debatable. From the measurement in columns $c_{0,1}$ = 300 g/l and $c_{0,2}$ = 300 g/l the error of the measurement is assumed to be ± 18 Pa.

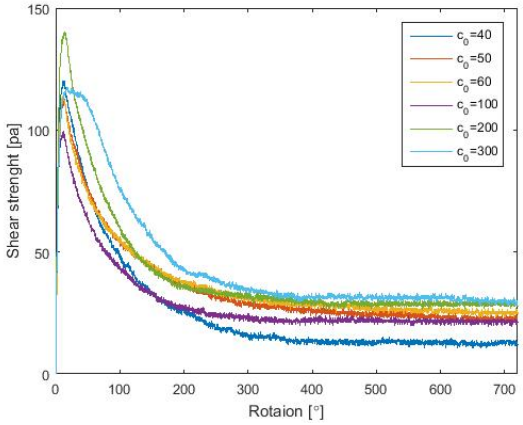

Figure 4.10: Vane tests results. Only the first two rotations are plotted in this graph for a better presentation of the peak.

Column c_0 [g/l]	τ_p [Pa]	c_u [Pa]
40	120.0	13.6
50	112.2	25.8
60	114.0	28.2
100	98.4	22.8
200	139.2	27.0
200 duplicate	138.1	30.2
300	115.2	31.8
300 duplicate	94.2	13.8
400	309.0	76.2

Table 4.8: Vane test results settling column experiments.

For the results from table 4.3.1 and fig 4.10 the vane is lowered to a specific depth that is kept constant for each test. On the device a marking makes it possible to lower the van in the same position. The vane is lowered 30 mm into the sediment. This constant measuring depth makes it easier to compare measurements between columns. However, not comparable with the study of Markermeer sediment by Hendriks [2016], who performed measurements at varying depths depending on the height of the bed.

4.3.2. Vane test at different depths

In the settling column experiment case $c_0 < c_{gel}$ the height of the bed was sufficiently high to perform multiple vane tests over depth. The vane was first lowered 30 mm into the bed, measuring from the lowest point of the vane to the surface. The results of these vane tests are presented in table 4.3.1. After the first vane test at the surface the vane was lowered 5 or 10 cm for the next measurement. Table 4.9 show the remoulded strength determined by the vane test at a given height in the column. These results show an increase in strength while decreasing in height in the column.

Table 4.9: Vane tests in columns at variable heights. Note that the duplicate settling columns are here denoted by the number 2 in the subscript. The results from column $c_{0,2} = 300$ g/l are considerably lower comparing to column $c_{0,1} = 300$ g/l. An explanation for this is that the equipment was moved from one location to another prior to this measurement which might have influenced the calibration of the torque transducer.

$c_0 = 400$		$c_{0,1} = 200$		$c_{0,2} = 200$	$c_{0,1} = 300$		$c_{0,2} = 300$	
height [mm]	c_u [Pa]	height [mm]	c_u [Pa]	c_u [Pa]	height [mm]	c_u [Pa]	height	c_u [Pa]
309	77	159	27	30	249	31	245	14
259	104	109	66	76	149	81	195	29
209	130	59	95	122	49	122	145	70
159	168						95	83
109	186						45	102
59	193							

From the increasing strength over a varying height in the column the fractal dimension can be derived. The remoulded shear strength is determined from a measuring volume. This measuring volume has an average density, derived from measurements in section 4.4, from which an average $\bar{\phi}$ can be determined. When the c_u is plotted over ϕ on double logarithmic scale equation 4.1 can be fitted to the data. From the slope of the curve the fractal dimension can be derived $n = 2/3 - n_f$. The remoulded strengths from the sediment in columns $c_{0,1} = 200$, $c_{0,2} = 200$, $c_{0,1} = 300$, $c_{0,2} = 300$ and $c_0 = 400$ are presented in figure 4.11. By curve fitting equation 4.1 [Kranenburg, 1994] to the data, shown in figure 4.12, the parameters A and n_f are determined.

$$c_u = A\left(\phi_s^m\right)^{\frac{2}{3-n_f}} \tag{4.1}$$

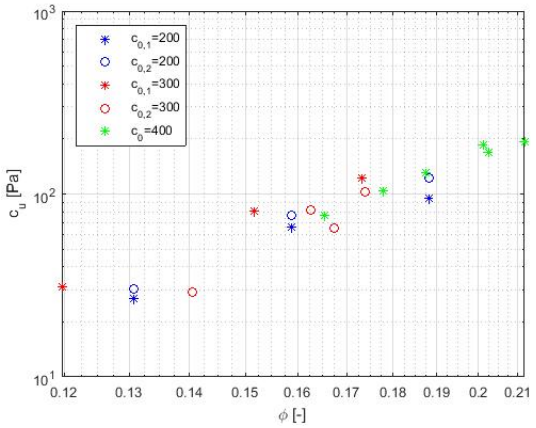

Figure 4.11: Shear strength measured at variable depths plotted over $\bar{\phi}$. In the figure the star and circle marker should be close for each measured strength. The columns with $c_0 = 200$ g/l show resemblance. The columns $c_0 = 300$ g/l show little resemblance in this plot. Column $c_0 = 400$ g/l has no duplicate.

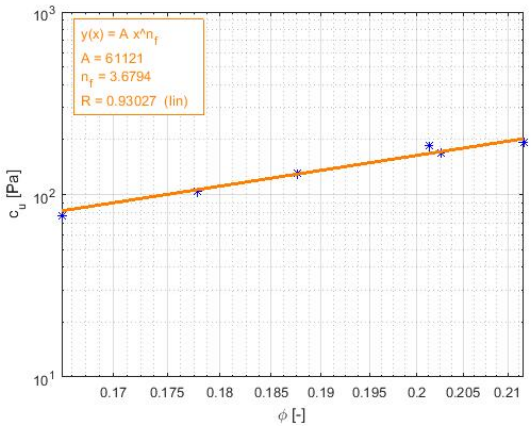

Figure 4.12: Parameters A and n_f obtained by fitting equation 4.1 to the data from column $c_0 = 400$ g/l.

In table 4.10 the parameters A and n_f for each column are presented. What is expected is that the fractal dimension should be similar from the result of the settling column experiments. So the obtained fractal dimension in table 4.10 are expected to be close to 2.70. However, this is not the case for these results. An explanation for these lower fractal dimension can be ascribed to the strength measurement. The rheometer at the Deltares FCL has a fixed rotation speed. The rotation speed has an effect on the result of the strength measurement. A high rotation speed resolves in a high peak strength and a low undrained shear strength. Therefore, these results resolve in a lower fractal dimension. This explanation can be validated if the measurements are repeated in a similar settling column experiment with a vane test at a lower rotation speed. Due to this questionable low strengths and large measuring error, the conclusions in this research will not be based on this data.

Table 4.10: Obtained parameters by curve fitting equation 4.1 ($\bar{\phi} - c_u$) to the data from vane tests and settling column experiments.

Column	A [Pa]	n_f [-]
$c_{0,1} = 200$	34224	2.42
$c_{0,2} = 200$	79991	2.48
$c_{0,1} = 300$	89115	2.47
$c_{0,2} = 300$	99236	2.49
$c_0 = 400$	61121	2.46

4.4. Density profile

The density profile was derived in two ways. First, by measuring with the UHCM as described in section 3.4 and second, by a 1-DV model, which solves the Gibson equation.

4.4.1. Density measurement

The density measurements in the columns were performed on t=67 days of the settling column experiment. The final bed height of the experiment is reached at this time. In each column one or two measurement were performed. Except for column c_0 = 300 g/l, because the sediment from this column was already used for a SIC test. In column c_0 = 40 g/l, c_0 = 50 g/l, c_0 = 60 g/l and c_0 = 100 g/l the measurement is done twice to assess the accuracy of the UHCM measuring device and repeatability of a measurement, see figure 3.4 that shows column c_0 = 100 g/l. The measured density profiles are all similar. This proves that the instrument is consistent and provides reliable measurements and the bed homogeneously distributed in the horizontal plane. Turn to appendix C for the derivation of the measuring error of the UHCM device. As mentioned before in section 3.4 at the bottom and surface the UHCM measures unrealistic values, see also figure 4.13. This also holds when gas trapped in the sediment comes in the measuring volume of the UHCM. The spikes seen in the density profile of figure 4.14 suggest that there is gas trapped in the sediment. The presence of gas in the sediment is also confirmed by the observed gas bubbles that floated towards the surface during the measurement. This is caused by disturbing the bed that allows trapped gas to escape.

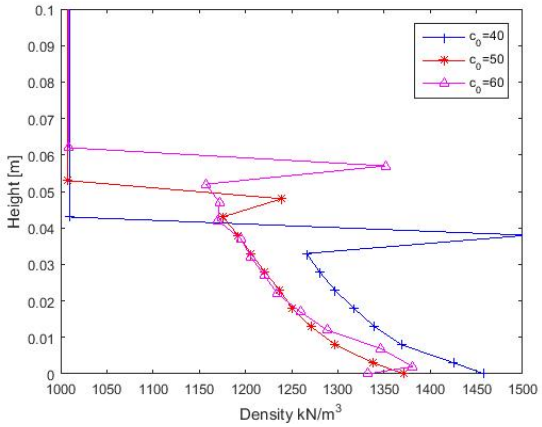

Figure 4.13: Density profiles settling column experiment case $c_0 < c_{gel}$. The spikes in the measurement are due to the measuring volume being only partly submerged in the mud, which gives unrealistic high values.

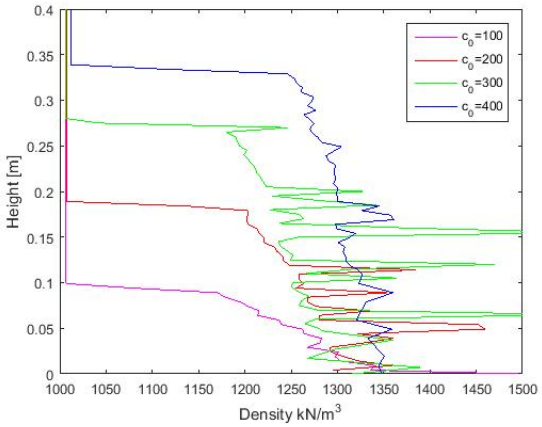

Figure 4.14: Density profiles settling column experiment case $c_0 > c_{gel}$. The spikes in the measurement are due to gas trapped in the sediment.

4.4.2. Analysis density measurement

Other research, such as Been and Sills [1981] Merckelbach [1998b] has shown the development of the density profile over time. A bed will show a concave shape which is shown in figure 4.16 and 4.17 in the early stage of consolidation. A fully consolidated bed has a density profile with a convex shape. The density profiles measured from case $c_0 > c_{gel}$ show this convex shape. In figure 4.13 this convex shape is difficult to recognise, while the density profile of the bed should follow this shape. This is proven by many other researchers and should also hold for this case. An explanation for this discrepancy might be due to segregation of particles or an error in the measurement. The first explanation suggest that a larger fraction of particles can settle faster

in the water column and form a denser lower layer, see figure 4.15. The layer above should then follow the convex shape, except for the highest point in the profile, which is an unrealistic value due to a measurement error explained earlier. The second explanation suggest that there is an error in the measurement. It might be the case that a smaller volume due to a lower bed height influences the accuracy negatively. The measurements are adjusted with a correction factor to satisfy the conservation of mass, so the profile is multiplied with a factor. This correction factor is an indicator of the accuracy of the measurement. The profile of column c_0 = 40 g/l is multiplied with a factor 1.11, while the the columns from case $c_0 > c_{gel}$ the factor is of the order 1.007. The derivation of this correction factor is explained in appendix C. Figure 4.13 shows this error clearly. The profile of column c_0 = 40 g/l is shifted beyond the profile of column c_0 = 50 g/l. This explanation suggests that measuring in smaller volumes, due to lower bed heights induces a greater error. For this reason it is questionable if these density profiles are valid results.

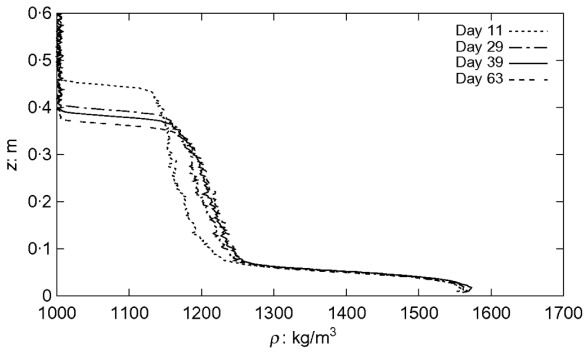

Figure 4.15: Density profile with a high density in the lower layer. This is caused by segregation of particles, sand particles with a higher particle density are in the lower layer of the bed [Merckelbach and Kranenburg, 2004b].

Figure 4.14 also shows a shape more difficult to recognise. Gas trapped in the sediment produces peaks in the density profile, but a similar shape can be seen in figures 4.16 and 4.17. These density profiles follow the convex shape of a consolidated bed.

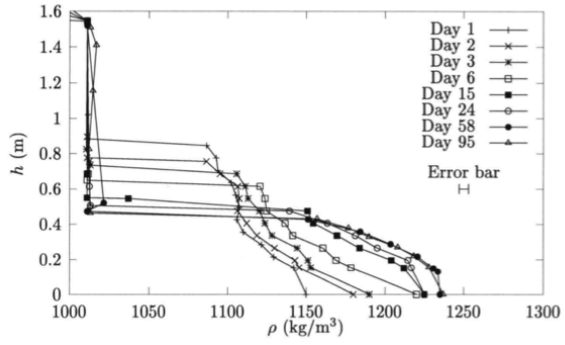

Figure 4.16: Density profile from clayey silt $\rho_0 = 1120 kg/m^3$ [Merckelbach, 1998b].

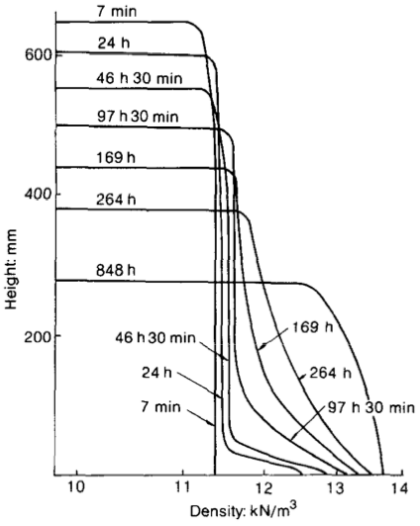

Figure 4.17: Density profiles from Caland-Beer mud [Been and Sills, 1981].

4.4.3. Density profile by 1-DV modelling

The 1-DV model produced density profiles for two cases. The first case is $c_0 < c_{gel}$ and the second is $c_0 > c_{gel}$. To simulate a settling column experiment from the second case a swelling coefficient is added to the model.

This allows the top layer of the bed to have a lower density than the initial density or initial concentration c_0. This is called swelling, water has to flow into the bed. The swelling coefficient c_s is chosen to be 0.1-0.2 times the consolidation coefficient c_v. This is further explained in appendix D.

For the first case $c_0 < c_{gel}$ a simulation is performed with the initial concentration c_0 = 60 g/l. Several time steps are displayed in figure 4.18, which show very clear the evolution of the density profile over time. The shape of the profile changes from a concave shape in the early stage of consolidation to a convex shape when consolidation comes closer to equilibrium. After 7 days the bed level and the shape of the density profile does not encounter any significant changes, other than the lowering of the bed height. In figure 4.19 the result from the model and the measurement from the UHCM are compared. The similarities are under debate. The convex shape does show in the measurement as clearly as in the model. The deviation can be ascribed to a measuring error from the UHCM or to the segregation of particles described in the previous section.

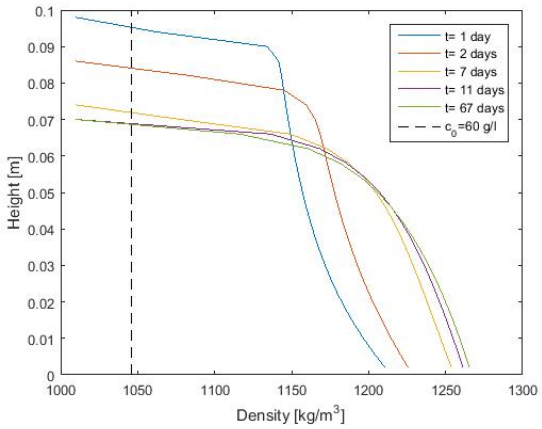

Figure 4.18: Density profiles c_0 = 60 g/l, c_{gel} = 80 g/l from 1-DV model over time

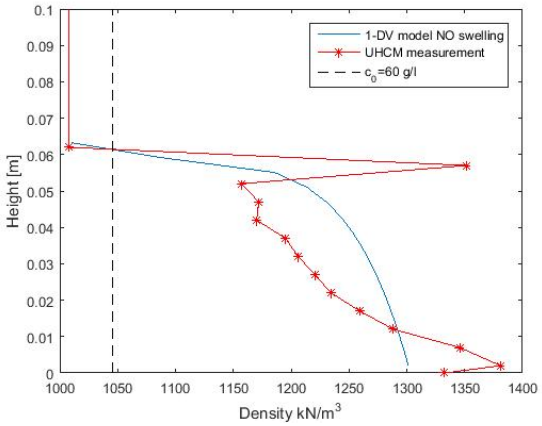

Figure 4.19: Comparing density profiles measured with UHCM and 1-DV model c_0 = 60, g/l c_{gel} = 80 g/l at t= 67 days

For the second case $c_0 > c_{gel}$ a simulation is performed with the initial concentration c_0 = 300 g/l. With the material parameters from the low initial concentration settling column experiments, see table 4.6. Several time steps are displayed. The intervals are taken differently in comparison to figure 4.18, because the time scale of the consolidation of the high concentrations is longer. The evolution of the density profile can be seen clearly. The initial density is indicated in the figure, which shows the swelling behaviour of a high density slurry that is consolidating. The model output and the UHCM measurement show reasonable similarities. The shape of the profile follows the convex shape as described by theory. Only the final bed height is predicted with an error of 5 cm, which is assumed to be reasonable. The material parameters that where obtained from the low initial concentration experiments ($c_0 < c_{gel}$) where used as input to simulate the density profile of the high initial concentration experiments. The model derives the final bed height from the material parameters. That is why the final bed height from the model deviates from the measurement. Using the material parameters determined from $c_0 < c_{gel}$ experiments serves as an estimate. Later the density profiles will be modelled with material parameters determined for the higher initial concentration experiments. The peaks in the measured profile are due to gas trapped in the density profile.

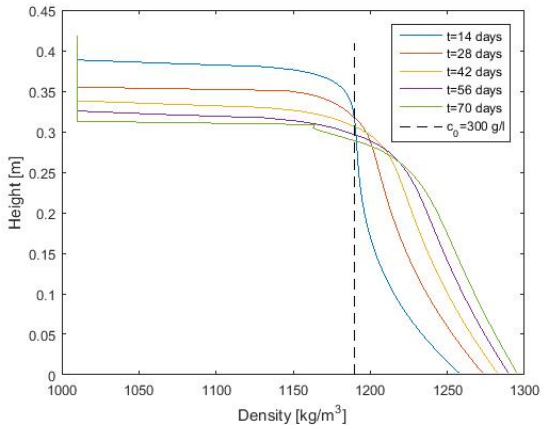

Figure 4.20: Density profiles c_0 = 300 g/l c_{gel} = 80 g/l from 1-DV for different time steps to show the evolution of the density profile. The initial concentration is indicated by the dashed line. In the top layer the density profile is below the initial density, this area experiences swelling.

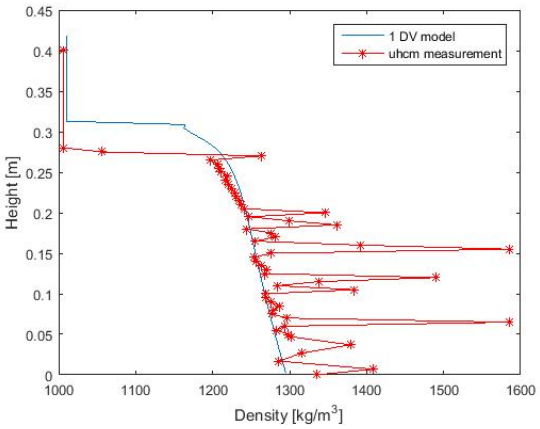

Figure 4.21: Density profiles c_0 = 300 g/l c_{gel} = 80 g/l at t=67 days. The model prediction deviates from the measurement due to the material parameters that were determined from the low initial concentration experiments ($c_0 < c_{gel}$). The peaks in the measured profile are due to gas trapped in the density profile.

4.5. Seepage Induced Consolidation (SIC) test

During this research three SIC tests were performed. The first test SIC300 proved to be a learning experience and the results will be analysed carefully in section 4.5.1 before any conclusions can be drawn. The data will analysed in two methods. The first method fits the material functions of the fractal theory to the SIC data. The material functions from fractal theory are here repeated, see equation 4.2 and equation 4.3, in which $n = 2/(3 - n_f)$. Note that ϕ_s^{sa} is left out of the equations. The sediment used for this research is sieved. So, there are no fractions present in the sediment larger than 63μm. This means there is no sand in the sediment used in this research. Thus, ϕ_s^{sa} equals zero and can be left out of the equations. For practical use of the equation the factor $K_{p,0}$, accounting for creep is assumed to be zero. However, this assumption might not be right, because creep can be observed during the SIC test. But, from literature it is not clear how to determine the creep factor and for the sake of simplicity is assumed to be zero [Merckelbach and Kranenburg, 2004a].

$$\sigma' = K_p \left(\phi_p^m\right)^n \tag{4.2}$$

$$k = K_k \left(\phi_p^m\right)^{-n} \tag{4.3}$$

The second method fits equation 4.4 and equation 4.5 to the SIC test data to obtain the DELCON parameters: A_p, B_p, A_k and B_k. This second method allows the results to be compared with other research.

$$\sigma' = \left(\frac{e}{A_p}\right)^{\frac{1}{-B_p}} - Z \tag{4.4}$$

$$k = A_k e^{B_k} \tag{4.5}$$

4.5.1. Analysis SIC test

The first SIC test was prepared directly after the end of the settling column experiment. During the settling experiment the lights where turned on throughout the day. Due to another experiment that was present in the room that needed lights to be switched on. It is suspected that due to the presence of light a large amount of organic growth was present, see figure 4.22. During the SIC300 test the formation of gas was observed. The amount of gas present in the sample was calculated, the procedure and results are described in appendix E. The pressurised system in the SIC apparatus had to be depressurised to clear out gas in the system that influences the measurement by the pressure sensor. The formation of gas was also observed during the density measurements described in section 4.4.1. So it is likely that the sediment produces gas due to a large amount of organic material that grows due to the exposure to light.

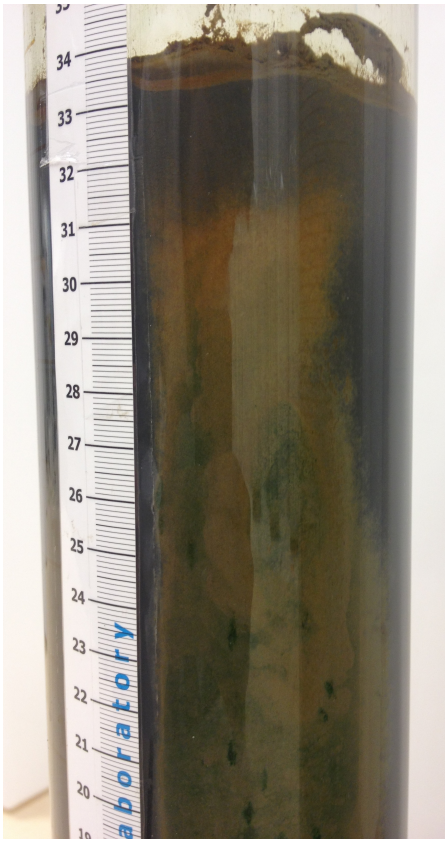

Figure 4.22: At the end of the settling column experiment t=67 days there was a significant amount of organic growth in the settling columns. The green and brown spots on the side of the column are peculiar. Mainly organic growth was observed on top of the bed.

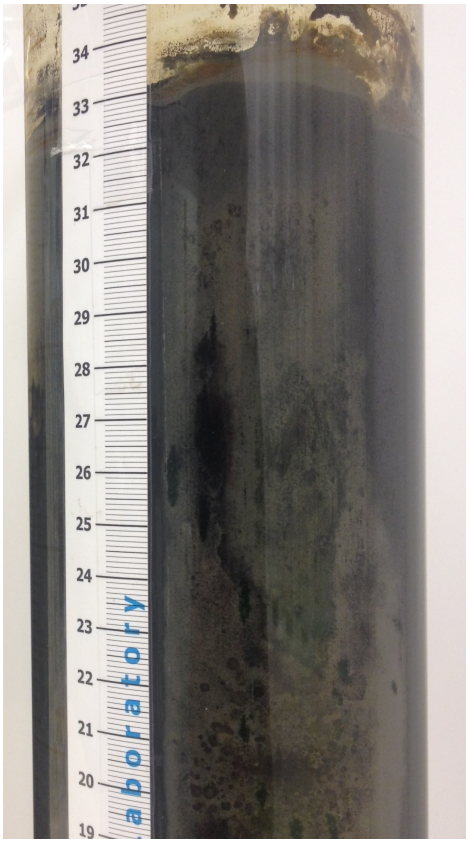

Figure 4.23: Settling column experiment t=97 days. During the SIC300 test there was no exposure to light which led to almost no organic growth in the column.

During the SIC200 and SIC400 test the sediment did not produce an extended amount of gas requiring the system to be cleared of gas. There was a discrepancy in the pretreatment of the sediment. All the columns were exposed to light during the settling column experiment. When the the settling column experiments reached equilibrium the sediment of column c_0 = 300 g/l was homogenised by gently mixing and directly placed in the SIC sample ring. At the Deltares FCL lab there is only one SIC device. To perform multiple SIC tests the sediment from columns c_0 = 200 g/l and c_0 = 400 g/l was stored for a waiting period in the column without being disturbed. The planning of the SIC tests and the amount of days that the sediment was stored prior to the SIC test is presented in table 4.11. During this waiting period the columns c_0 = 200 g/l and c_0 = 400 g/l were stored at room temperature (20-23 C°) with no exposure to light. The discrepancy in pretreatment lies in the exposure to light. The sediment of column c_0 = 300 g/l did not have a waiting period. Therefore, the sediment had a high amount of organic material, it is assumed that the high amount of organic material is responsible for the gas production during the SIC300 test. The waiting period (without exposure to light) for columns c_0 = 200 g/l and c_0 = 400 g/l reduced the amount of organic material and therefore the gas production during the SIC test.

Table 4.11: Starting dates of SIC tests and waiting period for each test. The differences in waiting time induce a different sediment pretreatment per SIC test.

Test ID	waiting period	start date	end date
SIC300	0 days	12-07-2016	15-08-2016
SIC200	39 days	23-08-2016	13-09-2016
SIC400	64 days	17-09-2016	07-10-2016

The sediment for SIC200 and SIC400 was not exposed to light for respectively, 39 days and 64 days. This has decreased the amount of organic growth, see figure 4.23 which shows the same column as figure 4.22. It is

assumed that the high amount of organic growth is responsible for the gas formation during the SIC300 test.

The settling curve of test SIC300 is presented in figure 4.24. What is very noticeable in in the settling curve is that for the first four load steps the settlement did not change significantly. The void ratio e and the volumetric concentration ϕ are determined from the settling of the sample. If e or ϕ do not change, while the load that is applied increases, this can indicate that the material is really stiff or the filter stone above the sample is jammed in the sample holder ring. However, it is known that the material is fluffy and from experience it is recognised that the filter stone is prone to be jammed in the sample ring. Figure 4.24 shows that the settlement only increases after the load step 100 N is applied. From this point the filter stone jumped loose and got unjammed. During SIC200 and SIC400 the filter stone was also jammed during the early stages of the test. The event of the filter stone jumping loose is displayed in figure 4.25. At several occasions this phenomenon was observed. There is a sudden drop in force and the settlement increases gradually. Normally the settlement first increases with a steep gradient and later the gradient becomes gradually less until close to zero.

The cause of the jamming filter stone was due to a new filter stone produced by the manufacturer. The new filter stone used during the three SIC tests was 0.15 mm larger in diameter than the previous filter stone. This change in the design of the filter stone was not made clear by the manufacturer. Unfortunately this minor difference in diameter was only discovered after the third SIC test. A very simple solution for this problem is to widen the diameter of the sample ring by 0.15 mm.

This phenomenon, the jamming filter stone, influences the results. The settlement is influenced by the filter stone in the early stages of the SIC tests. This makes the values of e and ϕ unrealistic. For that reason these data points are left out while processing the data to get a good result. To check the repeatability and the error of a SIC test the SIC300 test should be repeated. Unfortunately due to the duration of this research this was not possible. What also should be noted is that the time length of the first SIC test SIC300 was longer, approximately 7 days. Due to inexperience with the device it took longer to operate and complete the test. Applying a load longer than necessary also induce creep effects. Creep shows when the settlement has reached equilibrium, but the settlement still increases under a very mild gradient. The other SIC tests were performed in a shorter time period, also because of practicality. In appendix E the settling curves from test SIC200 and SIC400 can be found.

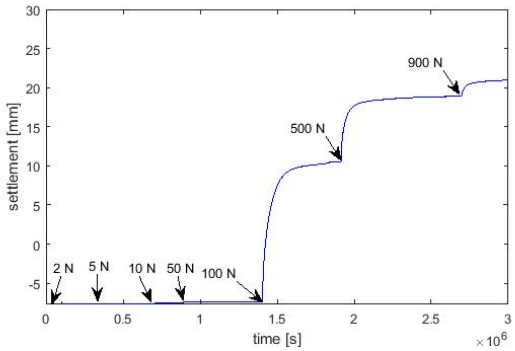

Figure 4.24: Settling curve test SIC300. What can be seen is that settlement only starts after the load 100 N is applied. Which indicates that the sample did not settle in the first phase of the test due to the filter stone that was stuck.

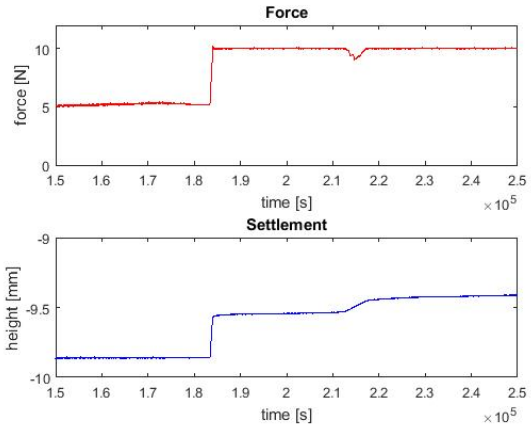

Figure 4.25: During SIC200 a sudden drop in the force at $2.15 * 10^5$ seconds and an increase in settlement indicates the jumping loose of the filter stone.

4.5.2. SIC test results

To account for the questionable data due to the jamming filter stone of the SIC tests the measurements from the lower load steps are not taken into account in the processing of the data. In the sense that the data is not used to fit the power law equations from section 4.5. The data is presented in figure 4.26, 4.27, 4.28 and 4.29. In general less data makes fitting equations less accurate. However, for these SIC tests this is not the case as the data points that were left out are not valid. This gives the material parameters from the fractal theory and the DELCON parameters that are presented in tables 4.12 and 4.13. The parameters can be compared per method, the first method following the fractal theory and the second to obtain the DELCON parameters.

Method 1 - fractal theory

The material parameters determined from the SIC tests are presented in table 4.12. The angle of each fitted curve gives a value for the fractal dimension. The fractal dimension is derived for the $\phi - k$ and $\phi - \sigma'$ relations. Comparing these two different fractal dimensions per SIC test shows that the results are within a certain range. However, all the fractal dimensions from the SIC tests have a lower value than the fractal dimensions from the settling column experiments. This is a very peculiar result. Following the fractal theory, a bed with a higher ϕ (denser packing) would have a higher fractal dimension than a bed with low ϕ (looser packing). The expected n_f was a value closer to 3. An explanation for this result could be that because of the range of ϕ in which the sediment exists during the settling column experiments and SIC tests. The range of ϕ for the settling column experiments goes up to 0.1. For the SIC tests this range is higher. Ranging from approximately 0.2 going beyond 0.4. The fractal dimension is obtained from curve fitting equations to the data. The range of data points to which an equation is fitted influences the accuracy of the determined parameters. When curve fitting is applied to a set of data with a low range this gives a lower accuracy than curve fitting to a wide range of data. In this case the settling column experiments have a lower range of ϕ, therefore curve fitting overestimates n_f. This is an explanation why n_f originating from the settling column experiments is higher than n_f originating from the SIC test. However, a very important note here is that two different experimental methods are being compared, but the difference between the fractal dimensions is minor and can be considered as a valid result. It is questionable if it is scientifically correct to compare data from two different experimental methods with each other.

The material parameters K_k and K_p are more or less in the same order of magnitude. The range in values originating from the SIC tests is larger than the range from the settling column experiments. However, it is likely that the rabge of the material parameters for these SIC tests are within the variability of the test.

Table 4.12: Material parameters obtained by fitting material function from fractal theory to SIC data, in which the factor n and n_f is determined from the relation $\phi - k$ or $\phi - \sigma'$

Test	K_k	$n(k)$	$n_f(k)$	K_p	$n(\sigma')$	$n_f(\sigma')$
SIC200	1E-11	5.432	2.63	6.25E+6	5.945	2.66
SIC300	4E-12	5.916	2.66	1.63E+7	6.261	2.68
SIC400	7E-12	6.154	2.68	8.40E+6	5.979	2.67

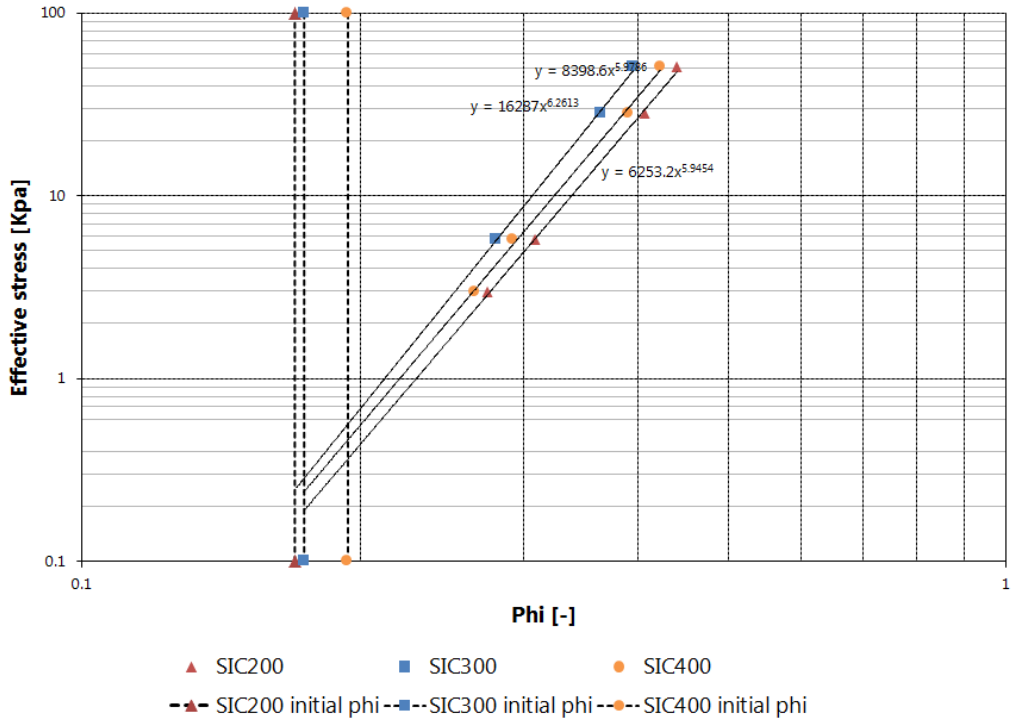

Figure 4.26: SIC test results for the $\phi - \sigma'$ relation. Due to the jamming filter stone the data is limited. The initial void ratio of the samples prior to the SIC tests are indicated in the figure by a marker and dashed line.

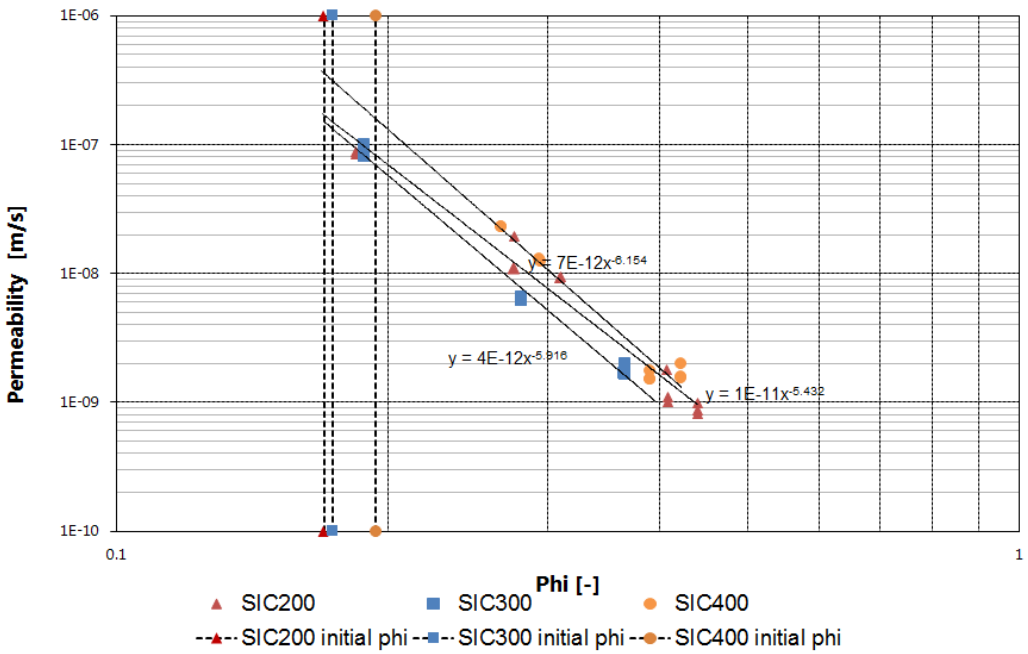

Figure 4.27: SIC test results for the $\phi - k$ relation. The initial void ratio of the samples prior to the SIC test are indicated in the figure by a marker and dashed line.

Method 2 - DELCON parameters

The obtained DELCON parameters obtained from the SIC test are comparable in relation $\sigma' - e$ and $k - e$. The variation in results between each SIC test can be due to a difference in sample preparation. The accuracy of the test is most affected by the preparation of the sample. However, this range of results is within the bounds of what can be considered as the same order of magnitude.

The second method of data processing is done to compare the SIC test data with SIC tests from other research. This is done to check if the SIC tests represents a valid result. The results are compared in table 4.13. The results of all the performed SIC tests are within the range of typical values from Winterwerp and Van Kesteren [2004]. The results from van Olphen [2016] are similar to the results from the SIC200, SIC300 and SIC400 tests. There is a deviation, but this can be ascribed to the presence of sand in the sediment that was used during the performed tests of van Olphen [2016]. The differences between SIC1 and SIC2 are assumed to be within the range in which the results of a SIC can vary, this also holds for the results of SIC200, SIC300 and SIC400.

From the comparison between the results it can be concluded that the SIC tests have produced valid data. This method of data processing is only used to compare data. Method 1, fitting the SIC test data to the material functions from fractal theory, is further utilised in this research.

Table 4.13: DELCON parameters obtained by fitting to SIC test data and comparable data from other research.

Test	A_p	B_p	Z	A_k	B_k
SIC200	3.8262	0.29	0	4E-10	3.784
SIC300	3.8917	0.24	0	1E-10	4.327
SIC400	4.6659	0.25	0	4E-10	4.039
SIC1 [van Olphen, 2016]	3.1900	0.11	-	1E-11	7.000
SIC2 [van Olphen, 2016]	2.5490	0.15	-	1E-10	6.041
Range [Winterwerp and Van Kesteren, 2004]	1−100	0.1−1	0−E+5	E-8−E-14	1−10

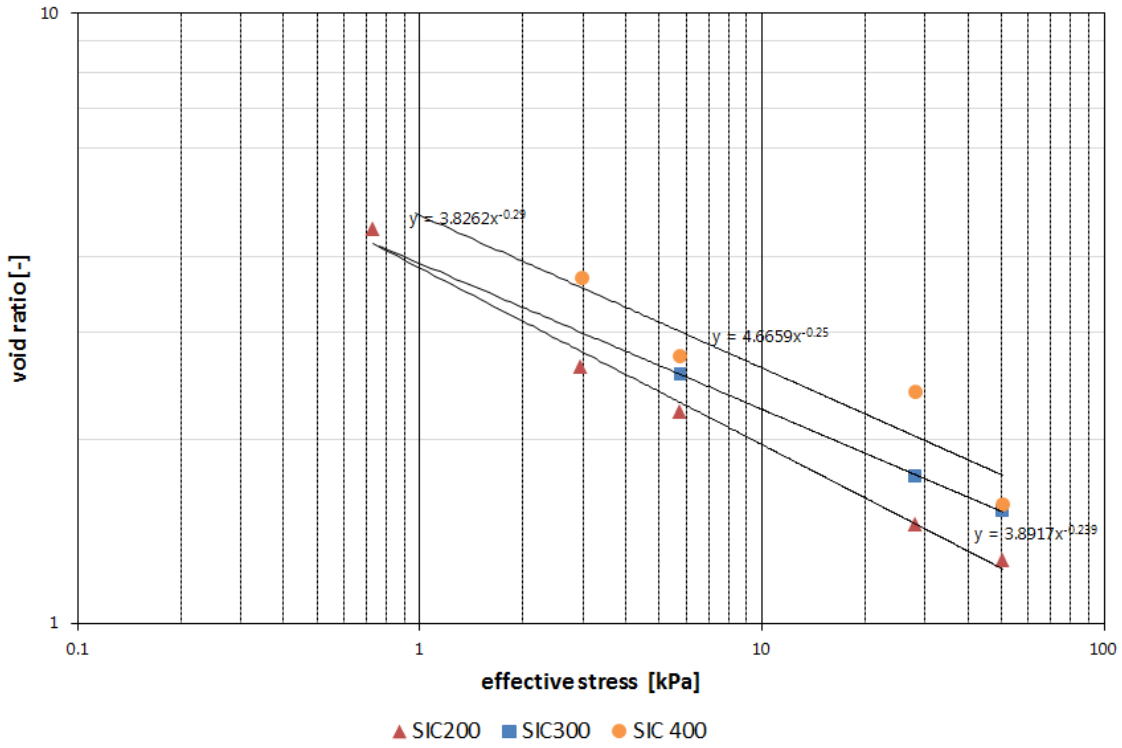

Figure 4.28: SIC test results $e - \sigma'$ to determine DELCOM parameters.

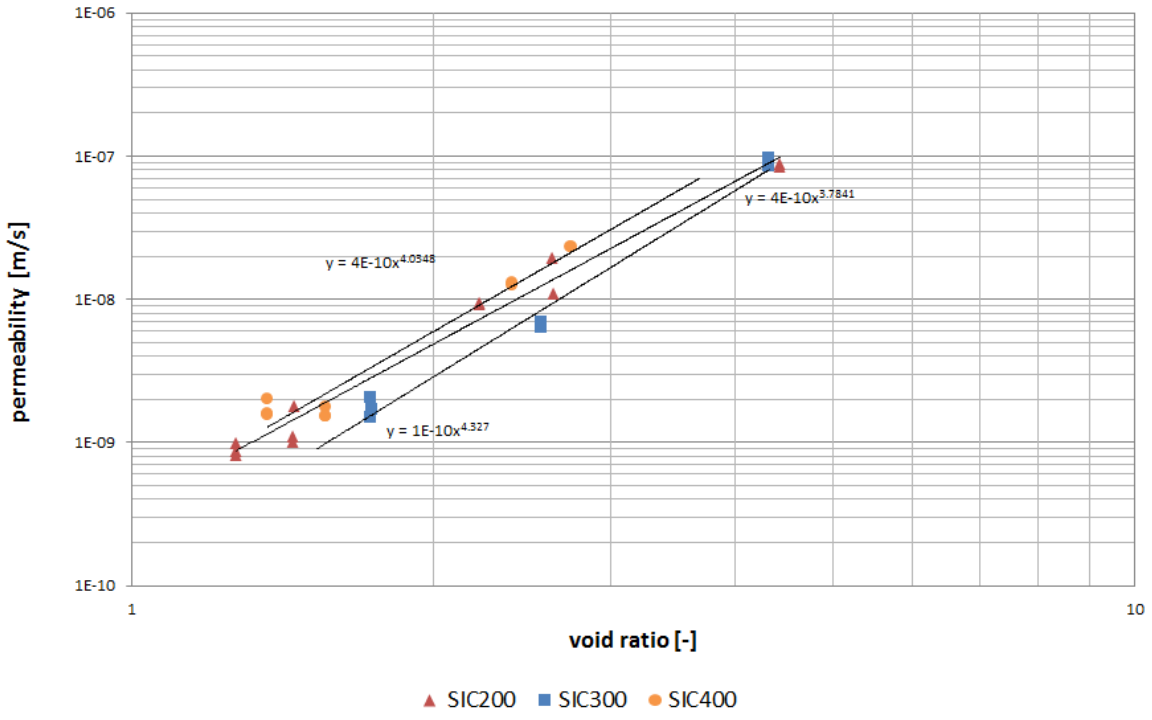

Figure 4.29: SIC test results $k - e$ to determine DELCOM parameters.

4.5.3. Comparing settling column experiment with SIC tests data

In this section the data from the SIC tests is compared with the settling column experiment data. This was done for the material functions from the fractal approach, equation 2.14 and 2.15. The material parameters obtained from the two experimental methods are repeated in table 4.14. At four time intervals during the settling column experiments ϕ was determined, these values are presented in table 4.15. The material functions are plotted for these values of ϕ and the material parameters from the settling column experiments and the SIC tests. This is shown in figures 4.30 and 4.31.

Table 4.14: Material parameters obtained from SIC tests and $c_0 < c_{gel}$ settling column experiment.

experiment	K_k	K_p	n	n_f	Γ_c
SIC200	1.00E-11	6.25E+6	5.8824	2.66	3.75E-8
SIC300	4.00E-12	1.63E+7	6.2610	2.68	3.58E-8
SIC400	6.00E-12	8.40E+6	5.9790	2.67	2.89E-8
Settling columns	1.74E-13	1.26E+7	6.4545	2.70	1.51E-9

The SIC test data is extrapolated to the range of ϕ from the settling column experiment, see table 4.15 and figures 4.30 and 4.31. In figures 4.30 and 4.31 the higher range of ϕ represents the SIC test data and the lower range of ϕ represent the extrapolated SIC test data. This makes it possible to compare the two experimental methods. The transition between the two plotted ranges of ϕ is an indication of the relation between the settling column experiment and the SIC test. A well fitted transition between the two experimental methods is characterised by two material functions that are in line.

Table 4.15: Volumetric concentration ϕ at different intervals from the settling column tests.

Column	$\phi_1(t = 4000s)$	$\phi_2(t = 100000s)$	$\phi_3(t = 1400000s)$	$\phi_4(t = 6000000s)$
$c_0 = 200$ g/l	0.0819	0.0919	0.157	0.1728
$c_0 = 300$ g/l	0.1209	0.1232	0.1531	0.1756
$c_0 = 400$ g/l	0.1653	0.1667	0.1782	0.1980

The extrapolated values are also compared to the material functions with the settling column data. These material parameters were determined from the $c_0 < c_{gel}$ settling column experiment. This material function forms a reference to compare the results from the SIC test. The material function from the settling column experiments represent only one line in figures 4.30 and 4.31 because only one set of material parameters was obtained from the settling column experiments, see table 4.14.

Figures 4.30 and 4.31 contain three sets of data. The first set is SIC data, the second set is the extrapolated SIC test data and the third set is the settling column experiment data. The material parameters obtained from the SIC test are extrapolated in the figures 4.30 and 4.31 and can be compared with the settling column experiment data.

In figure 4.30, which shows the $\phi - \sigma'$ relation, can be seen that the material parameters obtained from the SIC test show a well fitted transition between the SIC test data and the extrapolated SIC test data. The material parameters obtained from the SIC test are within the same order of magnitude, with the results from SIC300 as the exception. This will be explained later.

The settling column experiment data shows a well fitted transition to the SIC data for the $\phi - \sigma'$ relation. However, the the settling column data and SIC data for the $\phi - k$ relation does not show a well fitted transition, see figure 4.31. There is a discrepancy between these two data sets by an order of magnitude. The material parameters from the SIC test obtain a better fitting transition for the $\phi - k$ relation.

Which data set shows the best relation to the SIC data depends on how well fitting the transition is. For the relation $\phi - \sigma'$ the settling column experiment data shows a better fitting transition than for the relation $\phi - k$. For the relation $\phi - \sigma'$ both the data sets show a well fitting transition to the SIC data. Only the results from SIC300 test are out of the range from the other curves. This can be explained by the jamming filter stone. The limited amount of load steps due to the jamming of the filter stone influenced the accuracy of the material parameters obtained by curve fitting. Therefore, the SIC300 data is not within the range of the other SIC tests.

The reason why the settling column parameters do not show a well fitting transition, for the $\phi - k$ relation, might be due to many factors that influence the permeability. The amount of gas in the sample and the volumetric concentration ϕ influence the permeability and thus the coefficient of permeability K_k. The

material parameter K_k is determined in two different ranges of ϕ for the settling column experiments and the SIC experiments. During the SIC test and settling column experiments the amount of gas and the range of ϕ was different. This is a possible explanation for the deviation between the K_k from the settling columns and the SIC tests.

The data sets: extrapolated SIC data and settling column data plotted in the figures 4.30 and 4.31 are here presented in the tables 4.16 and 4.17.

Table 4.16: Effective stress for volumetric concentration ϕ at a specific time interval during the settling column experiment. ϕ was determined at four intervals during the settling column experiments, presented in table 4.15. The $\phi - \sigma'$ data is for the settling column experiment and the extrapolated SIC data.

Data set	$\sigma'(\phi_1)$ [Pa]	$\sigma'(\phi_2)$ [Pa]	$\sigma'(\phi_3)$ [Pa]	$\sigma'(\phi_4)$ [Pa]
SIC200 extrapolated	2.53	4.98	116.76	205.12
SIC300 extrapolated	179.24	197.49	640.37	1343.70
SIC400 extrapolated	128.78	135.48	203.82	391.11
$c_0 = 200$ g/l	1.94	4.07	129.55	240.35
$c_0 = 300$ g/l	24.03	26.98	109.85	266.04
$c_0 = 400$ g/l	180.55	190.40	292.02	577.93

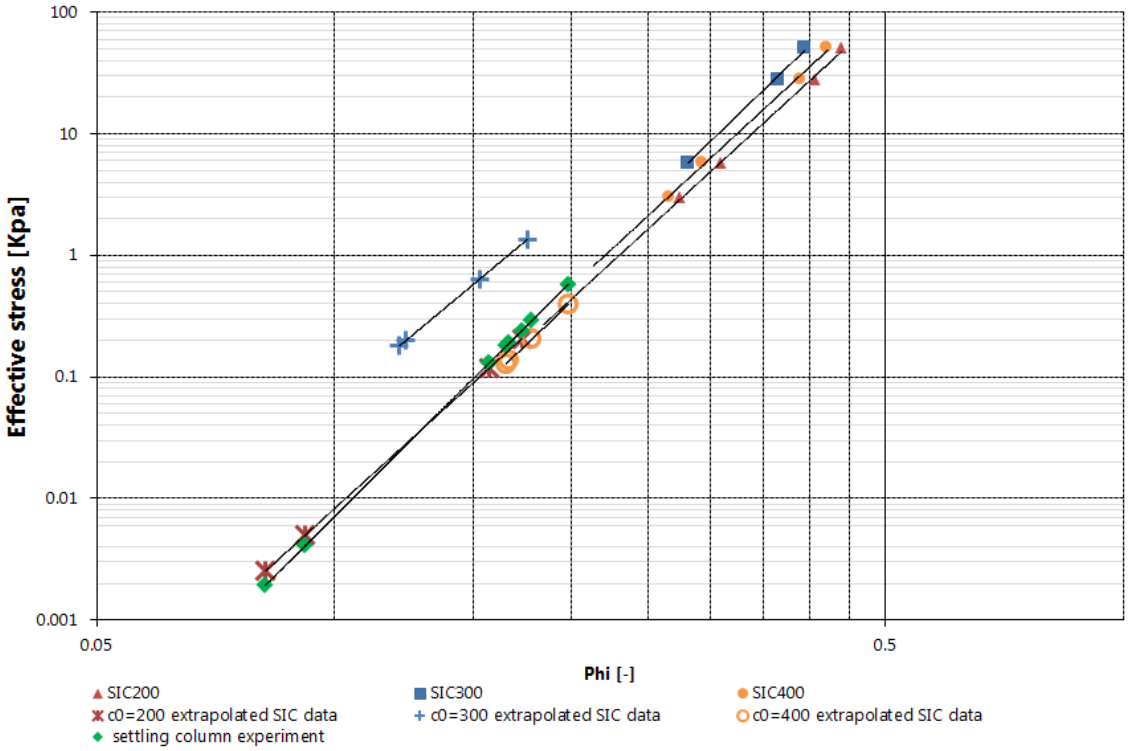

Figure 4.30: SIC test data, extrapolated SIC test data and settling column experiment data for the relation $\phi - \sigma'$ is presented in one graph. A well fitted transition between the two experimental methods is characterised by two material functions that are in line. For the relation $\phi - \sigma'$ both the settling column data and the extrapolated SIC data show a well fitting transition. Only the SIC300 data is not in line and is off by an order of magnitude, this can be ascribed to the jamming filter stone.

Table 4.17: Permeability for volumetric concentration ϕ at a specific time interval during the settling column experiment. ϕ was determined at four intervals during the settling column experiments, presented in table 4.15. The $k-\sigma'$ data is for the settling column experiment and the extrapolated SIC data.

Data set	$k(\phi_1)$ [m/s]	$k(\phi_2)$ [m/s]	$k(\phi_3)$[m/s]	$k(\phi_4)$ [m/s]
SIC200 extrapolated	9.89E-06	5.02E-06	2.14E-07	1.22E-07
SIC300 extrapolated	9.09E-07	8.25E-07	2.54E-07	1.21E-07
SIC400 extrapolated	3.91E-07	3.72E-07	2.47E-07	1.29E-07
$c_0 = 200$ g/l	1.64E-06	7.82E-07	2.46E-08	1.32E-08
$c_0 = 300$ g/l	1.33E-07	1.18E-07	2.90E-08	1.20E-08
$c_0 = 400$ g/l	1.76E-08	1.67E-08	1.09E-08	5.51E-09

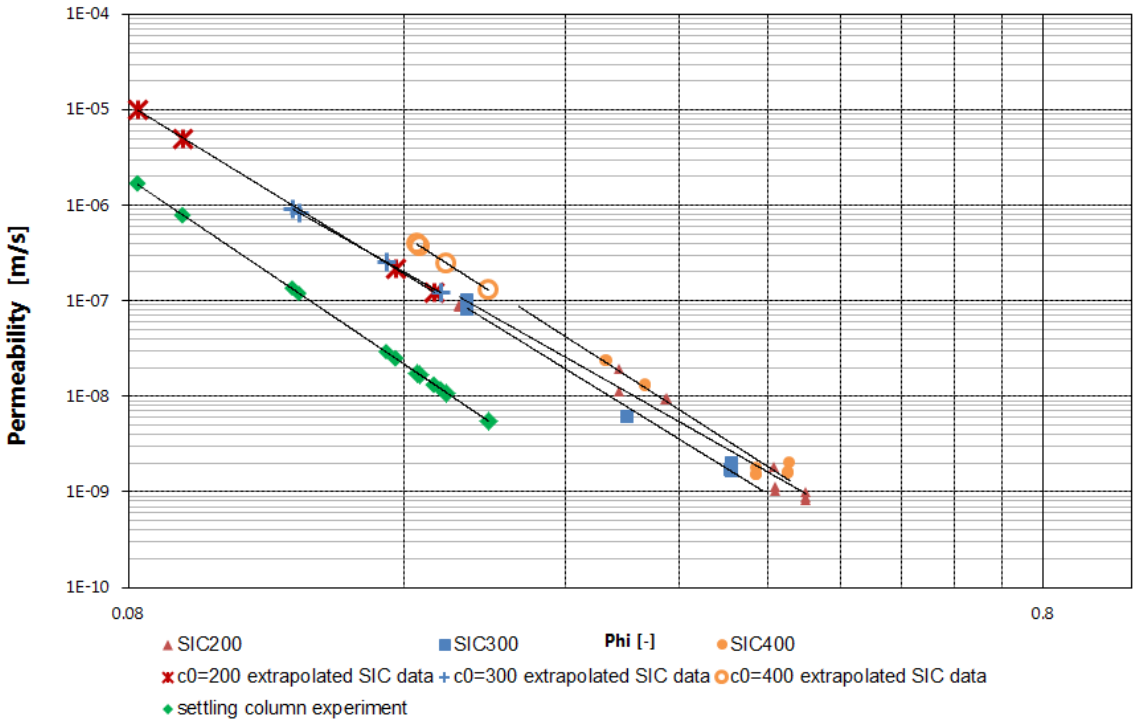

Figure 4.31: SIC test data, extrapolated SIC test data and settling column experiment data for the relation $\phi - k$. For the relation $\phi - k$ only the extrapolated SIC data set shows a well fitting transition. Tha settling column experiment data is off by an order of magnitude.

5

Discussion

In this chapter the experimental results will be discussed. It is argued that there is no trend in the material parameters. This is demonstrated by comparing the result with data from other research and in practice by modelling density profiles with different sets of material parameters. As a practical example an additional hypothetical consolidation experiment is modelled to put the results in the context of the Marker Wadden project.

5.1. Discussion settling column experiment results

The results obtained from settling column experiments ($c_o < c_{gel}$) suggest that the bed from each experiment with its own initial concentration have similar material parameters. The results in table 4.6 are in the same order of magnitude and show resemblance. From these results it can be concluded that the material parameters of a bed is not dependent on the initial concentration if the statement $c_0 < c_{gel}$ holds. This has already been proven by other researchers, this research confirms these earlier findings. Results from the settling column experiment are compared with other research with similar sediment, see table 5.1. This also indicates that the experiment provided valid results. In table 5.1 the range of the parameters K_k and K_p can be off by one or two orders of magnitude. Applying this range on the results of the settling column experiment of this research shows that the range of the material parameters are within the boundaries of what can be considered as the same order of magnitude.

Table 5.1: Determined parameters K_k, K_p and n_f from settling column experiments ($c_o < c_{gel}$) compared to other research.

Reference	Sediment	n_f [-]		K_k [m/s]		K_p [Pa]	
Current	Markermeer LC	2.69	2.70	1.23E-13	2.18E-13	0.81E+07	1.26E+07
[Hendriks, 2016]	Markermeer IJ02	2.67	2.69	4.14E-14	1.28E-13	2.13E+07	6.46E+07
[Barciela Rial, 2015]	Markermeer IJ02	2.64	2.75	1.63E-16	6.66E-14	1.41E+07	6.66E+09
[De Lucas Pardo, 2014]	Markermeer	2.67	2.68	7.85E-14	9.03E-14	1.10E+07	2.50E+07
[Merckelbach, 2000]	Caland-Beer	2.72	2.75	9.90E-16	2.20E-14	7.00E+07	4.00E+09

5.1.1. Sensitivity of the method to determine the permeability coefficient

To determine the parameters K_k and n_f equation 2.9 is fitted to the settling curve. The section of the settling curve to which this equation is fitted is the consolidation phase C-I. This section is chosen by assuming a time interval. There is a degree of subjectivity in the method by choosing the time interval. How the limits of the section are chosen affects the angle n_f of the fitted curve. The variation of the angle results in a variability of the K_k of a few orders of magnitude. Figures 5.1 and 5.2 show an extreme example of how the choice of time interval influences the angle of the fitted curve. The results in table 5.2 show that K_k can deviate by three orders of magnitude. Therefore, this method is prone to errors. To reduce the error in the determination of the K_k a different method should be used with less subjectivity.

Table 5.2: Results from curve fitting to different sections of the settling curve.

Section [s]	K_k	n	n_f
Δt =1E+3-1E+4	1.09E-11	5.1314	2.61
Δt =9E+3-9E+4	7.06E-14	6.68084	2.71

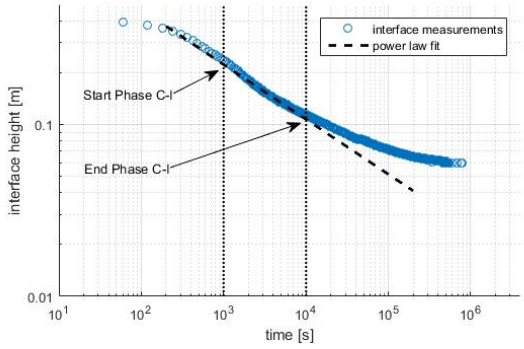

Figure 5.1: Curve fitting to determine the permeability coefficient. In the figure the limits are indicated for which section of the settling curve the fitting is performed. Δt =1E+3-1E+4 s.

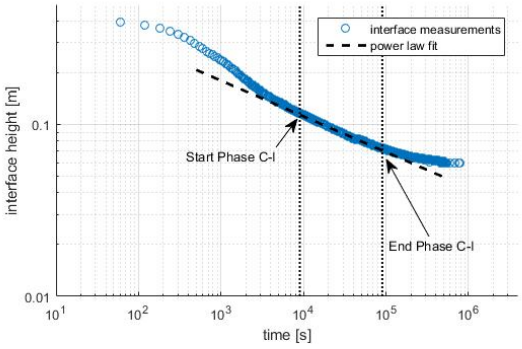

Figure 5.2: Curve fitting to determine the permeability coefficient. In the figure the limits are indicated for which section of the settling curve the fitting is performed. Δt =9E+3-9E+4 s.

5.1.2. Influence of the particle density

In the initial phase of this research the particle density was estimated to be $\rho_s = 2650$ kg/m^3. This is a common assumption made by many researchers and engineers. Later particle density measurements showed the particle density to be $\rho_s = 2540$ kg/m^3 [Barciela Rial, 2015]. The results from the settling column experiments were calculated again for this measured particle density. The measured particle density had an influence on the newly calculated material parameters. The material parameters based on $\rho_s = 2650$ kg/m^3 and $\rho_s = 2540$ kg/m^3 are summarised in tables 5.3 and 5.4. When the density profile is modelled with the 1-DV model a difference in final bed height is observed. The final bed height is over estimated with the model input for $\rho_s = 2650$ kg/m^3. Figure 5.3 shows that the material parameters for the measured particle density give a better result. This suggests that the particle density affects the final conditions. Therefore, the particle density should be measured to determine the material parameters for simulating consolidation behaviour with the 1-DV model to obtain valid results.

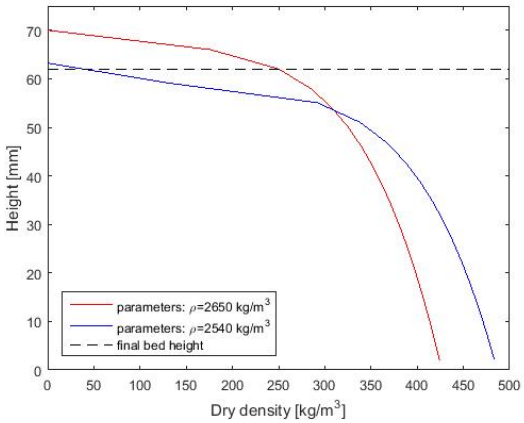

Figure 5.3: Density profile from 1-DV model for column c_0 = 60 g/l. The density profile determined for $\rho_s = 2650$ kg/m^3 overestimates the final bed height. The density profile modelled with $\rho_s = 2540$ kg/m^3 shows a bed height that fits better to the measured final bed height.

Table 5.3: Material parameters based on $\rho_s = 2650$ kg/m^3.

c_0 [g/l]	K_k [m/s]	n_f [-]	K_p [Pa]	c_v [m^2/s]
40	1.14E-13	2.70	2.97E+7	2.23E-9
50	2.04E-13	2.69	1.16E+7	1.51E-9
60	1.63E-13	2.70	1.84E+7	1.97E-9

Table 5.4: Material parameters based on $\rho_s = 2540$ kg/m^3.

c_0 [g/l]	K_k [m/s]	n_f [-]	K_p [Pa]	c_v [m^2/s]
40	1.23E-13	2.70	1.12E+7	0.93E-9
50	2.18E-13	2.69	0.81E+7	1.15E-9
60	1.74E-13	2.70	1.26E+7	1.51E-9

5.1.3. Settling behaviour in high concentration mud

During the high concentration settling column experiment the mud-water interface was observed moving down following a linear trend (figure 4.8). However, this settling behaviour was not expected. An explanation for this linear trend is that the density exceeds the equilibrium density in the top layer of the mud bed. Strength and density are directly related by fractal theory, so the top layer is denser and stronger than the equilibrium strength or density. This excess of density or strength in the top layer is an overburden which presses down on the lower part of the slurry in the column. This means that there is an overburden that makes the interface move down linearly, until the force balance is recovered. The upper part of the mud is over consolidated. This phenomenon can be described as the piston effect (JC Winterwerp, personal communication, June, 2016), see figure 5.4. The slurry's density is too high and it pushes the particles down as a piston until it reaches a point where the particles build up enough strength to carry the load. The force balance is restored, then the bed follows consolidation behaviour by slowly decreasing in height.

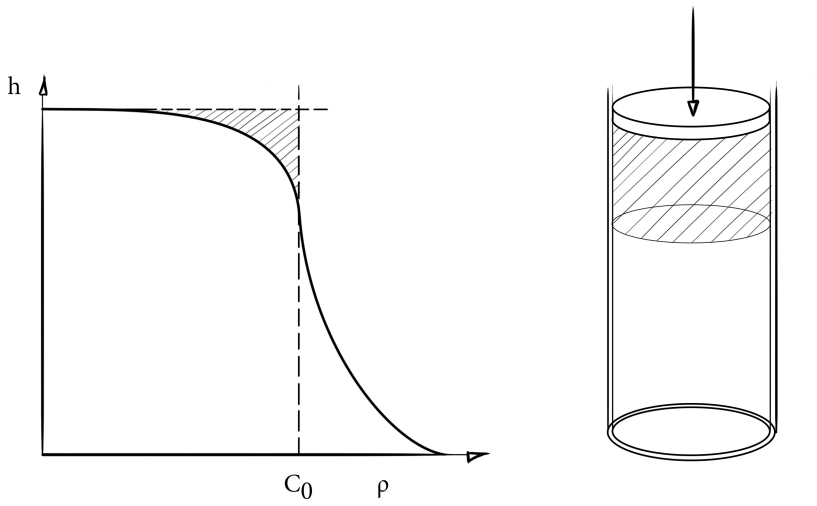

Figure 5.4: At t_0 of a settling column experiment $c_0 > c_{gel}$ the top part the equilibrium density profile (for $c_0 > c_{gel}$) is exceeded by to the initial concentration c_0. This is an overburden indicated in the shaded area. The overburden pushes the particles down like a piston following a linear trend. This phenomenon is called the piston effect and explains why the settling curve shows settling behaviour even though the initial concentration exceeds the gelling concentration.

In previous research by van Olphen [2016] the settling behaviour for the high initial concentrations was also noticed. However, in this research the pseudo settling behaviour for the high concentration mud was considered as the hindered settling phase. The method of Merckelbach and Kranenburg [2004a] was utilised to determine the gelling concentration, fractal dimension and material parameters. The results from this approach resolve in values that are out of bounds of the spectrum that is indicated in table 5.1. From this it can be concluded that the linear trend in the beginning of the settling curve cannot be considered as a hindered settling phase.

5.2. SIC test results

The largest influential factor on the results of the SIC test is the pretreatment of the sediment. A variation in the results in figures 4.26 and 4.27 is observed. It was expected that at higher stresses the results would converge. Theoretically, the results should converge, because the initial concentration does not affect the

volumetric concentration ϕ at the higher stress levels. In practice the results are expected to converge under the assumption that measurement is accurate and the experimental procedure is consistent and repeatable. The lack of reproducibility is a explanation for this variation. This explanation requires additional duplicate experiments.

In the data there is no trend observed. As mentioned earlier it is expected that the results should converge to the same line. This is under the assumption that the samples are remoulded and the there is no effect of the structure within the sample. The results in figures figures 4.26 and 4.27 follow the same slope, but are shifted from each other. This shift is explained by the test conditions, such as sediment pretreatment, that were not the same.

The influence of the test conditions is described by van Olphen [2016], which shows a variation in results of two SIC tests due to a discrepancy in the sediment pretreatment. Thixotrophy effects and different resting duration of the samples prior to the SIC test has affected the results. Thixotrophy effects can be shown by a vane test. The strength of the mud will increase over time. In this research there was not a sufficient amount of sample left after the preparation of the SIC test to perform a valid vane test. However, van Olphen [2016] has shown thixotrophy effects in the sediment used, which is similar to the sediment used in this research. Thus, thixotrophy effects are also expected in the sediment used in this research.

During the SIC test besides the pretreatment of the sample other errors are induced. These errors are induced during the operation of the SIC device or by the interpretation of the data. For further elaboration on these errors turn to appendix E.

5.3. Material parameters related to initial concentration

The objective of this research is to determine if the consolidation behaviour is a function of the initial conditions. There is no trend observed in the material parameters obtained from the settling column experiments and the SIC tests. Taking into account the accuracy of the SIC tests, the range of material parameters given by other research (table 5.1) and the lack of trend in the obtained material parameters, the material parameters obtained from the settling column experiment and SIC tests do not show effect of the initial concentration if evaluated per case ($c_0 < c_{gel}$ and $c_0 > c_{gel}$).

Figures 5.5 and 5.6 show the material parameters determined per initial concentration. The results have been compared to results from Hendriks [2016] and De Lucas Pardo [2014], which both have used similar sediment from lake Markermeer. In the figures no trend can be observed in the material parameters. What can be observed is that the material parameter K_k from the SIC test and settling column experiment differ by an order of magnitude. So, when both cases are evaluated the initial concentration does have an effect on the material parameters. A good physical explanation for this difference is not known yet. However, it is known that gas and volumetric concentration influence the permeability. These two factors were different in the two experimental methods, so the explanation could relate to this difference. There is no significant difference in the order of magnitude in the material parameters K_p. What can be observed is that the variation in the material parameters for the higher initial concentrations have a higher variability than the results obtained from the settling column experiments. This can be explained by a larger error in the SIC test.

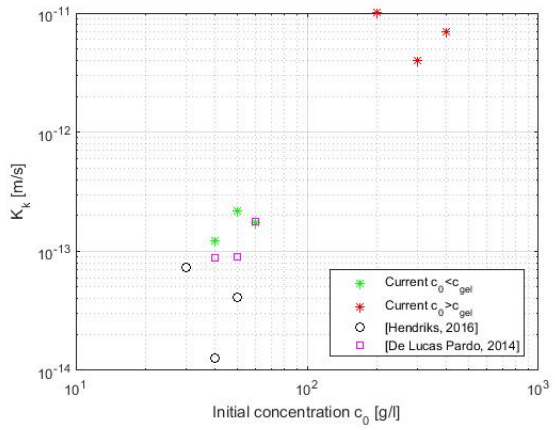

Figure 5.5: Permeability coefficient K_k determined for initial concentrations from settling column experiment $c_0 < c_{gel}$ and SIC tests compared results to other research.

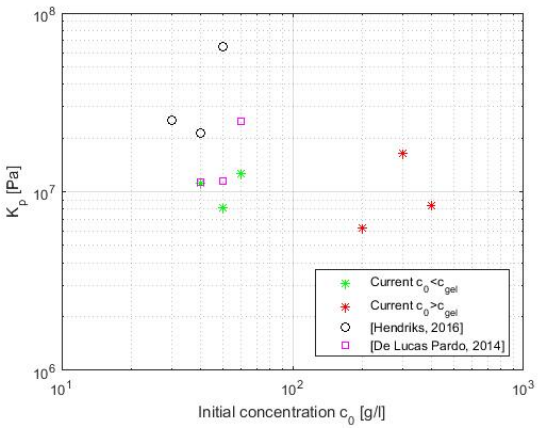

Figure 5.6: Effective stress coefficient K_p determined for initial concentrations from settling column experiment $c_0 < c_{gel}$ and SIC tests compared results to other research.

The fractal dimension does not show a trend for the initial concentration. In figure 5.7 no trend can be seen. Comparing the fractal dimensions determined from settling column experiments and SIC tests show similar results. The fractal dimension from the SIC test is lower. However, the results are very similar and can be considered within the error of the experimental methods.

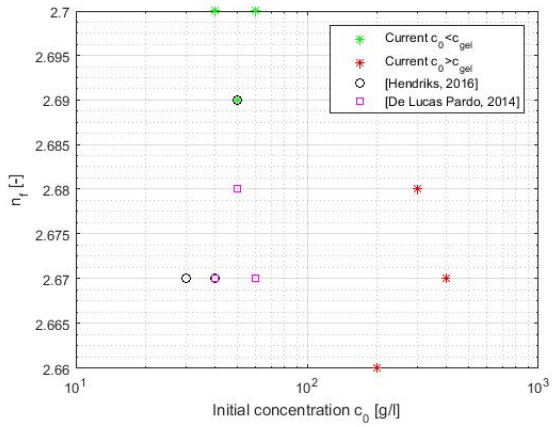

Figure 5.7: Fractal dimension n_f determined for initial concentrations from settling column experiment $c_0 < c_{gel}$ and SIC tests compared results to other researcher.

5.4. Material parameters model comparison

There is no trend observed in the material parameters obtained from the SIC test. To show this in practice the 1-DV model was utilised to determine the effect of the material parameters on the density profile and height of the final bed. The same 1-DV model including the swelling coefficient as described in section 4.4.3 was used. The modelled density profiles are based on the material parameters from the SIC tests and settling column experiments, presented in table 5.5. The model results are then compared to the measured density profile with the UHCM device. The measured density profiles in section 4.4 show peaks in the measurement due to gas. In this section the peaks in the density profiles, which is considered to be noise in the measurement, are corrected. The peaks are reduced to an average value of the measured density from the point above and below the peaks. This correction is explained further in appendix C.

Table 5.5: Material parameters obtained from SIC tests and $c_0 < c_{gel}$ settling column experiment.

experiment	K_k	K_p	n	n_f	Γ_c
SIC200	1.00E-11	6.25E+6	5.8824	2.66	3.75E-8
SIC300	4.00E-12	1.63E+7	6.261	2.68	3.58E-8
Settling columns	1.74E-13	1.26E+7	6.4545	2.70	1.51E-9

In figure 5.8 and figure 5.9 the 1-DV model output the density profiles for the material parameters from the settling column experiments and the SIC tests. These modelled density profiles are compared with the measured density profile. The modelled density profiles for column c_0 = 200 g/l both show a good fit to the measured density profile, based on visual observation. Both the model results predict the final bed height well and the density profile follows the measured density profile. However, the density profile modelled with the material parameters from the SIC200 test fits better to the measured density profile, with respect to the final bed height. The density profiles modelled for column c_0 = 300 g/l show a higher deviation in figure 5.9. The modelled result from the material parameters obtained from the SIC300 test show a better fit to the measured density profile, with respect to profile and bed height.

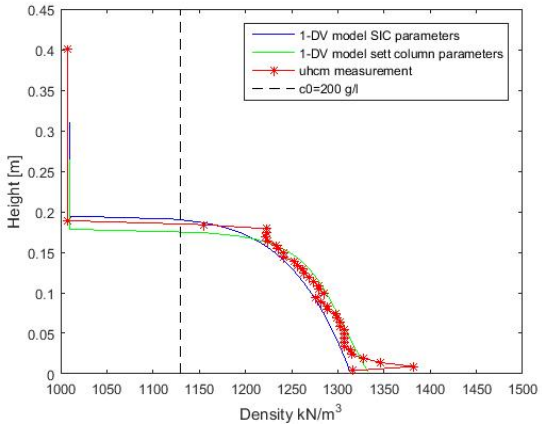

Figure 5.8: Density profiles c_0 = 200 g/l modelled with material parameters obtained from the settling column experiment and SIC test. These profiles are compared with UHCM measurement at t=67 days. Both sets of material parameters predict the density profile and final bed height well. The differences are minor, but the SIC material parameters give a better fitting density profile with respect to the final bed height.

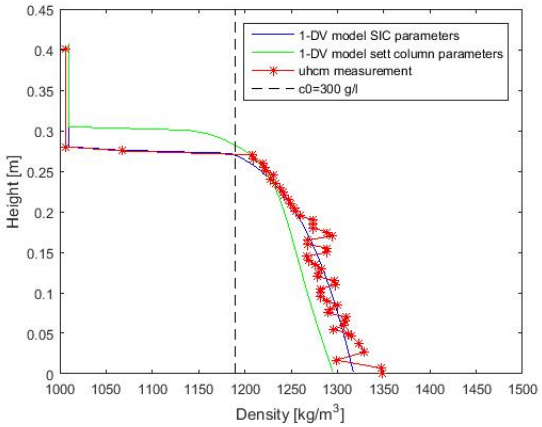

Figure 5.9: Density profiles c_0 = 200 g/l modelled with material parameters obtained from the settling column experiment and SIC test. These profiles are compared with UHCM measurement at t=67 days. The material parameters from the SIC test model a density profile that fits better to the measurement.

The performance of how well a modelled density profile fits to actual measurements is quantified in table 5.6. This is done by determining the percentage of offset of the fit for two parameters. The first parameter is the density of the profile and second the bed height. The offset for the density profile is determined by subtracting the dry density of the modelled profile from the dry density of the measured profile. The offset is determined for each measurement in the measured density profile until the bed height of the modelled profile is reached. This offset is converted to a percentage of offset. From these offsets percentages the average percentage of offset is derived. The offset percentage of bed height is determined by the difference in bed height divided by the measured final bed height. Thus, now the fit from a modelled density profile is quantified with respect to density profile and bed height. This provides a better method to analyse the fit between the density profiles.

Table 5.6: Offset of modelled density profiles compared to the measured density profile.

c_0 = 200 g/l Parameters	offset profile [%]	offset bed height [%]	c_0 = 300 g/l Parameters	offset profile [%]	offset bed height [%]
Settling columns	2.45	7.41	Settling columns	7.80	9.31
SIC200	2.05	1.59	SIC300	3.70	0.36
SIC300	8.60	7.41	SIC200	4.61	5.82

The modelled density profiles in figures 5.8 and 5.9 predict the density profile and the final bed height reasonably well. So, apparently the material parameters obtained from the settling column experiments are a good method to make a first estimate for a density profile of a consolidated bed, based on the offset of this scale.

To determine if there is an effect of the initial concentration on the density profile, the material parameters obtained from test SIC300 are used to model the density profile of column c_0 = 200 g/l. Subsequently, this profile is compared with the density profile modelled with the material parameters from the SIC200 test, shown in figure 5.10. The same procedure is performed for the column c_0 = 300 g/l, shown in figure 5.11.

In both figures 5.10 and 5.11 the modelled density profiles show similar results, but there is a difference in the determined offsets. The density profiles modelled with an initial concentration different from the initial concentration of the SIC test fit less well. The difference is shown in table 5.6.

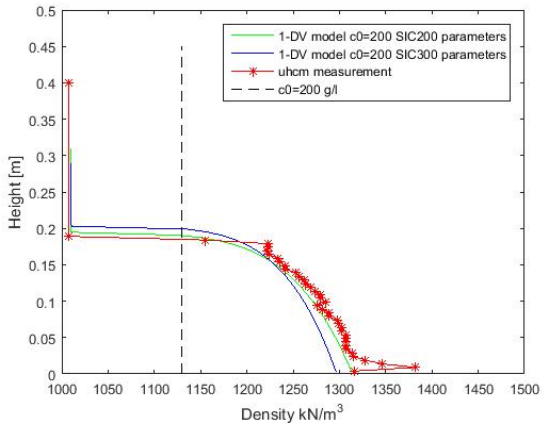

Figure 5.10: Density profiles modelled from column c_0 = 200 g/l with material parameters obtained from SIC200 and SIC300 and compared to the measures density profile.

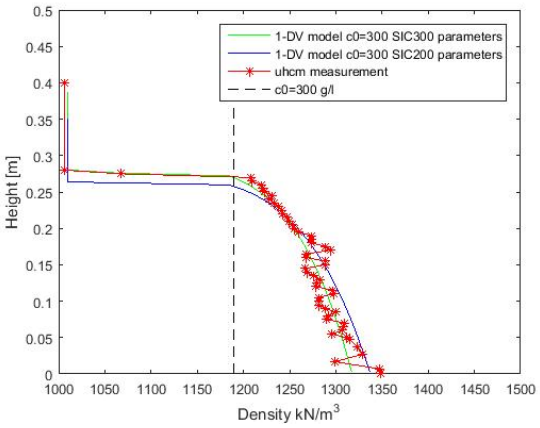

Figure 5.11: Density profiles modelled from column c_0 = 300 g/l with material parameters obtained from SIC200 and SIC300 and compared to the measures density profile.

The material parameters obtained from the settling column experiments are a good first estimate to predict the final conditions. There are deviations in the results, especially for column c_0 = 300 g/l, in which the bed height is overestimated. However, utilising the material parameters from the $c_0 < c_{gel}$ settling column experiments to model the final density profile is from an engineering point of view a good method for a prediction on this small scale. Material parameters obtained from a relative simple and quick experiment are able to reasonably predict the final conditions of a high concentration ($c_0 > c_{gel}$) settling column experiment. From the figures 5.10 and 5.11 it can be concluded that there is evidence of the effect of the initial concentration on the final conditions of the bed. However, the significance of the effect is not known. It should be noted that the offset of the density profile is within the reproducibility of the measurement. The error is based on the reproducibility of the density measurement with the UHCM device. For further explanation turn to appendix C. However, even though the offsets are within the error it still does not explain why there is a difference.

5.5. Hypothetical settling column experiment

To show the effect of the difference in the material parameters from the settling column experiments and the SIC tests in practice, the consolidation behaviour of a slurry in a hypothetical column is modelled for realistic conditions. A 5 m high settling column experiment with the initial concentration of c_0 = 300 g/l is modelled with the 1-DV model, as described in section 4.4.3. The results will predict the behaviour of the mud as in practice. The mud that is deposited in the construction of the Marker Wadden has approximately the same initial height. Therefore, this is a good method to show the consolidation behaviour of a slurry in practice.

In figure 5.12 the density profiles are modelled with the material parameters obtained from the settling column experiment and the SIC300 test, presented in table 5.7. The profiles are modelled at three time intervals. The profiles modelled with the SIC material parameters show a convex profile, which indicates that the consolidation reaches its equilibrium state. However, the concave shape of the profile modelled with the material parameters from the settling column experiment suggest that the consolidation of the bed is not close its equilibrium state.

Table 5.7: Material parameters obtained from SIC300 test and $c_0 < c_{gel}$ settling column experiment.

experiment	K_k	K_p	n	n_f	Γ_c
SIC300	4.00E-12	1.63E+7	6.2610	2.68	3.58E-8
Settling columns	1.74E-13	1.26E+7	6.4545	2.70	1.51E-9

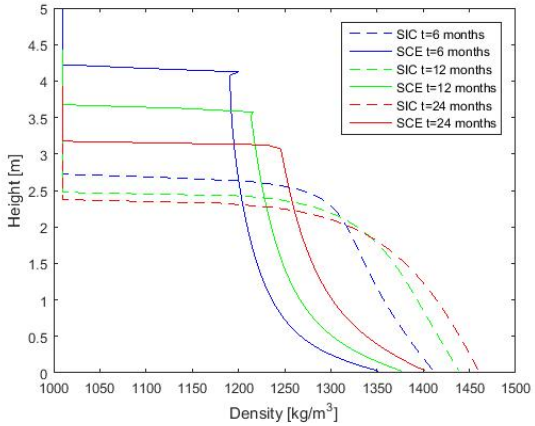

Figure 5.12: Density profiles from c0=300 g/l modelled at time intervals 6, 12 and 24 months in a 5 m high column with material parameters from the SIC300 test and the settling column experiment (denoted as SCE).

The settling curves of the two modelled slurries in figure 5.13 show that the equilibrium bed height is reached much earlier by the simulation with the SIC300 material parameters. The consolidation time for the settling column experiment material parameters is more than six times as long. However, when the final bed height is reached the density profiles have a similar profile. Figure 5.14 shows that the final bed heights of both experiments are similar. The consolidation time depends on the permeability parameter. The difference in K_k is approximately a factor of 20, which induces this long consolidation time. The final bed height from the experiment with material parameters from SIC300 is reached at 24 months, while the bed height of the settling column material parameters is not in equilibrium. Based on these model simulations it can be concluded that the material parameters obtained from a simple low concentration ($c_0 < c_{gel}$) settling column experiment cannot be used to accurately predict the consolidation behaviour on a larger scale. However, the final bed heights and profiles are very similar. This was expected, because K_p is in the same order of magnitude. So, for a dredging project in which time is more or less equivalent to money it is still needed to perform a SIC test to determine a valid permeability coefficient.

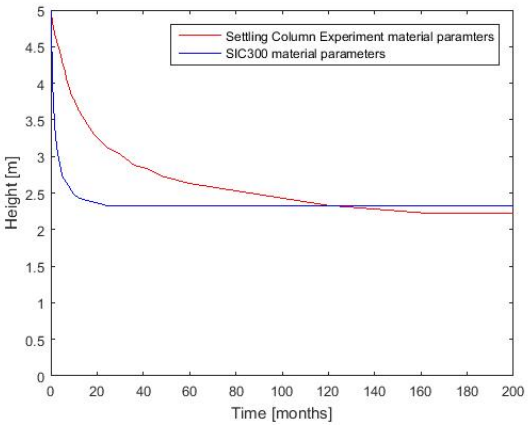

Figure 5.13: Settling curves from c0=300 g/l settling column experiment modelled in a 5 m high column. The time needed for the material parameters from the settling column experiment to reach the final bed height is significantly longer.

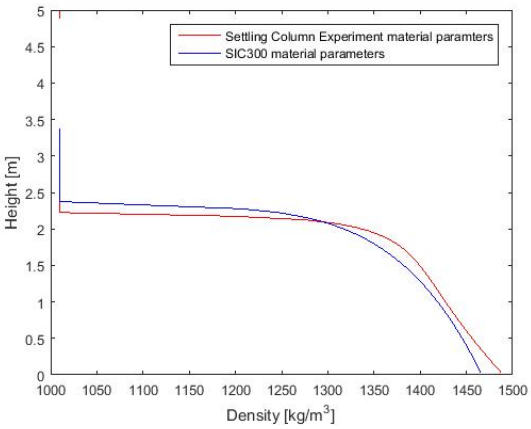

Figure 5.14: Final density profiles from c0=300 g/l settling column experiment modelled in a 5 m high column. The final density profiles are reached at different times, this is seen in the settling curve in figure 5.13.

6

Conclusions & recommendations

This chapter reflects upon the objective of this research and whether it is met. The objective of this research is to determine if the consolidation behaviour is a function of the initial conditions. The research questions are used to reach the objective stated in chapter 1. In the first section conclusions answer the research questions. In the final section recommendations for further research and the industry will be given.

The outcome of this research is relevant for land reclamations with mud as a filling material. The increasing demand for space to live and work in coastal zones and the scarcity of granular sediments contributes to the importance of this research. When the objective is reached this research will be a contribution to the prediction and understanding of the consolidation behaviour of mud. When the consolidation of mud is better predictable, it will be possible to use dredged mud as a filling material for land reclamations.

6.1. Conclusions

The objective of this research is to determine if the consolidation behaviour is a function of the initial conditions. The 1-DV model is used in the analysis of the results. The relevant parameters for the consolidation behaviour are fractal dimension n_f, permeability coefficient K_k and effective stress coefficient K_p. Two cases are compared, in which the first case the low initial concentration is below the gelling concentration ($c_0 < c_{gel}$) and in the second case the high initial concentration that exceeds the gelling concentration ($c_0 > c_{gel}$). The main focus is on the high initial concentration mud mixtures, when the gelling concentration is exceeded.

Consolidation behaviour

The consolidation of a low initial concentration ($c_0 < c_{gel}$) mud suspension shows three phases; hindered settling phase, consolidation phase C-I and consolidation phase C-II. The density profile of the bed changes from a concave shape in phase C-I to a convex shape in phase C-II. High initial concentration ($c_0 > c_{gel}$) mud mixtures also follow three phases during consolidation. The first phase observed is a mud water interface that moves down linearly over time. This would suggest a hindered settling phase. However, it is known that according to fractal theory the particles cannot settle anymore, because the gelling concentration is exceeded. This settling behaviour is caused by the initial density profile that exceeds the equilibrium density profile in the top part of the column. Strength and density are directly related by fractal theory, so the top layer is stronger than the equilibrium strength. This creates an overburden that pushes down like a piston until the force balance is recovered. From this point the consolidation phase C-I starts following the settling curve. This phenomenon is called the piston effect. Furthermore, the top part of the density profile is below the initial concentration of the mud. The density of top layer of the bed is below the initial density by water that is flowing into the bed. This behaviour is called swelling. The swelling of the bed is showed by the density profiles from the 1-DV model that simulates the consolidation behaviour of high initial concentration mud. So, the consolidation behaviour of high initial concentration mud mixtures is different from the lower initial concentration mud, based on the piston effect and swelling. Therefore, it can be concluded that the consolidation behaviour depends on the initial concentration.

Final conditions

Material parameters obtained from the SIC tests were used to simulate the high initial concentration settling column experiments with the 1-DV model. The material parameters from the SIC tests were used to model the density profiles from the high initial concentration settling column experiments. A comparison is made between the modelled and measured density profile. The modelled density profiles show similar results to the measured density profile. This was done for two initial concentrations, c_0 = 200 g/l and c_0 = 300 g/l. For both initial concentrations, the modelled density profiles using the material parameters obtained from the SIC tests are comparable with the measured density profile. Thus, even though these two methods are completely different the conclusion is that the results from these two methods are consistent.

To investigate wether the initial concentration has an effect on the consolidation behaviour, density profiles of a column were modelled for material parameters. This was done for columns c_0 = 200 g/l and c_0 = 300 g/l. The sets of material parameters describing the sediment in these columns are denoted by SIC200 and SIC300, respectively. First, the density profile is modelled with its own material parameters. Second, the material parameters were interchanged. So, column c_0 = 200 g/l was modelled with material parameters obtained from the tests SIC200 and SIC300. The same procedure was done for column c_0 = 300 g/l. These profiles are then compared to the measured density profile. The offset between the modelled and the measured profile is determined. Offset is a measure of how well a modelled density profile fits to the measurement. It is observed, that when the material parameters from the columns were interchanged these density profiles fit less well to the measurement. The accuracy of the fit is based on how well the bed height and density profile from the model compares to the measured density profile. The bed height and density profile deviate more, when material parameters were interchanged. So, the density profiles with interchanged material parameters have a worse fit. Therefore, it can be concluded that the initial concentration has an effect on the final conditions. However, it is not known whether the observed deviation in the density profiles is significant. Whether the effect of the initial concentration is of any significance should be investigated further.

Material parameters

To obtain material parameters for high initial concentration mud mixtures SIC tests have to be performed. A SIC test is a time consuming and costly test to perform. Preferably the material parameters are determined by a simpler method, such as a low initial concentration settling column experiment. Sets of material parameters obtained from the SIC tests and settling column experiments are not the same order of magnitude. The fractal dimension n_f and effective stress coefficient K_p are similar in both sets. However, the permeability coefficient K_k differs by approximately a factor of 20 or more. Therefore, the material parameters are dependent on the initial concentration. However, this dependency only shows between the low concentration $c_0 < c_{gel}$ and high concentration $c_0 > c_{gel}$ case. The K_k determined from the SIC test is different from the settling column experiment. There is no relation between these two experimental methods for the effective stress, but based on the data from this research there is a relation for permeability. An increase in concentration gives a different permeability coefficient. K_k is a parameter that affects the time in which the final bed height is reached and the final bed height is related to K_p. The material parameters obtained from SIC test and settling column experiments are used to model density profiles. Results from the 1-DV model are compared with the measured density profiles from the settling columns. The density profile modelled with the material parameters obtained from the settling column experiments fits less well than the density profile modelled with the SIC material parameters. There are differences in bed height and density profile, but in small scale settling columns with relative small bed heights the differences look reasonable. However, when the two sets of material parameters obtained from a SIC test and settling column experiment are used to model a hypothetical settling column experiment of 5 m high considerable differences are observed. The final bed heights are similar, due to the K_p that is in the same order of magnitude in both sets of material parameters. However, the effect of K_k is clearly observed. A lower value of K_k results in a longer consolidation time. Due to the smaller K_k obtained from the settling column experiment the time to reach the final bed height is more than six times longer. Thus, the K_k is a sensitive parameter for modelling consolidation behaviour on a larger realistic scale. Therefore, it can be concluded that the material parameters obtained from a low concentration settling column test are not suitable to model a high concentration mud mixture with respect to consolidation time.

The permeability coefficient is determined by curve fitting the Gibson equation to the settling curve from a low concentration ($c_0 < c_{gel}$) settling column experiment. Determining K_k is based on a subjective method in which a section of the settling curve is chosen to which the gibson equation is fitted. Which section is

chosen of the settling curve affects the K_k. The effect can be two or three orders of magnitude. However, this is the common method currently used to determine the permeability coefficient. Therefore, a different method to determine the permeability coefficient is needed, which is based on a less subjective approach.

6.2. Recommendations

From this research two sets of recommendations follow. The first set of recommendations is aimed to investigate the aspects that were left untouched due to the scope of this research. These recommendations are focussed to improve the knowledge on the consolidation behaviour of soft cohesive sediments. The second set of recommendations is aimed on the practical application of this research. They serve as a tool to better predict consolidation behaviour for commercial purposes.

6.2.1. Further research

Effect of initial concentration

From this research it can be concluded that there is an effect from the initial concentration on the final conditions. However, it is not known whether this effect is of significance. So, this is a topic for further research. From modelling it is observed that material parameters have a clear effect on simulations of settling columns with a larger height. Therefore, it is proposed to also perform physical settling column experiments with a larger height.

Settling column experiments

During the settling column experiments and the SIC tests the presence of gas in the sediment was observed. The gas trapped in the sediment influenced the measurements. Organic material present in the sediment is responsible for the production of gas. The amount of organic material increases when the sediment is exposed to light. So, it is recommended to limit the exposure of light. This will reduce the gas production in the sediment, which will improve the accuracy of the SIC test and the density measurement.

Permeability coefficient

The determination of the permeability coefficient K_k is prone to errors. K_k is determined by fitting the Gibson equation to a specific section of the settling curve [Merckelbach and Kranenburg, 2004a]. The section of the settling curve to which the Gibson equation is fitted is subjectively chosen. It has been demonstrated that the fit to a section can affect the K_k by three orders of magnitude. To reduce the variability in the permeability coefficient K_k, a different method should be used. One that uses a less subjective approach is recommended.

Vane test

When remoulded shear strengths of a settling column experiment are plotted on double logarithmic scale over volumetric concentration ϕ, the angle of the curve gives the fractal dimension n_f [Kranenburg, 1994]. However, the fractal dimension derived from strength measurements in this research do not match with the fractal dimension determined from the settling column experiments or the SIC tests. An explanation for these lower fractal dimensions can be ascribed to the strength measurement. The rotation speed of the rotovisco measuring system Haake M1500 is fixed to 0.5 rpm. It is suspected that the rotation speed is too high, which influences the measurement. To provide a reliable measurement it is recommended to use a different vane test at a lower rotation speed. Another recommendation is to use higher columns. Higher columns produce higher bed heights, which will provide more space between the measurements for less disturbance, better accuracy and possibly more measurements.

SIC test

In the early stages of the SIC tests the filter stone was jammed in the sample ring. This was a problem that also occurred in other tests prior to this research, but it did not happen as often as during this research. The manufacturer changed the diameter of the filter stones used in this research. Unfortunately, the change in diameter and the solution to this problem was found when all the tests were performed. The new filter stone has a diameter which is 0.15 mm larger than the old one, therefore the diameter of the sample holder ring should be increased to fit the new filter stone. This minor adjustment makes it possible to include a lower range of ϕ in the processing of the data. Which will increase the accuracy of the test and when the test is extrapolated to the range of ϕ of the settling column tests. These low load steps are essential for finding a relation between the settling column experiments and the SIC tests. In further research SIC tests with these

low load steps should be included. A second recommendation regarding the SIC tests is to investigate the material functions from the fractal approach and their application on the SIC test data. The material functions are specifically applicable for settling column experiments. To properly fit these equations to the SIC test data, the assumptions and the empirical coefficients from Merckelbach and Kranenburg [2004b] should be revised.

Experimental error

The governing error in the settling column experiments and SIC tests is induced by variations in the pretreatment of the sample. For the settling column experiment this is the mixing of the sediment and for the SIC test this is the resting period and the amount of organic material of the sample prior to the test. To determine the error replicate experiments should be performed following the same protocol. This makes it possible to evaluate the reproducibility of the experiment. A valid result should be reproducible within the error when the same procedure is followed.

Fitting performance model to measurement

Density profiles obtained from the 1-DV model were fitted to the measured density profiles. The performance of the fit is based on the average percentage of offset in the density profile and bed height. To increase the accuracy of the fitting, the method of Van Wijngaarden et al. [2016] can be used.

Statistical analysis

The measured density profiles by the UHCM device showed noise in the measurements. It is assumed the noise was caused by gas trapped in the sediment. The peaks were adjusted by interpolation following an approach that has a degree of subjectivity. To increase the accuracy the adjustment of the gas peaks should be done following a statistical analysis.

1-DV model

In this research part of the analysis was based on the density profiles from the 1-DV model. However, the settling curve can also be determined by the 1-DV model. This procedure is time consuming and therefore did not fit in the scope of this research. When the settling curve are determined it is possible to determine the K_k and n_f from this settling curve. The results should be consistent to the parameters that were put into the model. This procedure is proposed to evaluate the accuracy of the method to determine K_K [Merckelbach and Kranenburg, 2004b].

6.2.2. Recommendations for the industry

Particle density

The particle density ρ_s is commonly estimated to be 2650 kg/m^3. During this research this estimation was adjusted to the measured particle density $\rho_s = 2540$ kg/m^3 [Barciela Rial, 2015]. This changed several parameters which affect the modelled density profile, settling curve and final bed height. For commercial purposes overestimating or underestimating consolidation can have a great impact. The sludge depot the Slufter in the Netherlands, which design was oversized by overestimation, is an example of this. Dredging is a costly operation that is optimised constantly to reduce costs. In an early stage of a project this important parameter should be measured, because the effect is considerable and measuring the particle density is a minor effort.

Modelling consolidation

Density profiles from the 1-DV model [Winterwerp, 1999] that includes the swelling behaviour of mud and the material parameters determined from a SIC test show consistent results compared to the measured density profile in the settling column experiment. So, even though the density profile is derived in two different methods they are consistent. Therefore, this 1-DV model that includes the swelling behaviour is proposed to be used as a tool to predict the consolidation behaviour of mud for projects similar to the Marker Wadden.

Experimental method

To determine material parameters for a soft cohesive sediment two experimental methods can be used. A relative simple settling column experiment or a more elaborate and costly SIC test. These material parameters are used to predict the behaviour and final conditions of a consolidating bed. When only the final conditions should be known and consolidation time is not of interest, material parameters of a settling column experiment are sufficient to model the final conditions with the 1-DV model. When it is important to know at which time the final conditions are reached, then the material parameters should be determined by a SIC test.

Predictability

Mud deposited in an enclosed area is not homogeneously distributed. The initial concentration is varying locally within the enclosed area. In this research it is concluded that there is an effect of initial concentration on the consolidation behaviour and final conditions. To predict the consolidation behaviour and final conditions of mud with multiple initial concentrations, multiple sets of material parameters should be determined from SIC tests. Performing multiple SIC tests is costly and time consuming. Therefore, it is recommended to investigate whether the consolidation of the mud in the whole enclosed area can be predicted by one set of material parameters determined by one SIC test.

List of Figures

List of Tables

References

ASTM, D. (1989). 4648-87, 1989. *Standard test method for laboratory miniature vane shear test for saturated fine-grained clayey soil. Annual Book of ASTM Standards*, 4:868–873.

Barciela Rial, M. (2015). *Sediment heterogeneity in Lake Markermeer*. Internal report.

Been, K. and Sills, G. (1981). Self-weight consolidation of soft soils: an experimental and theoretical study. *Geotechnique*, 31(4):519–535.

Berkhout, N. (1994). Manual uhcm, ultra-sonic high concentration meter. *Delft Hydraulics, The Netherlands*.

Berlamont, J., Ockenden, M., Toorman, E., and Winterwerp, J. C. (1993). The characterisation of cohesive sediment properties. *Coastal Engineering*, 21(1):105–128.

Berlamont, J. and Van Goethem, J. (1984). Avoiding mud accumulation in harbours and their entrances. *Report to SBBM, Hydraulics Laboratory, KU Leuven (in Dutch)*.

Dankers, P. (2006). *T., 2006, On the hindered settling of suspensions of mud and mud-sand mixtures*. PhD thesis, PhD thesis, Technical University of Delft.

Dankers, P. and Winterwerp, J. C. (2007). Hindered settling of mud flocs: theory and validation. *Continental shelf research*, 27(14):1893–1907.

De Lucas Pardo, M. (2014). *Effect of biota on fine sediment transport processes: A study of Lake Markermeer*. PhD thesis, TU Delft, Delft University of Technology.

Evans, D. (2012). Building the european unions natura 2000 network. *Nature conservation*, 1:11.

Geretsen, P. (2014). Design research houtribdijk marker wadden. *Vista Svasek Hydraulics, The Netherlands*.

Gibson, R., England, G., and Hussey, M. (1967). The theory of one-dimensional consolidation of saturated clays: 1. finite non-linear consildation of thin homogeneous layers. *Geotechnique*, 17(3):261–273.

Hendriks, E. (2016). *The effect of pH and the solids composition on the settling and self-weight consolidation of mud*. MSc-thesis Delft University of Technology, Delft, The Netherlands.

Johansen, C. (1998). *Dynamics of cohesive sediments*. PhD thesis, Videnbasen for Aalborg UniversitetVBN, Aalborg UniversitetAalborg University, Det Teknisk-Naturvidenskabelige Fakultet. The Faculty of Engineering and Science.

Kranenburg, C. (1994). The fractal structure of cohesive sediment aggregates. *Estuarine, Coastal and Shelf Science*, 39(6):451–460.

Krone, R. B. (1986). The significance of aggregate properties to transport processes. In *Estuarine cohesive sediment dynamics*, pages 66–84. Springer.

Lintern, D. G. (2003). *Influences of flocculation on bed properties for fine-grained cohesive sediment*. PhD thesis, University of Oxford.

Liu, J.-C. and Znidarčić, D. (1991). Modeling one-dimensional compression characteristics of soils. *Journal of Geotechnical Engineering*, 117(1):162–169.

Mehta, A. J. (2014). *An introduction to hydraulics of fine sediment transport*. World scientific.

Merckelbach, L. M. (1998a). Laboratory experiments on consolidation and strength evolution of mud layers. Technical report, TU Delft, Department of Hydraulic Engineering.

Merckelbach, L. M. (1998b). Laboratory experiments on consolidation and strength evolution of mud layers. Technical report, TU Delft, Department of Hydraulic Engineering.

Merckelbach, L. M. (1999). Consolidation and strength evolution of dollard mud: Measurement report on laboratory experiments. Technical report, TU Delft, Department of Hydraulic Engineering.

Merckelbach, L. M. (2000). *Consolidation and strength evolution of soft mud layers*. TU Delft, Delft University of Technology.

Merckelbach, L. M. and Kranenburg, C. (2004a). Determining effective stress and permeability equations for soft mud from simple laboratory experiments. *Géotechnique*, 54(9):581–591.

Merckelbach, L. M. and Kranenburg, C. (2004b). Equations for effective stress and permeability of soft mud–sand mixtures. *Géotechnique*, 54(4):235–243.

Meshkati Shahmirzadi, M., Staelens, P., Claeys, S., Cattrysse, H., Van Hoestenberghe, T., Van Oyen, T., Vanlede, J., Verwaest, T., and Mostaert, F. (2015). Experimental investigation on consolidation behaviour of mud: Subreport 1-methodology study. *Journal of Geophysical Research: Oceans*, Version 5.0.

Michaels, A. S. and Bolger, J. C. (1962). Settling rates and sediment volumes of flocculated kaolin suspensions. *Industrial & Engineering Chemistry Fundamentals*, 1(1):24–33.

Migniot, C. and Hamm, L. (1990). Consolidation and rheological properties of mud deposits. *Coastal Engineering Proceedings*, 1(22).

Monroe, J. S. and Wicander, R. (2011). *The changing earth: exploring geology and evolution*. Cengage Learning.

Noordhuis, R., van Zuidam, B. G., Peeters, E. T., and van Geest, G. J. (2015). Further improvements in water quality of the dutch borderlakes: two types of clear states at different nutrient levels. *Aquatic Ecology*, pages 1–19.

Townsend, F. and McVay, M. (1990). Soa: Large strain consolidation predictions. *Journal of geotechnical engineering*, 116(2):222–243.

Van Kessel, T. and Kranenburg, C. (1996). Gravity current of fluid mud on sloping bed. *Journal of Hydraulic Engineering*, 122(12):710–717.

Van Mieghem, J., Smits, J., and Sas, M. (1997). Large-scale dewatering of fine-grained dredged material. *Terra et Aqua*, pages 21–28.

van Olphen, e. J. C. (2016). *Consolidation behaviour of soft cohesive soils, the correlation between different scale model tests*. MSc-thesis Delft University of Technology, Delft, The Netherlands.

van 't Hoff, J. and Nooy van der Kolff, A. (2012). *Hydraulic Fill Manual: For Dredging and Reclamation Works*, volume 244. CRC press.

Van Wijngaarden, W., Van Paassen, L., Vermolen, F., Van Meurs, G., and Vuik, C. (2016). A reactive transport model for biogrout compared to experimental data. *Transport in Porous Media*, 111(3):627–648.

Welton, J. E. (1984). *SEM petrology atlas*. American Association of Petroleum Geologists Tulsaˆ eOklahoma Oklahoma.

Winterwerp, J. C. (1999). *On the dynamics of high-concentrated mud suspensions*. PhD thesis, TU Delft, Delft University of Technology.

Winterwerp, J. C. (2002). On the flocculation and settling velocity of estuarine mud. *Continental shelf research*, 22(9):1339–1360.

Winterwerp, J. C. and Van Kesteren, W. G. (2004). *Introduction to the physics of cohesive sediment dynamics in the marine environment*, volume 56. Elsevier.

Znidarčić, D., Miller, R., Van Zyl, D., Fredlund, M., and Wells, S. (2011). Consolidation testing of oil sand fine tailings. In *Proceedings of Tailings and Mine Waste*.

A

Useful relations

This appendix provides useful relations that were used in this thesis.

Volumetric concentration:

$$\phi = 1 = \phi_s + \phi_w + \phi_g \tag{A.1}$$

Volumetric concentration solids phase:

$$\phi_s = \frac{V_s}{V_t} = \frac{c}{\rho_s} = \frac{1}{1+e} \tag{A.2}$$

Void ratio:

$$e = \frac{V_e}{V_s} = \frac{\phi_w + \phi_g}{\phi_s} = \frac{1-\phi_s}{\phi_s} \tag{A.3}$$

Bulk density:

$$\rho_b = \frac{M_t}{V_t} \tag{A.4}$$

Dry density:

$$\rho_{dry} = c = \frac{\rho_b - \rho_w}{1 - \rho_w/\rho_s} = \frac{M_s}{V_t} \tag{A.5}$$

Water content by weight:

$$W = \frac{M_w}{M_t} \tag{A.6}$$

B

Additional undrained shear strength data

The strength of the bed in a settling column is measured by a vane test. The experimental procedure is explained in section 3.3. Results from the vane tests are summarised in section 4.3.

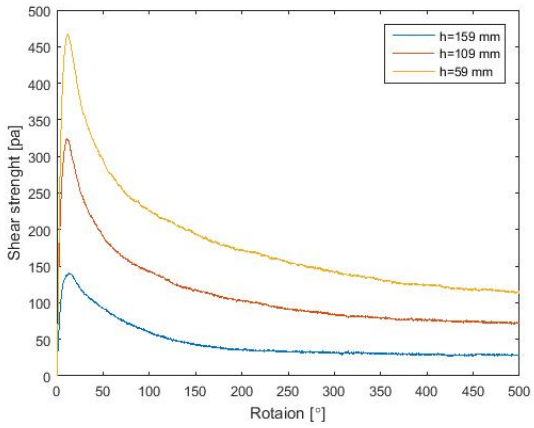

Figure B.1: Vane test in column $c_{0,1}$ = 200 g/l

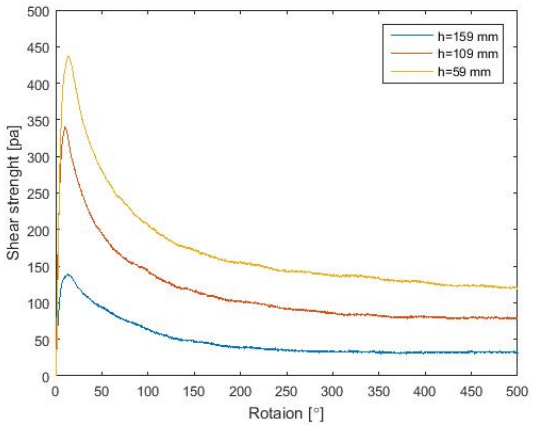

Figure B.2: Vane test in column $c_{0,2}$ = 200 g/l

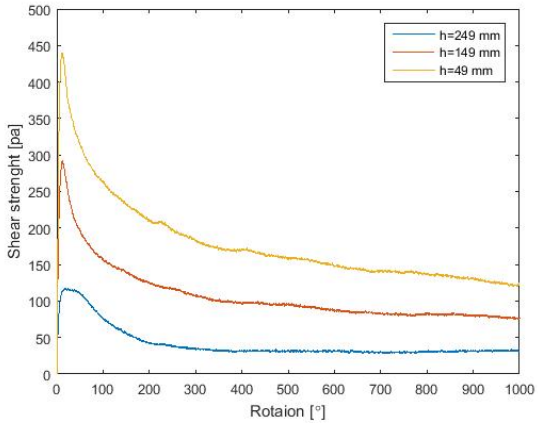

Figure B.3: Vane test in column $c_{0,1}$ = 300 g/l

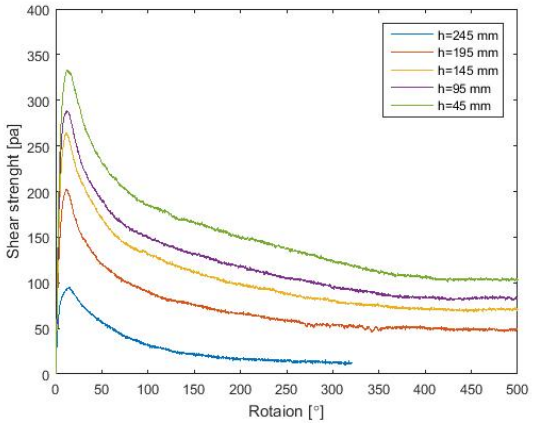

Figure B.4: Vane test in column $c_{0,2}$ = 300 g/l

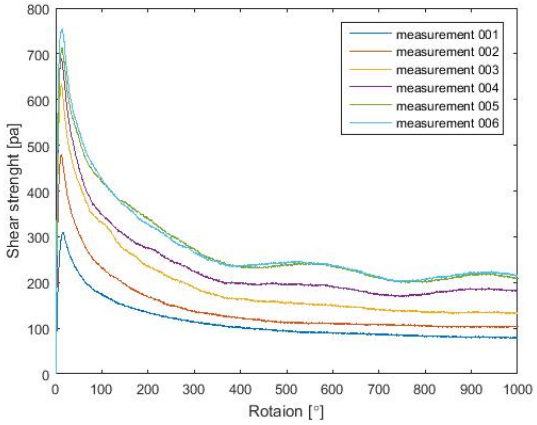

Figure B.5: Vane test in column c_0 = 400 g/l

C

Density profile measurement

In this appendix is explained how the data is processed from the density measurements. The measuring principle and procedure is explained and the factors that are implied to adjust the data are given. The measurements were done with the UHCM (Ultrasonic High Concentration Meter) device. The measuring principle is based on the attenuation of ultra sound by particles suspended between a pair of acoustic transducers, a transmitter and a receiver. From this measuring principle the density profiles are derived.

Before the measurement in the columns the UHCM device was calibrated. The calibration was done with sediment from column $c_{0,1}$ = 300 g/l, that was used for a SIC test before density measurements could be done. It is important to use the same sediment for calibration, because the type of sediment and composition can influence the attenuation of ultra sound energy. For better accuracy the calibration was done for 6 known densities. Calibrating the device for multiple points increases the accuracy.

To perform the measurement in the column the transducers are placed in a measuring gauge. This allows the transducers to be lowered into the bed accurately. Each 5 mm a measurement is performed. This gives the measurement a high resolution. After the each measurement in a column a zero check was done. The transducers are dipped in water to see if the volt output was zero, i.e. a density of 1000 kg/m^3. The distance between the transducers highly influences the measurement. This is a good method to check the reliability of the measurements between each column.

During the measurement high peaks in the volt output were observed. High peaks in the measurements are due to gas trapped in the sediment or a measurement close to the surface or bottom of the sediment in a column. When gas is present in the measuring volume between the transmitter and receiver the output of the measuring device will give an unrealistic high value Van Kessel and Kranenburg [1996]. This also holds for measurements close to the surface and the bottom of the bed. At the surface the measuring volume between the transmitter and receiver is not completely submerged in the mud, which gives an unrealistic output and a measurement close tot the bottom of the bed is affected by the glass bottom of the column.

When all the measurements are done the volt output can be converted to density by utilising the calibration. When the density over height is plotted a density profile is created. This preliminary density profile has an error. The error is based on the principle of mass conservation. When a a settling column experiment is started the initial mass of the sediment in the column is known. The mass based the density profile measured with the UHCM device can calculated. The difference between the initial mass and the mass based on the density profile is a systematic error.

To determine the mass from a density profile the settling column is divided in segments of 5 mm. The volume per segment can be calculated from the inner diameter of the column. The density per segment was measured by the UHCM device. So, with the density and volume the mass per segment can be calculated. The total mass of the segments is then compared to the initial mass of the settling column experiment. The difference can be compensated for by adjusting the density of each segment with a factor α. The density of each segment is multiplied by this factor α until the total mass of the measurement is equal to the initial mass of the experiment. In this first adjustment of the density profile the peaks in the measurements in figures 4.14 and 4.21 are not corrected.

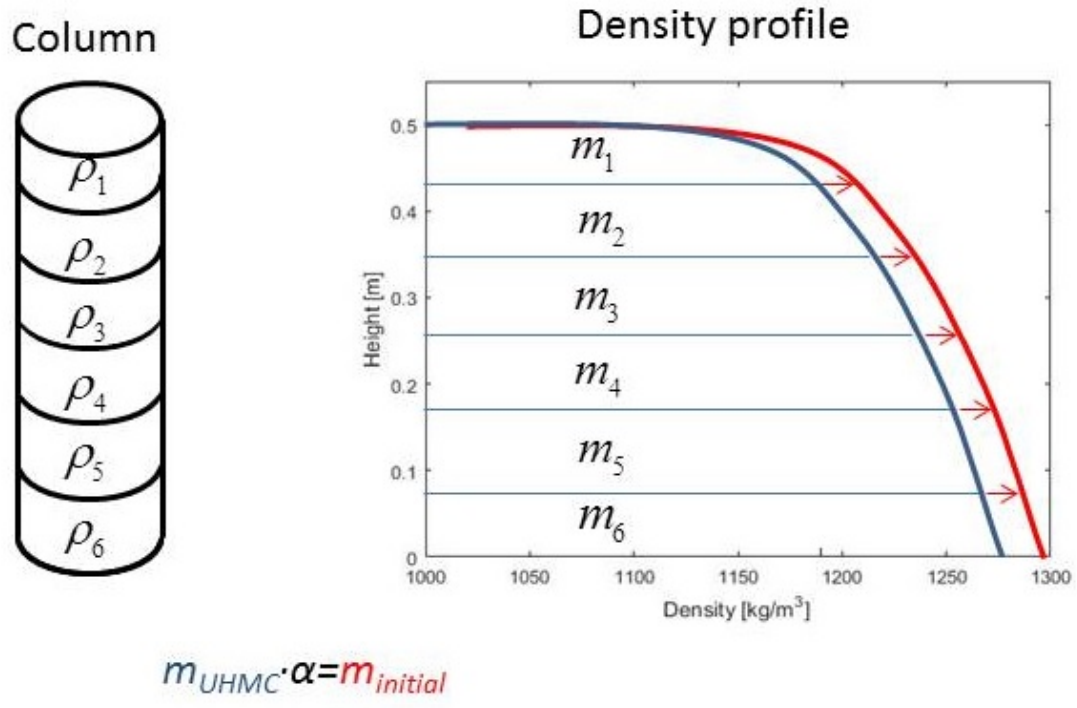

Figure C.1: Schematically explanation for determining the measured density profile. The density profile is measured by the UHCM device. The column is divided in sections and for each section the mass based on the measured density and the volume of that section. The total mass based on the UHCM measurement is then multiplied by a adjustment factor α to match the initial mass of the sediment that is present in the column ($m_{UHCM} * \alpha = m_{initial}$).

The factor α is the systematic error of the measured density profile per column. A higher adjustment factor suggest a lower accuracy, the adjustment factors are presented in table C.1. This is the case for the lower initial concentration settling column experiments $c_0 < c_{gel}$. The higher initial concentration experiments $c_0 > c_{gel}$ show a better accuracy due tot he lower α. It is suspected that a smaller bed height induces a lower accuracy. This can be seen in figure 4.13, in which the density profile of c_0 = 40 g/l is shifted to higher densities well beyond the density profiles of the columns c_0 = 50 g/l and c_0 = 60 g/l. While these high densities are not expected.

Table C.1: α factor used to adjust the measured density profile to meet the principle of mass conservation

c_0 [g/l]	α [-]
40	1.11
50	1.04
60	1.02
100	1.02
200	1.005
200 duplicate	1.007
300 duplicate	0.986
400	1.022

In this first adjustment of the density profile the peaks in the measurements in figures 4.14 and 4.21 are not corrected. The peaks in the measurement due to gas influence the value of the adjustment factor α. To better adjust the density profile to the principle of mass conservation the peaks in the density profile were corrected. This is done by taking the average density from the point above and below the peak and and replace the peak density with this average density. This resolves in a smooth density profile. The data analysis as described in figure C.1 is then repeated on this new density profile without peaks. The adjustment factor

increases, because removing the peaks effects the mass of the sediment derived from the UHCM density profile. Figures C.2 and C.3 show the density profile with peaks and the density profile without peaks, but with an extra adjustment needed. The density profile is shifted due to the increasing adjustment factor α. The new determined alpha is presented in table C.2. The corrected density profiles are used in section 5.4.

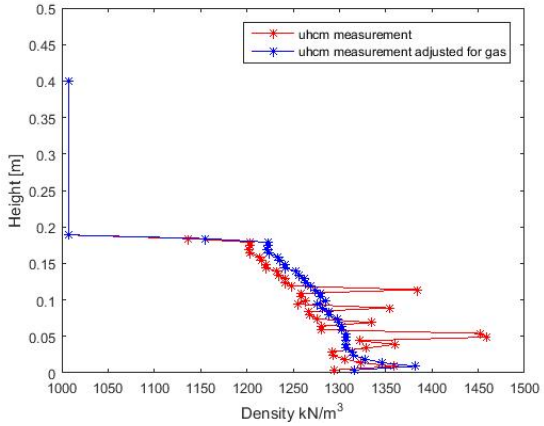

Figure C.2: Density profiles column c_0 = 200 g/l. In the new density profile the peaks are corrected and adjusted with a new α factor to match the initial mass of the experiment. Due to the correction of the peaks the new adjustment factor is higher and shifts the density profile.

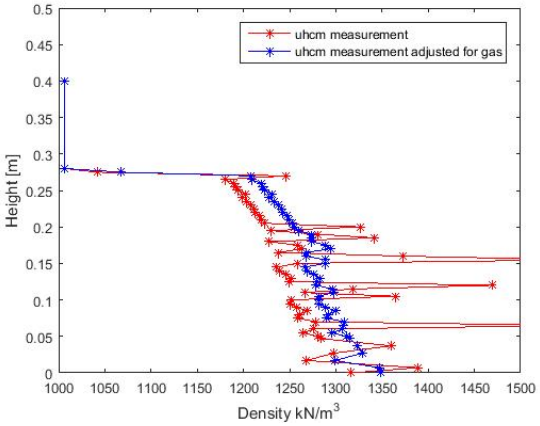

Figure C.3: Density profiles column c_0 = 200 g/l. In the new density profile the peaks are corrected and adjusted with a new α factor to match the initial mass of the experiment.

Table C.2: α factor used to adjust the measured density profile after the correction of the noise in the measured density profile

c_0 [g/l]	α [-]
200	1.022
300 duplicate	1.009

An estimation of the measuring error for the UHCM device is made based on the reproducibility of the measurement. In figure 3.5 the reproducibility of a measurement is shown. The derived density profiles shows a similar density profile. This indicates a good reproducibility of the measurement. The error is determined by averaging the differences between each profile. The determined measuring error is ± 24 kg/m^3. This can be presented as an error bound on the density profiles. The error bound is shown in figures C.4 and C.5, which shows that the modelled density profiles with the material parameters from the SIC tests are within the reproducibility of the measurement.

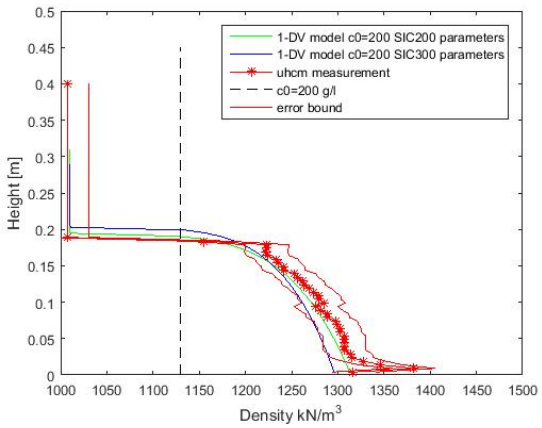

Figure C.4: Density profiles modelled from column $c_0 = 200$ g/l with material parameters obtained from SIC200 and SIC300 and compared to the measures density profile with indicated error bounds

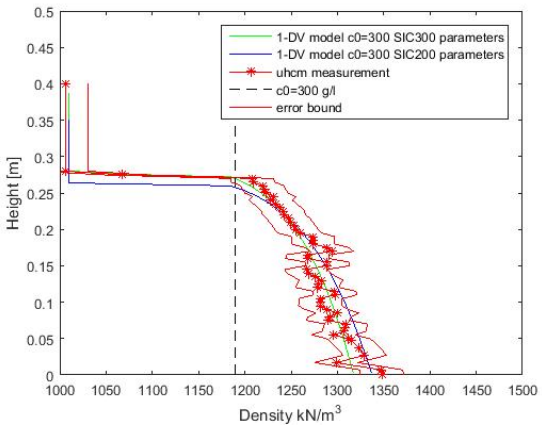

Figure C.5: Density profiles modelled from column $c_0 = 300$ g/l with material parameters obtained from SIC200 and SIC300 and compared to the measures density profile with indicated error bounds

D

Swelling of high concentration suspensions

In this appendix the swelling behaviour is explained. Swelling occurs for high initial concentration mud that consolidates. When a high initial concentration mud mixture is set to consolidate the density profile will move to its equilibrium profile at that time on the settling curve. The density profile evolves from a concave to convex shape. The top layer of the bed will have a density that is lower than the initial concentration. Water has to flow into the bed to dilute the suspension to be able to lower the concentration of the bed below the initial concentration. Figure 4.20 demonstrates this behaviour. To implement this swelling behaviour in the 1-DV model a swelling coefficient is added to the Gibson equation. The Gibson equation follows:

$$\frac{\partial \phi}{\partial t} - \left(\frac{\rho_s - \rho_w}{\rho_w}\right) \frac{\partial (w_s + k\phi)\phi}{\partial z} - D\frac{\partial^2 \phi}{\partial z^2} = 0 \tag{D.1}$$

in which w_s is the hindered settling formulation and D is either the consolidation coefficient or the swelling coefficient. The behaviour of the coefficient D depends on the concentration at a certain height in the bed.

$$c(z) > c_0 : \qquad \frac{\partial \phi}{\partial t} - \left(\frac{\rho_s - \rho_w}{\rho_w}\right) \frac{\partial (w_s + k\phi)\phi}{\partial z} - \Gamma_c \frac{\partial^2 \phi}{\partial z^2} = 0 \tag{D.2}$$

$$c(z) < c_0 : \qquad \frac{\partial \phi}{\partial t} - \left(\frac{\rho_s - \rho_w}{\rho_w}\right) \frac{\partial (w_s + k\phi)\phi}{\partial z} - c_s \frac{\partial^2 \phi}{\partial z^2} = 0 \tag{D.3}$$

In these two equations c is the concentration, Γ_c is the consolidation coefficient and c_s is the swelling coefficient. In the top few centimetres of the bed the local concentration is lower than the initial concentration, then swelling equation D.3 applies. For the lower part of the bed the local concentration exceeds the gelling concentration, then consolidation equation D.2 applies.

E

SIC test results

This appendix contains additional results and information regarding the performed SIC tests.

Sediment parameters

The sediment from the settling column experiment was used for the SIC tests. After the settling column tests the bulk density, water content by weight and gas content by volume were determined by drying a subsample in an oven at 105°C for 24 hours and presented in table E.1. This is denoted by c_0 due to its origin from the initial concentration from the settling column experiment. These values are the parameters of the sediment that is used in the SIC tests. Only the percentage of gas is determined for the situation in the settling column at the end of the experiment. When the sediment is transferred to the SIC test it was homogenised by gently mixing. It is assumed that the mixing extruded all the gas from the sediment. Total extrusion of gas in sediment is very much dependent on the way of mixing and preparing the sample after mixing. However, this assumption is made to set a reference to determine the amount of gas in the sediment after the SIC test.

Table E.1: Parameters determined from the final beds from the settling column experiments before it is used for the SIC tests

Experiment	w% $=\left(\frac{M_w}{M_t}\right)$	ρ_b $[kg/m^3]$	gas %
$c_0 = 200$	0.654	1269.9	2.0%
$c_0 = 300$	0.639	1282.8	3.9%
$c_0 = 400$	0.616	1306.6	0.03%

After the SIC tests the height of the sample is measured. The bulk density and water content by weight are derived by drying a subsample in an oven at 105°C for 24 hours. The gas percentage by volume is calculated by determining the volume of pores for the final SIC sample based on the height of the sample and the volume of water based on the water content by weight. Subtracting these values will give the volume of gas in the sample. These determined parameters are presented in table E.2. What can be seen in table E.1 and E.2 is that column c_0 = 300 g/l has considerably more gas in the sediment. This is also the case for the SIC300 test. The gas present in the sample from SIC300 is a factor 10 higher than that from the other test. The presence of gas was observed during the test itself while operating the SIC device.

Table E.2: Parameters determined from the sample after the SIC tests

Experiment	w% $=\left(\frac{M_w}{M_t}\right)$	ρ_b $[kg/m^3]$	$h(t_0)$ $[mm]$	$h(t_{end})$ $[mm]$	gas %
SIC200	0.42	1553	56	26.5	1.1%
SIC300	0.40	1582	56	29.0	11.6%
SIC400	0.40	1581	56	29.0	1.4%

Results

The settling curves from SIC200 and SIC400 are shown in figure E.1 and E.2. The settling curve from SIC300 can be found in section 4.5.1.

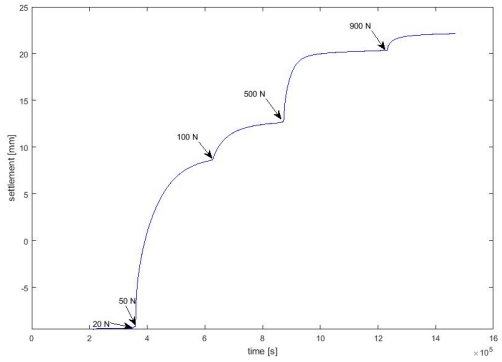

Figure E.1: SIC200 settlement including loadsteps

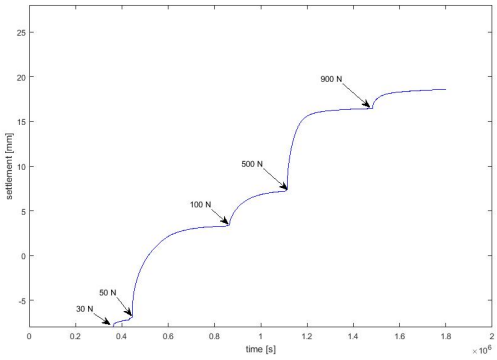

Figure E.2: SIC400 settlement including loadsteps

After each SIC tests vane tests where performed on the sediment that came out of the SIC test. The vane tests settings are presented in table E. Note the the sediment is much more stiffer than that of the settling column tests, therefore the vane use had a different size. The vane test measurements are presented in the figures E.3, E.4 and E.5.

Table E.3: Settings vane test Haake M1500 after SIC test

Variable	Setting
Rate of rotation	0.5 rpm
Vane	FL1000
Vane diameter	10 mm
Vane height	9 mm
Vane depth	19 mm

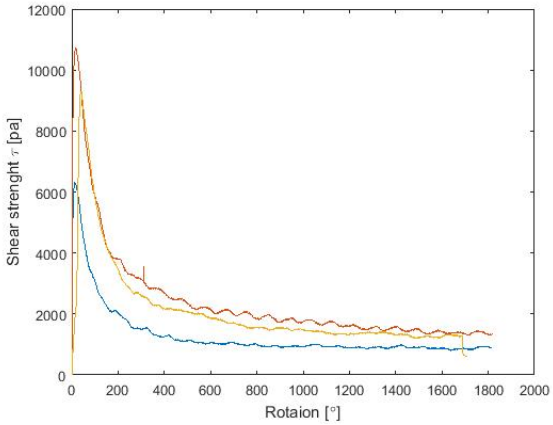

Figure E.3: SIC200 vane tests

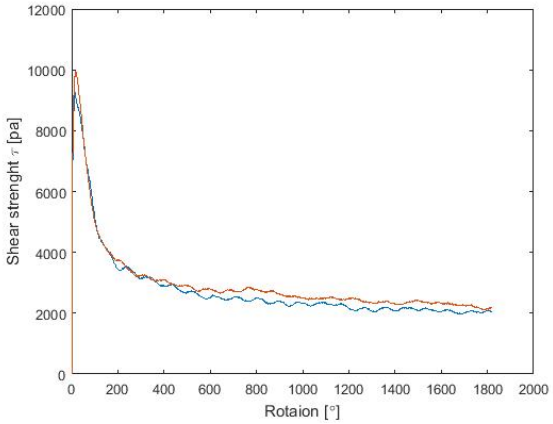

Figure E.4: SIC300 vane tests

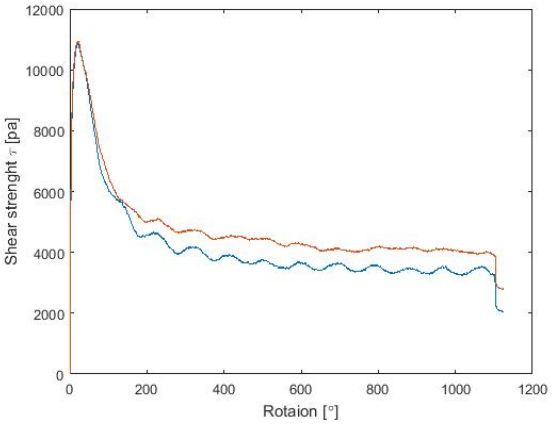

Figure E.5: SIC400 vane tests

Potential errors

The biggest error in the SIC test is induced by the sample pretreatment. The sample pretreatment is highly affecting the results. Other factors that induce error are discussed here. These errors are induced during the operation of the SIC device and by the interpretation of the data.

During the operation of a SIC test an error is induced by the stabilising of the differential pressure. The pressure difference between the top and the bottom is measured during the test. Based on the hydrostatic pressure in the sample there is an equilibrium differential pressure assumed. During a SIC test at different load steps flow rates are induced on the sample, i.e. a permeability step. The SIC measurement device displays a differential pressure signal. During a permeability step a pressure increase in differential pressure is observed. When the induced flow rate is stopped the pressure increase stabilises again to the equilibrium pressure. However, due to a number of reasons the pressure can deviate from the equilibrium differential pressure. This deviation induces the error. The error is calculated by $\Delta p_{eq,up} - \Delta p_{eq,up}$. This is explained in figure E.6.

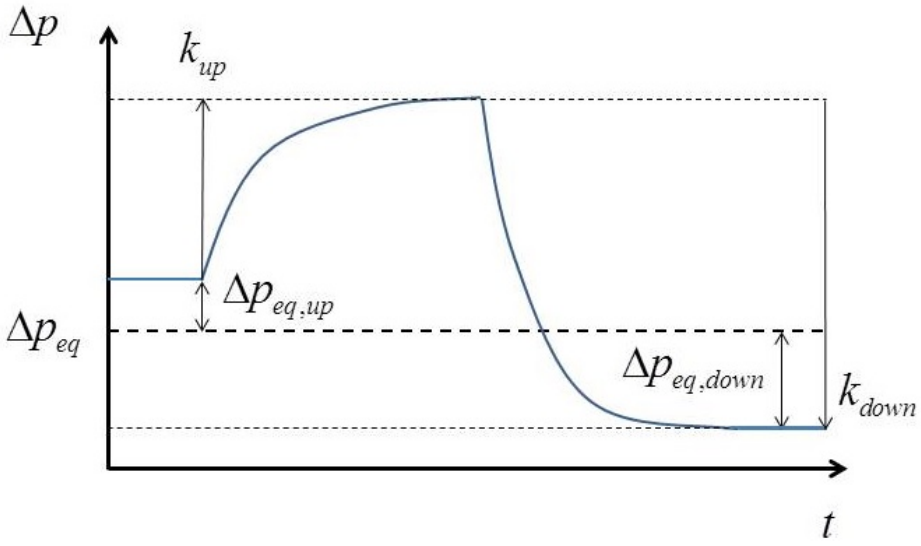

Figure E.6: Schematised differential pressure signal during SIC test. The differential pressure deviates from the assumed equilibrium. From this deviation the error is derived error= $\Delta p_{eq,up} - \Delta p_{eq,up}$.

Another kind of error can be induced by the data processing, this is a systematic error. The volumetric concentrations ϕ is derived from the sample prior to the SIC test and the settlement during the SIC test. The SIC test produces a settlement curve of the sample which is based on the signal of an electronic measuring gauge. To determine the volumetric concentrations at different load steps it is important to set the right zero setting for the start of the settlement of the sample. The zero settling of settlement should be when the load piston is lowered on the sample and it pushes down on the sample. This is a very subtle transition in the settling curve. How this point is chosen affects the volumetric concentration throughout the course of the test. Therefore, it is a systematic error. During the data processing of the SIC tests the same protocol was followed. So, if there is a systematic error due to this phenomenon it will be the same in all the three SIC tests.